WIND ENGINEERING STUDY OF THE MOBILE SERVICE TOWER AND SPACE SHUTTLE FOR SLC-6, VANDENBERG AFB, CALIFORNIA

by

G. K. Kiely*
J. E. Cermak**
J. A. Peterka***

for

Sverdup and Parcel and Associates, Inc.
800 North 12th Boulevard
St. Louis, Missouri 63101

Fluid Mechanics and Wind Engineering Program
Fluid Dynamics and Diffusion Laboratory
Department of Civil Engineering
Colorado State University
Fort Collins, Colorado 80523

May 1979

*Graduate Research Assistant
**Director, Fluid Dynamics and Diffusion Laboratory
***Associate Professor

ACKNOWLEDGEMENTS

The support of Sverdrup & Parcel and Associates in carrying out this study is gratefully acknowledged.

Construction of the MST, PCR and auxiliary structures was accomplished by personnel of the Engineering Research Center Machine Shop.

Construction of the force and moment balances and data collection was accomplished principally by Max Pettago (Sr. Electronics Spec.) and Morgan Downing (Research Associate).

Mr. James A. Garrison supervised the photography and motion picture sessions.

Typing of this report was performed by Mrs. Arlene Nelson and Technical Typing staff.

TABLE OF CONTENTS

LIST OF FIGURES

LIST OF TABLES

LIST OF SYMBOLS

Symbol	Definition
U	Local mean velocity
H	Characteristic dimension (building Height)
B	Characteristic dimension
A	Characteristic Area
ν, ρ	Kinematic viscosity and density of approach flow
$\frac{UD}{\nu}$	Reynolds number
E	Mean voltage
A, B, n	constants
U_{rms}	Root-mean-square of fluctuating velocity
E_{rms}	Root-mean-square of fluctuating voltage
U_H	Reference mean velocity at top of building
U_{30}	Reference mean velocity corresponding to 30 ft full-scale
$X.Y$	Horizontal coordinates
Z	Height above surface
δ	Height of boundary layer
T_u	Turbulence intensity $\frac{U_{rms}}{U_H}$
$C_{p_{mean_{30}}}$	Mean pressure coefficient, $\frac{(p-p_{30})_{mean}}{0.5\ \rho\ U_{30}^2}$
$C_{p_{rms_{30}}}$	Root-mean-square pressure coefficient, $\frac{\left((p-p_{30})-(p-p_{30})_{mean}\right)_{rms}}{0.5\ \rho\ U_{30}^2}$
$C_{p_{max_{30}}}$	Peak maximum pressure coefficient, $\frac{(p-p_{30})_{max}}{0.5\ \rho\ U_{30}^2}$

Symbol	Definition
$C_{p_{min_{30}}}$	Peak minimum pressure coefficient, $\frac{(p-p_{30})_{min}}{0.5\ \rho\ U_{30}^2}$
$(\ )_{min}$	Minimum value during data record
$(\ )_{max}$	Maximum value during data record
p	Fluctuating pressure at a pressure tap on the structure
p_{30}	Static pressure in the wind tunnel corresponding to 30 ft in full scale (i.e., 3.6 in. in model scale)
A_1	The projected frontal area of orbiter and external tank and boosters viewed from the wind direction 270°.
H_1	The height from top of launch pad to top of external tank
B_1	The radius of the external tank
A_2	The projected frontal area of orbiter only
H_2	The height of orbiter
B_2	The radius of the external tank
A_3	The projected area of external tank
H_3	The height from top of launch pad to top of external tank
B_3	The radius of the external tank

Abbreviations

SSV	Space Shuttle Vehicle
ET	External Tank
LM	Launch Mount
MST	Mobile Service Tower
PCR	Payload Change Room
AT	Access Tower

1. INTRODUCTION

The magnitude of the wind induced loads on the Space Shuttle in a stationary ground position is a significant factor in its launch-site assembly and support against wind and design of the surrounding buildings. Factors influencing the loads are 1) meteorological variables, such as approach wind speed and direction, and 2) the geometry and configuration of the Shuttle and surrounding buildings.

The purpose of this study was to determine the flow patterns and forces and moments on the Space Shuttle and Mobile Service Tower: The study was divided into five different parts as follows:

A) mean velocity and turbulence profiles of the simulated atmospheric boundary layer

B) forces and moments on the Mobile Service Tower (with no other buildings in place)

C) pressure measurements on the Mobile Service Tower using 100 external and 56 internal pressure taps

D) forces and moments on the Space Shuttle in six different configurations and

E) flow visualization studies by addition of smoke was recorded on still and motion pictures.

The study was performed in the Environmental Wind Tunnel in the Fluid Dynamics and Diffusion Laboratory. This facility permitted modeling of the Space Shuttle and auxiliary buildings to a scale of 1:100. Modeling of the wind flow over and around these complex geometries requires special consideration of flow conditions in order to guarantee similitude between model and prototype. A detailed discussion of the

similarity requirements can be found in References (1), (2) and (3). In general, the requirements are that the model and prototype be geometrically similar, that the approach mean velocity at the model location have a vertical profile shape similar to the full-scale flow, and that the turbulence characteristics of the flows be similar. For sufficiently high Reynolds number ($> 2 \times 10^4$) the airflow patterns about bluff bodies will be essentially constant for a large range of Reynolds numbers. Typical values encountered are 10^6-10^7 for the full-scale and 10^4-10^5 for the wind tunnel model. In this range acceptable flow similarity is achieved without precise Reynolds numbers equality.

2. EXPERIMENTAL CONFIGURATION

2.1 Wind Tunnel

The study was performed in the Environmental Wind Tunnel located in the Fluid Dynamics and Diffusion Laboratory at Colorado State University. The wind tunnel is an open-circuit facility driven by a 50 hp variable speed propeller. The test section is nominally 12 ft wide, 7 ft high and 57 ft long fed through a 3.35:1 contraction ratio. The roof is adjustable to maintain a zero pressure gradient along the test section. The mean velocity can be adjusted continuously from 1 to 30 fps. A diagram of the wind tunnel is shown in Figure 1.

2.2 Models

In the determination of forces and moments on the MST building, scaled models made of aluminum and plastic were used. The model was mounted on an aluminum base plate located below the tunnel floor. The base plate was securely fixed to a six-component strain gage force and moment balance (Figure 2). This arrangement was positioned on a turntable centered 45 ft from the test section entrance. The system was viscously damped by a set of masonite cross-fins moving in a viscous fluid to prevent motion of the model (Figure 2). The damping system worked satisfactorily and did not affect the magnitude of the mean forces and moments.

To determine the the local pressures on the MST building, a Plexiglas model containing 100 pressure taps on the outside faces and 56 taps on the inside was fabricated. The location of the taps on the structure are shown in Figures 4a to 4j (see Figure 3 for wall indentifications). Dimensions and elevations are given in both full-scale feet and model inches.

In order to determine the forces and moments on the Space Shuttle, two separate strain gage balances were used: One, a two-component force balance with a range of 0.02 to 3 lbs in both orthogonal directions (Figures 5a and 5b); the other, a three-component moment balance with a range of 0.01 to 20 inch-lb (Figures 6a and 6b). Each was separately set in position below the tunnel floor in a layout similar to that of the six-component force balance (Figure 2). The model of the orbiter and external tanks was mounted on an aluminum base plate located below the tunnel floor. The base plate was securely fixed to either the two-component force balance or the three-component moment balance. As with the MST building, the different Space Shuttle configurations were viscously damped by sets of brass or Plexiglas fins (Figures 5 and 6). The damping system worked satisfactorily and did not affect the magnitude of the mean forces and moments.

2.3 Test Configurations

For the force and moment measurements on the MST building, measurements were made for six different configurations and five different angles of wind approach (see Figure 3 for coordinate system). This is a total of thirty individual runs. The configurations are shown in Figures 7a to 7f.

Table a
MST Configurations vs. Wind Angle

Configuration	Angle of Wind
1	90, 135, 180, 225, 270
1A	"
2	"
3	"
4	"
5	"

For the force and moment measurements on the Space Shuttle, measurements were made for six different configurations and five different angles of wind approach.

Table b
SSV Configurations vs. Wind Angle

Configuration	Angle of Wind
A	90, 135, 180, 225, 270
B	"
C	"
E-2	"
$E\text{-}2_2$	"
D-2	"

These configurations are depicted in Figures 8a to 8f. All configurations requiring an MST model used configuration 5 of the MST.

The pressure measurements on the MST were done on the 272 ft high building with the sides fully clad and identical to configuration 5 of Table a (Figure 7f). A photograph of the pressure model is shown in Figures 4g and 4h.

2.4 Experimental Arrangement

The models were mounted on a 12 ft diameter turntable centered 45 ft downstream from the test section. The turntable was calibrated to indicate azimuthal orientation to 0.3 degrees. The region upstream from the model was covered with 1/4 in. thick pegboard with 1/4 in. diameter, 1/2 in. long wooden pegs inserted to form a pattern of roughness which would produce the desired approach flow. Spires were installed at the test section entrance to provide a thicker boundary layer than would otherwise be available. The spries were approximately triangularly shaped

pieces of 1/2 in. thick plywood 6 in. wide at the base and 1 in. wide at the top, extending from the floor to the top of the test section. They were placed so that the broad side intercepted the flow. Splitter plates, triangular in cross-section and made to fit the shape of the spires, were placed downstream from, but in contact with, the spires to form streamlined obstructions in the airflow path. An additional flow trip consisting of 7 in. high bricks standing on end spaced approximately at 1 ft was placed 8 ft upstream of the spires in the intake transition section. This combination of spires and trip provided a boundary layer thickness of approximately 4 ft and an approach velocity profile power-law exponent similar to that for flow over smooth terrain. A photograph of the MST building in the tunnel is shown in Figure 7g.

Velocity profiles were taken at 4 locations as shown in Figures 10, 11 and 12. These 4 velocity profiles were taken to define the approach flow in the absence of buildings.

Velocity measurements were made at 6 strategic locations as indicated in Figure 9. These were taken to discern the flow velocity behavior in the vicinity of the SSV complex.

3. INSTRUMENTATION AND DATA ACQUISITION

3.1 Flow Visualization

Making the airflow visible in and around the different models is helpful in defining areas of high or low velocity, flow channeling or other flow characteristics which may increase or decrease loading. Titanium tetrachloride smoke was released from sources on and near the model to make the flow lines visible to the eye and to make it possible to obtain motion picture records of the tests. A guide to the motion picture scenes is given in Table c. Results of these smoke studies are discussed in Section 4.1 and the conclusions stated in Section 5.1.

3.2 Velocity Profiles

Mean velocity and turbulence intensity profiles were measured upstream of the model to determine the characteristics of the approach wind. Measurements were also taken at the center of the turntable and the profile data is shown in Figures 10, 11 and 12.

Velocity measurements were made with a single hot-wire anemometer. The probe was mounted with its axis horizontal and was supported from a vertical traverse which was positioned behind the model so as not to create a disturbance near the model. The instrumentation used was a Thermo Systems constant temperature anemometer (model 1050) with a .001 in. diameter platinum film sensing element .02 in. long. Output from the anemometer was fed to an on-line data acquisition system, consisting of a Hewlett-Packard 21 MX computer, disc unit, card reader, printer, Digi-Data digital tape drive and a Preston Scientific analog to digital converter. The data was processed immediately into mean velocities, turbulence intensities and corresponding heights and stored on a computer disc for printout and further analysis.

Calibration of the hot-wire was performed using a Thermo Systems Calibrator (Model 1125). The calibration data were fit to a variable exponent King's Law relationship,

$$E^2 = A + BU^n$$

where E is the hot-wire output voltage, U the approach velocity and A, B and n are effective coefficients selected to fit the data. The above relationship was used to determine the mean velocity at measurement points using the measured mean voltage data. The fluctuating velocity in the form U_{rms} (root-mean square velocity) was obtained from

$$U_{rms} = \frac{2E\ E_{rms}}{BnU^{n-1}}$$

where E_{rms} is the root-mean square voltage output from the anemometer. The turbulence intensity is then the ratio U_{rms}/U_H.

3.3 Force and Moment Measurements

For the force and moment measurements of the MST building an Inca six-component strain gage balance was used. Wind forces and moments were measured in the X, Y and Z directions in a coordinate system fixed to the MST building as shown in Figure 3. The force F_Z was not recorded. Each strain-gage bridge of the Inca balance was monitored by a Honeywell Acudata 118 gage control/amplifier unit for signal conditioning. These units are characterized by a very stable excitation voltage and amplifier gain. Output from the Honeywell signal conditioners was fed to an on-line, analog to digital conversion unit. Calibration of the balance was accomplished in a test rig in which known forces and moments could be applied to the balance. From static (weight-over-pulley) calibration results a calibration matrix was developed for reducing the mean output of the strain gages. Load and

strain relationship is strictly linear for the range of loads applied in these tests. The balance capacity is 50 lbs force and 300 in.-lbs moment. Values measured during the MST tests were 4.33 lbs maximum force and 103 in.-lbs maximum moment (the latter corrected to floor level).

For the force measurements on the Space Shuttle a two-component force balance with a range of 0.02 to 3 lbs, was used. This recorded the forces in two orthogonal directions, i.e. F_y and F_x (or drag and lateral forces respectively). This balance is shown in Figures 5a to 5c. The balance measures accurately the total drag and the total lateral force on the Space Shuttle regarless of where the resultant of the drag or lift force is applied. The balance is, of course, a two-dimensional instrument but the mathematical verification is most simply explained by considering only the drag measuring section. That is, consider the balance is one-dimensional. Because of minute interactions between F_x and F_y the following proof is valid.

Figure 5d shows a constant resultant force applied at a position, ℓ, on a stiff rod which is inserted into the vertical receptical of the transducer. The force pushes the rod through a horizontal displacement, e. L is a constant, from level A to the bearings at level B. Consider ℓ as a variable, from level B to the resultant positon of the force. Two shearing forces, V_1 and V_2, and two restoring moments M_1 and M_2, are exerted on leg 1 and leg 2 respectively. T_{1A} is the tension in leg 1 and T_{2A} the compression in leg 2. W is the total weight of the instrument, considered as a concentrated load at the center.

Consider the free body diagram 1 shown in Figure 5e:

$$\Sigma F_x = 0 \tag{1}$$

then

$$F = P_1 + P_2 \tag{2}$$

and

$$\Sigma F_y = 0 \tag{3}$$

hence

$$W = T_{2B} - T_{1B} \tag{4}$$

Taking moments about hinge 1 gives:

$$\Sigma M_1 = 0 \tag{5}$$

then

$$T_{2B} = \frac{F\ell}{x} + \frac{W}{2} \tag{6}$$

thus

$$T_{1B} = \frac{F\ell}{x} - \frac{W}{2} \, . \tag{7}$$

Now consider the free body diagram 2 shown in Figure 5f:

$$e_1 = e_2 = e \tag{8}$$

from

$$\Sigma M_{A1} = 0 \tag{9}$$

$$M_1 = P_1 L - T_{1B} \, e \tag{10}$$

and

$$\Sigma M_{A2} = 0 \tag{11}$$

$$M_2 = P_2 L + T_{2B} \, e \, . \tag{12}$$

The total moment is

$$M_1 + M_2 = L\,(P_1 + P_2) + e\,(T_{2B} - T_{1B}) \tag{13}$$

or

$$M_1 + M_2 = LF + eW \tag{14}$$

but,

$L >> e$ and $F \simeq 0(w)$, therefore $LF >> eW$

thus,

$$M_1 + M_2 \tilde{=} LF. \tag{15}$$

From Equation (15), the conclusion can be drawn that the total moment depends only on the constant resultant force F and the constant distance L.

The above results were verified experimentally for F ranging from 0.1 lbs to 3 lbs and for ℓ ranging from 2 to 18 inches. Figure 5g is the calibration curve which was obtained by applying the various loads at one position of the stiff rod. The response did not change when the load was shifted to another position on the rod. Figure 5a shows the balance ready to be set in place in the wind tunnel.

For the moment measurements on the Space Shuttle a three-component moment balance with a range of 0.01 to 20 in.-lb was used. The balance measured the M_x, M_y, M_z moments. It is shown in Figures 6a to 6b. The mathematical proof of this instrument is related to the proof already given for the two-component force balance. As in the case of the force balance the operation of the moment balance was verified experimentally. Figure 6d is a plot of the calibration of the three quantities M_x, M_y and M_z. It is noted from these that each strain gage system (e.g., M_x)

were different, due to different stiffness for each component sense. It was also verified that the interactions between each of the three channels were minute.

In both the force and moment balances, it was found effective to install damping mechanisms. As in the six component inca-balance the damping system worked satisfactorily and did not affect the magnitude of the mean forces and moments.

3.4 Pressures on the MST

Mean and fluctuating pressures were obtained at each of the 100 external pressure taps and 56 internal on the MST Plexiglas model. Data was obtained for 5 wind directions (90, 135, 280, 225, and 270 degrees). Figures 4h and 4j are pictorials of the MST pressure study building. The model was made of 1/4 in. Plexiglas with brass tubes 1/8 in. O.D. inserted in its walls in a vertical position and on the roof in a horizontal position. Each brass tube was drilled through at desired locations to give a pressure tap on both the inside and outside (when either was blocked off). Pressure tap locations are marked in black on the back wall of Figure 4j and are shown diagramatically in Figures 4a to 4g. The brass tubes were connected to plastic tubing which in turn were connected to a pressure switch mounted below the tunnel floor. The pressure switch has the capacity of working with 76 pressure taps, however in this case it was operated with a maximum of 16 (this number being the number of vertical brass tubes). The switch was designed and built in the Fluid Dynamics and Diffusion Laboratory to minimize the attenuation of pressure fluctuations across the switch. Each of the 16 pressure taps was directed in turn by the switch to one of four pressure transducers mounted close to the switch. Four pressure input taps used for transmitting building

surface pressures were connected to a common tube leading outside the wind tunnel. This arrangement provides both a means of performing in-place calibration of the transducers and, by connecting this tube to a pitot tube mounted inside the wind tunnel, a means of automatically monitoring the tunnel speed. The switch is operated by means of a shaft projecting through the floor of the wind tunnel. A computer-controlled stopping motor stepped the switch into each of the 5 required positions. The computer monitored switch position but a digital readout of position was also provided at the wind tunnel.

The pressure trasducers used are Statham differential strain gage transducers (Model PM 283TC) with a 0.15 psid range. They were selected because of their stability and linearity in the required working range. Reference pressures were obtained by connecting the reference sides of the four transducers, using plastic tubing, to the static side of a pitot tube mounted in the wind tunnel free stream above the model building. In this way the transducer measured the instantaneous difference between the local pressures on the surface of the building and the static pressure in the free stream above the model.

Each pressure transducer contains a built-in bridge similar to a Wheatstone Bridge. The bridge is monitored by a Honeywell Accudata 118 Gage Control/Amplifier unit which provides excitation to the transducer bridge and amplifies the bridge output. These instruments are characterized by a very stable excitation voltage and amplifier gain. Output from the Honeywell signal conditioners was fed to an on-line data acquisition system consisting of a Hewlett-Packard 21 MX computer, disc unit, card reader, printer, Digi-Data digital tape drive and a Preston Scientific analog-to-digital converter. The data were processed immediately into

pressure coefficient form as described in Section 4.5 and stored for printout or further analysis.

All four transducers were recorded simultaneously for 16 seconds at a 250 sample per second rate. The results of an experiment to determine the length of record required to obtain stable mean and rms (root-mean-square) pressures and to determine the overall accuracy of the pressure data acquisition system is shown in Figure 4k. A typical pressure port record was integrated for a number of different time periods to obtain the data shown. Examination of a large number of pressure taps showed that the overall accuracy for a 16 second period was, in pressure coefficient form, 0.03 for mean pressures, 0.1 for peak pressures, and 0.01 for rms pressures. Pressure coefficients are defined in Section 4.5. Because tube lengths required to reach the upper portions of the structure were longer than normally used with this data acquisition system, frequency attenuation in the pressure tubes may result in slight underestimation of peak local pressures on the upper third of the MST.

4. RESULTS

4.1 Flow Visualization

A film is included as part of this report showing the characteristics of flow about the structures using smoke to make the flow visible. A listing of the contents of the film is shown in Table c.

Table c

MOTION PICTURE SCENE GUIDE

Run #	SSV Configuration	Wind Direction
1	A	90°
2	B	90°
3	C	90°
4	$E\text{-}2_2$	90°
5	A	135°
6	B	135°
7	C	135°
8	$E\text{-}2_2$	135°
9	A	180°
10	B	180°
11	C	180°
12	$E\text{-}2_2$	180°
13	A	225°
14	B	225°
15	C	225°
16	$E\text{-}2_2$	225°
17	A	270°
18	B	270°
19	C	270°
20	$E\text{-}2_2$	270°

Length = 1085 ft
Running time = 30 min

4.2 Velocity Profiles

Velocity and turbulence profiles are shown in Figures 11 and 12. These profiles were taken upstream from the model and are characteristic of the boundary-layer approaching the model. As shown in Figure 11, the boundary-layer thickness, δ, was 50 in. The corresponding prototype value of δ for this study is 415 ft. Because of the complex terrain near the complex, the prototype value is not known, but this value was established as a reasonable height for this study. The mean velocity profile has the form

$$\frac{U}{U_\delta} = \left(\frac{z}{\delta}\right)^p \quad .$$

The exponent p for the approach flow established for this study is shown in Figure 11.

The profile of longitudinal turbulence intensity is shown in Figures 11 and 12. The turbulence intensities are appropriate for the approach mean velocity profile selected. For the purpose of this report, turbulence intensity is defined as the root-mean-square about the mean of the longitudinal velocity fluctuations divided by the reference mean velocity U_H at the top of the building

$$Tu = \frac{U_{rms}}{U_H} \quad .$$

Mean velocity U/U_H, turbulence intensity U_{rms}/U_H, and largest effective gust at strategic measuring positions shown in Figure 9 were obtained to show velocity magnitudes near the SSV with MST and PCR in place. The 'peak' velocity representing roughly the largest effective gust velocity was calculated using:

$$U_{pk} = \frac{U + 3U_{rms}}{U_H} \quad .$$

A discussion of these values is given in Section 5.2 while data are listed in Tabe 4 for 5 wind directions.

4.3 Forces and Moments on MST

The computer output in Appendix A shows the forces and moments experienced by the model. The corresponding coefficients are with respect to a dynamic pressure of $1/2\ \rho U_{30}^2$ where U_{30} is the velocity at 30 ft in the full-scale. All coefficients are with respect to the pertinent wall areas and model dimensions used for each configuration.

The nondimensional coefficients pertinent to the MST study are defined in Table d.

Table d
Definition of MST Force and Moment Coefficients

$$C_{F_x} = F_x/q_{30}WH$$

$$C_{F_y} = F_y/q_{30}LH$$

$$C_{M_x} = M_x/q_{30}LH^2$$

$$C_{M_y} = M_y/q_{30}WH^2$$

$$C_{M_z} = M_z/q_{30}LH^2$$

$$q_{30} = 1/2\ \rho U_{30}^2$$

The following is a list of values used in the model tests.

U_H = 29.49 ft/sec (velocity at the top of building)

U_{30} = 0.69 U_H = 20.38 ft/sec

q_{30} = $1/2\ \rho U_{30}^2$ = 0.415 lb/ft^2

W = 9.9 in.
H = 37.8 in.
L = 16.26 in.

} model values Configurations 1 to 4

W = 9.9 in.
H = 33.0 in.
L = 16.26 in.

} model values Configuration 5

The only difference to the values for configurations 1 to 4 and 5 is the height:

H = 33.0 in.

Note that for all MST load measurements, U_H was

$U_H = U_{37.8}$

i.e., the height at which the pitot tube was placed in the wind tunnel and was held constant for the duration of the MST experiments (including configuration 5).

Sample calculations are included in the following pages.

AIR DENSITY

The density of air is dependent on the barometric pressure and temperature. It may be evaluated using the following relationship:

$$\text{Density} = \frac{\text{Barometric pressure in inches}}{(\text{Absolute temp}) \times 24.29697} \quad : \text{slugs/ft}^3$$

Absolute temp = temperature in °F + 459.69

SAMPLE FORCE AND MOMENT CALCULATIONS

The following example is used to explain the procedure for calculating full scale the forces and moments on the MST. Assume the following conditions at the site:

Temperature = 60°F

Barometric pressure = 30.3 in.

Wind speed at 30 ft = 80 mph = 117.3 ft/sec

Density $= \frac{30.3}{519.69 \times 24.297} = 0.0024$ slugs/ft^3

Building Dimensions: (full-scale)

H = 315 ft (ground level to roof level)

W = 82.5 ft (narrow side of building)

L = 135.5 ft (large side of building)

Configuration 1: wind approach angle 90°

Question--

What are the along wind force and the along wind overturning moment?

Step 1: F_y = ? (along wind force)

M_x = ? (along wind moment)

Step 2: $F_y = C_{F_y} q_{30} L H$

$M_x = C_{M_x} q_{30} L H^2$

Step 3: Dynamic pressure q_{30} = ?

$q_{30} = 1/2 \rho U_{30}^2$

$q_{30} = 1/2 \times 0.0024 \times 117.3^2 = 16.51$ lbs/ft^2

Step 4: $F_y = C_{F_y} q_{30} L H$

Computer output, Appendix A, read $C_{F_y} = 2.25$

$F_y = 2.25 \times 16.51 \times 135.5 \times 315 = 1.5856 \times 10^6$ lbs

$= 1585.6$ kips

Step 5: $M_x = C_{M_y} q_{30} L H^2$

Computer output, Appendix A, read $C_{M_x} = -1.04$

$M_x = -1.04 \times 16.51 \times 135.5 \times 315^2 = -230.9 \times 10^3$ kip-ft

4.4 Forces and Moments on the S.S.V.

The forces and moments measured on the six configurations pertinent to the SSV are shown in Table 2. The corresponding coefficients are with respect to the dynamic pressure of $1/2\ \rho U_{30}^2$ (as in the MST study) where U_{30} is the velocity at 30 ft, in the full scale. The coefficients are based on the reference lengths and areas respective to the particular configuration. The nondimensional coefficients pertinent to the SSV study are shown in Table e.

Table e
Definition of SSV Force and Moment Coefficients

$$C_{F_x} = \frac{F_x}{q_{30}A_i}$$

$$C_{F_y} = \frac{F_y}{q_{30}A_i}$$

$$C_{M_x} = \frac{M_x}{q_{30}A_iH_i}$$

$$C_{M_y} = \frac{M_y}{q_{30}A_iH_i}$$

$$C_{M_z} = \frac{M_z}{q_{30}A_iB_i}$$

A_iH_i and B_i for the respective configurations are given on the following page.

$i = 1$, 2 or 3.

The H_i value is measured from the top of the launch-mount.

The following is a list of values estimated from the model and their corresponding full-scale values (the latter not necessarily the exact values).

$U_{3.6\ in.}$ (model) = U_{30} (full-scale) = 20.38 ft/sec

$q_{30} = 1/2\ \rho U_{30}^2 = .415\ lbs/ft^2$

$A_1 = 116.2\ in^2$ $H_1 = 20\ in$ $B_1 = 1.5\ in$	model values configurations A,B,C,E-22	$A_1 = 8069.4\ ft^2$ $H_1 = 166.6\ ft$ $B_1 = 12.5\ ft$	corresponding full-scale values
$A_2 = 37\ in^2$ $H_2 = 12\ in$ $B_2 = 1.5\ in$	model values configuration E-2 (orbiter only)	$A_2 = 2570\ ft^2$ $H_2 = 100\ ft$ $B_2 = 12.5\ ft$	corresponding full-scale values
$A_3 = 60\ in^2$ $H_3 = 20\ in$ $B_3 = 1.5\ in$	model values configuration D-2 (tank only)	$A_3 = 4167\ ft^2$ $H_3 = 166.6\ ft$ $B_3 = 12.5\ ft$	corresponding full-scale values.

(See list of symbols for physical description of A_1, A_2, etc.)

During the experiments for load measurements on the SSV, the pitot tube was held at a constant height of 33.2 in. in the wind tunnel (i.e., at the MST building height). During data analysis this reference height velocity was converted to $U_{3.6\ in.}$ (i.e., U_{30} full-scale). The reason for this is that a better resolution of velocity is obtained near the free stream, which was at about 50 in. in the wind tunnel.

The procedure for calculating the full-scale forces and moments is similar to the example given in Section 4.3.

SAMPLE FORCE AND MOMENT CALCULATIONS - SSV

The following is an example used to explain the procedure of calculating the full-scale forces and moments on the SSV from the

force and moment coefficients of Table 2. Assume the following on-site conditions

Temperature = 60°F

Barometric pressure = 30.3 in.

Wind speed at 30 ft = 20 knots = 33.8 ft/sec

Density of air = $\frac{30.3}{519.69 \times 24.297}$ = .0024 slugs/ft^3

Question: Determine the drag force F_y and the corresponding moment M_x for configuration C at a wind angle of 225°. Also determine the force F_x and the corresponding moment M_y. Finally determine the torsional moment M_z for the same configuration and wind angle.

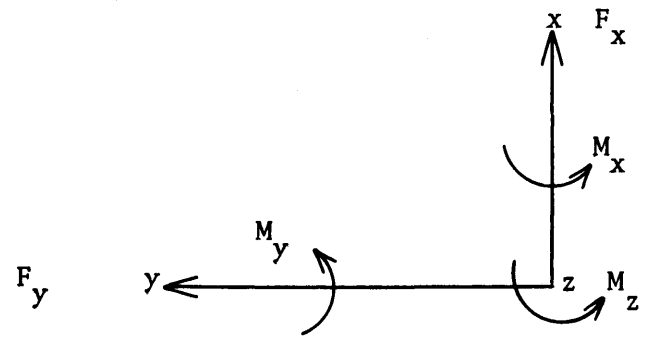

Right Hand Coordinate System

Note: $+F_x$ causes $+M_y$

$+F_y$ causes $-M_x$.

} true because F_x and F_y are applied physically above the x and y axes.

Structure Dimensions (full scale)

A = 8069.4 ft^2 (projected frontal area of orbiter & tank and boosters)

H = 166.6 ft (height from top of launch pad to top of external tank)

B = 12.3 ft (radius of external tank)

Determine: $F_x = ?$

$F_y = ?$

$M_x = ?$

$M_y = ?$

$M_x = ?$

Step 1. From Table 2.

Config.	Wind Angle	C_{F_x}	C_{F_y}	C_{M_x}	C_{M_y}	C_{M_z}
C	225°	-.93	-.80	.46	-.49	.45

Step 2. From Table e,

$$F_x = C_{F_x}\, q_{30}\, A$$

$$F_y = C_{F_y}\, q_{30}\, A$$

$$M_x = C_{M_x}\, q_{30}\, AH$$

$$M_y = C_{M_y}\, q_{30}\, AH$$

$$M_z = C_{M_z}\, q_{30}\, AB$$

Step 3. q_{30} = dynamic pressure at 30 ft

$$= 1/2\ \rho\ U_{30}^2$$

$$= 1/2 \times .0024 \times (33.8)^2 = 1.370\ \text{lb/ft}^2$$

Step 4.

$$F_x = C_{F_x}\, q_{30}\, A$$

$$= -.93 \times 1.370 \times 8069.4 = -10281\ \text{lbs}$$

$$= -10.281\ \text{kips}$$

$$F_y = C_{F_y} q_{30} A$$

$$= -.80 \times 1.37 \times 8069.4 = -8844 \text{ lbs}$$
$$= -8.84 \text{ kips}$$

$$M_x = C_{M_x} q_{30} AH$$

$$= .46 \times 1.37 \times 8069.4 \times 166.6 = 847217 \text{ ft-lbs}$$
$$= 847.22 \text{ ft-kips}$$

$$M_y = C_{M_y} q_{30} AH$$

$$= -.49 \times 1.37 \times 8069.4 \times 166.6 = -902470 \text{ ft-lbs}$$
$$= -902.47 \text{ ft-kips}$$

$$M_z = C_{M_z} q_{30} AB$$

$$= .45 \times 1.37 \times 8069.4 \times 12.5 = 62185.0 \text{ ft-lbs}$$
$$= 62.185 \text{ ft-kips}$$

It is emphasized that the characteristic areas and lengths are those values measured from the model and then scaled to those of full scale.

4.5 Pressures on the MST

For each of the pressure taps examined at each wind direction, the data record was analyzed to obtain four separate pressure coefficients. The first is the mean pressure coefficient $C_{p_{mean}} = (p - p_{30})_{mean}$ where the symbols $0.5 \rho U_{30}^2$ are defined in the List of Symbols. It represents the mean of the instantaneous pressure difference between the building pressure tap and the static pressure in the wind tunnel above the building model, nondimensionalized by the dynamic pressure

$$0.5 \rho U_{30}^2$$

at the reference velocity position. This relationship produces a dimensionless coefficient which indicates that the mean pressure

difference between building and ambient wind at a given point on the structure is some fraction less or some fraction greater than the dynamic pressure at the 30 ft height in full-scale. Using the measured coefficient, prototype mean pressure values for any wind velocity may then be calculated.

The magnitude of the fluctuating pressure is obtained by the rms pressure coefficient

$$C_{p_{rms}} = \frac{\left((p-p_{30}) - (p-p_{30})_{mean}\right)_{rms}}{0.5\ \rho\ U_{30}^{2}}$$

in which the numerator is the root-mean-square of the instantaneous pressure difference about the mean.

If the pressure fluctuations followed a Gaussian probability distribution, no additional data would be required to predict the frequency with which any given pressure level would be observed. However, the pressure fluctuations do not follow a Gaussian probability distribution so that additional information is required to show the extreme values of pressure expected. The peak maximum and peak minimum pressure coefficients are used to determine these values:

$$C_{p_{max}} = \frac{(p-p_{30})_{max}}{0.5\ \rho\ U_{30}^{2}}$$

$$C_{p_{min}} = \frac{(p-p_{30})_{min}}{0.5\ \rho\ U_{30}^{2}}$$

The values of $p-p_{30}$ which were digitized at 250 samples per second for 16 seconds, representing about one hour of time in the full-scale, are examined individually by the computer to obtain the most positive and

most negative values during the 16 second period. These are converted to $C_{p_{max}}$ and $C_{p_{min}}$ by nondimensionalizing with the 30 ft (full-scale) dynamic pressure.

The four pressure coefficients are calculated by the on-line data acquisition system computer and tabulated along with the approach wind azimuth in degrees from true north. The list of coefficients is included as Appendix B. The pressure tap code numbers used in the appendix are explained in Figures 4a to 4g.

To determine the largest peak loads acting at any point on the structure for cladding design purposes, the pressure coefficients for all wind directions were searched to obtain, at each pressure tap, the largest absolute value of peak pressure coefficient. Table 1 provides these pressure coefficients and associated wind directions. Included in Section 5.5 is an analysis of the coefficients of Table 1 including the maximum values obtained and where they occurred on the building. Because pressure differences across the shell were not measured simultaneously, peak pressures were not likely obtained at taps on opposite sides of the shell simultaneously. For this reason, peak pressures should be used with some care.

The pressure coefficients of Table 1 can be converted to full-scale loads by multiplication by a suitable reference pressure selected for the field site. This reference pressure is represented in the equations for pressure coefficients by the $0.5\ \rho\ U_{30}^2$ denominator. This value is the dynamic pressure associated with an hourly mean wind at the reference velocity measurement position at 30 ft elevation. In general, the method of arriving at a design reference pressure for a particular

site involves selection of a design wind velocity, translation of the velocity to an hourly mean wind at the reference velocity location and conversion to a reference pressure. Selection of the design velocity can be made from statistical analysis of extreme wind data obtained at the site or selected from wind maps contained in the proposed wind loading code ANSI A58.1 of the American National Standards Institute (4). Gust factors to reduce gust winds to hourly mean winds is given in reference (5).

The reference pressure associated with the design hourly mean velocity at the reference velocity location can be used directly with the pressure coefficients to obtain mean and peak local wind loads for cladding design.

Local, instantaneous peak loads on the full-scale MST are obtained by multiplying the reference pressure by the peak coefficients of Table 1. The maximum psf load given at each tap location is the absolute value of the maximum value found in the tests, irrespective of its algebraic sign. For ease in visualizing the loads on the structure, contours of equal peak pressure coefficient shown in Table 1 have been plotted on developed elevation views of the structure, Figures 41 to 4s. It should be noted that coefficients shown in Figures 41 to 4s on inside and outside portions of a given panel are not developed simultaneously.

5. DISCUSSION

5.1 Flow Visualization

Flow visualization patterns on the six SSV configurations showed that flow separation characteristics near the corners of the structures might produce moderately high suctions near the corners.

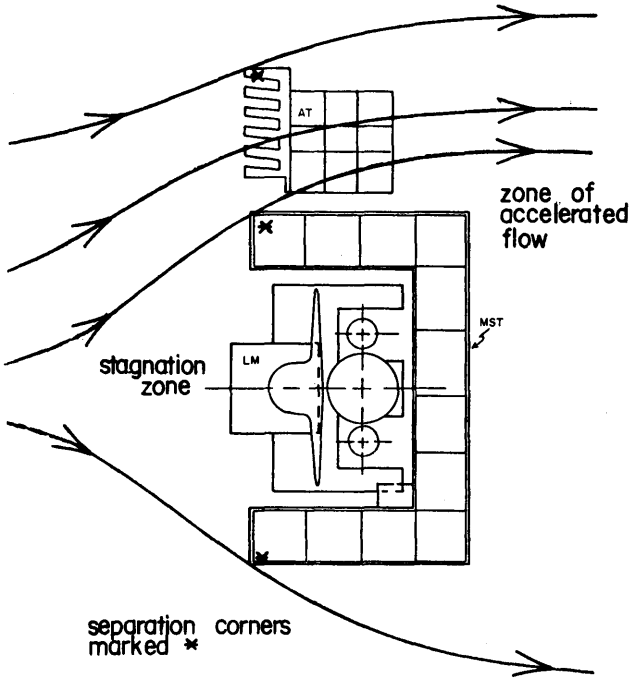

For a wind angle of 270° on configuration A the flow patterns, sketched above indicate that the MST creates a stagnation zone in front of the SSV and it appears that the MST behaves essentially as if all its walls were solid. This observation is borne out in the results shown in Table 2 indicating very low forces and moments on the SSV. It is also noted in the flow visualization movie that again for a 270° wind and configurations A, E and D it appears that there are high velocity zones between the top of the PCR building and the roof of the MST allowing this accelerated flow to bear down on the top of the external tank as shown on next page.

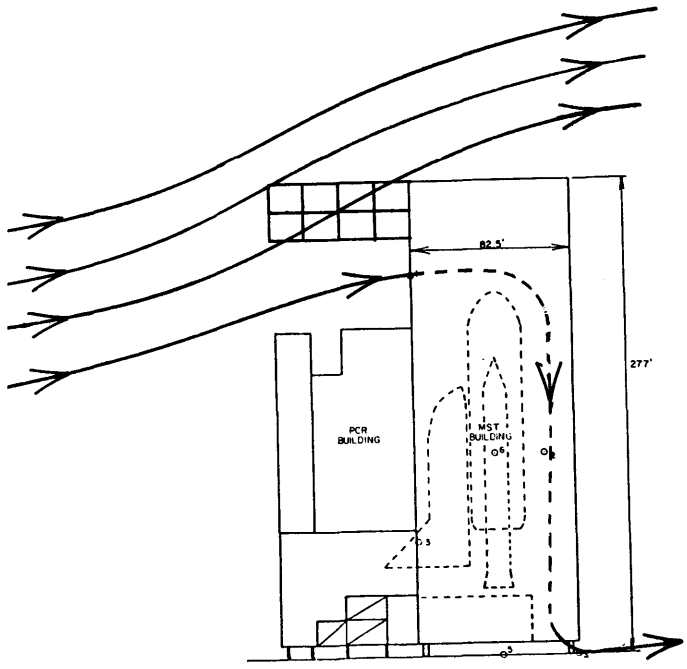

High negative pressures are noticeable on the roof where the flow separates at the roof corners. Wind flow patterns near the base of the structures showed higher velocities due to openings in the MST than would be expected if these openings did exist. It was clearly noticeable that the flow structure was strongly three-dimensional in nature and does not lend itself to simple explanations. It was observed that vortices were shed from the

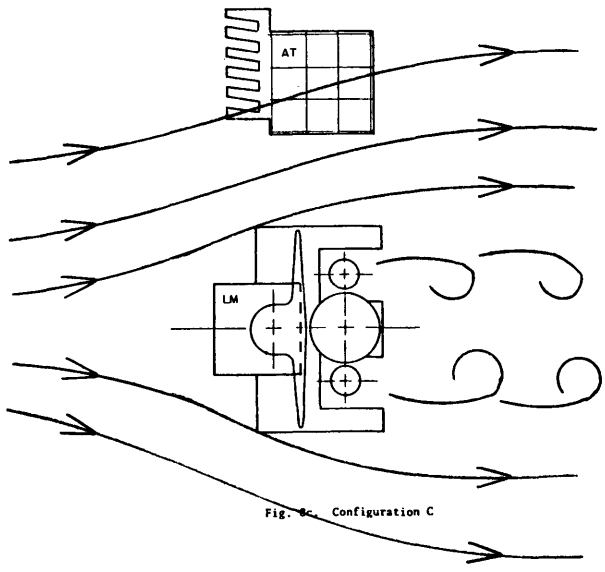

Fig. 8c. Configuration C

wings of the SSV and also from the tanks in configuration C. This phenomenon appeared to occur at most wind directions between 180° and 270°.

5.2 Velocity Profiles

Table 3 gives the ratios of the mean, rms and peak wind velocities to the mean velocity at the top of the MST expressed as percentages. Six different locations were studied and measurements at each location were made for both a horizontal and vertical orientation of the measuring sensor axis. The sensor measures the magnitude of velocity vector component perpendicular to the sensor axis. Thus, in the horizontal mode (axis parallel to the x axis) the sensor measured the velocity component in the y-z plane, while in the vertical mode (axis parallel to the vertical axis) the sensor measured the velocity component in the x-y plane the horizontal velocity component. For brevity. the data are referred to as horizontal component data (sensor axis vertical) or as vertical component data (sensor axis horizontal). The measurement locations are shown in Figure 9. Location 1 its highest U_{mean}/U_H horizontal component from a 225° wind. Flow visualization observations indicated accelerated flow in this area. In magnitude, its value was 85 percent which means it is close to the value of U_H. The turbulence magnitudes for the horizontal component were about 8 percent for all wind directions indicating that the turbulence in this location is not dominant. Location 2 showed higher vertical than horizontal components of mean velocity. Location 4, situated close to the ground in the opening on the main wall of the MST indicated a very high velocity component in the y-z plane. This is commensurate with dominant vertical components at location 2. The highest turbulent intensities are experienced at

location 5 for a 270° wind. Location 5 is in the opening on the side wall of the MST and the vertical fluctuating component is up to 24 percent.

5.3 Forces and Moments on the MST

Appendix A contains the force and moment coefficients on the MST in isolation. For configuration 1 the highest coefficient is C_{F_y} for a wind direction of 270°. This magnitude is 2.36 compared with the corresponding magnitude of 2.25 for the 90° wind. The small difference in these values indicates that the total drag on the MST is almost the same whether the incident wind is onto the solid back face or into the front cavity face. These two "drag" coefficients have appreciably different magnitudes of moment coefficients (1.48 and 1.04 for 270° and 90° winds). This is due to differing heights of the center of action of the drag force on the MST caused by different geometry of the respective face.

Configuration 1A has the overhang sides and top covered. It is noticed that this does not appear to make much different to either the lateral or the drag forces or their corresponding moments. It is believed, based on flow visualization studies, that this covering may have a more noticeable different on the uplift values which were not measured.

Configurations 1 and 5 are identical buildings except that 1 has a height of 315 ft and 5 has a height of 272 ft. A general comparison of the coefficients indicates somewhat lower values for configuration 5 even with the smaller value of H used in the coefficient. This can be explained by the fact that configuration 1 is 43 ft higher up into the boundary layer where the mean wind velocities are higher, consequently a higher velocity wind is acting at these higher elevations. It is also noticed that the trends of the values are very similar allowing for this smaller magnitude of values in configuration 5.

Some interesting observations are noticed in a study of the coefficients re' 'ing to configurations 2, 3 and 4. Configuration 2 does not have cladding on the perimeter of the top 43 ft. As is expected this should have reduced force and moment coefficients in comparison to configuration 1. The magnitudes are, in general, reduced by about 10 percent.

Configuration 3 has a 30 percent porous back wall and no cladding on the top 43 ft perimeter. As is expected, this dramatically reduces the drag (C_{F_y}) by about 30 percent for the significant wind directions of 90° and 270°. It is also noticed that for the quartering wind directions of 135° and 225° the lateral force (C_{F_y}) is increased by about 20 percent. This increase beyond that of configuration 1 may have the following explanation.

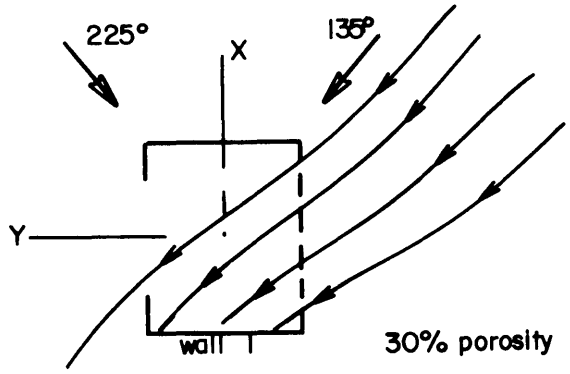

For the 135° wind direction in particular the wind can enter through the back wall cavities, into the interior of the building. Consequently more wind force is exerted on wall 1a. This build-up of internal pressures does not occur in configuration 4 where these side walls are also 30 percent porosity. For configuration 4 it appears that the drag (C_{F_y}) reduction over configuration 1 is about 20 percent. The corresponding lateral force (C_{F_x}) reduction however is not quite this large.

5.4 Pressures on the MST

Appendix B, shows the pressure data organized by wind direction for the tap locations shown in Figures 4a to 4g. Table 1 shows the largest peak pressure coefficients measured on the MST. The largest peak pressure coefficient was 6.56 measured at tap 1099 for a wind angle of 135°. This location is near the roof edge where the adjacent taps also have very high suction values due to the separated flow in these regions. Most peak wall pressures are moderate values of about 3.0 magnitude with few locations exceeding this value. It must be remembered that these pressure coefficients are to be used with the full-scale hourly mean velocity at 30 ft. From Table 1 and the contour peak pressure plots of Figures 41 to 4s, it can be seen for corresponding taps and walls that the internal magnitudes are generally less than the esternal magnitudes.

5.5 Forces and Moments on the SSV

The force and moment coefficients on the six configurations of the SSV are shown in Table 2. Figure 13 graphs the M_x and M_y model values measured for configuration E-2. This shows that the maximum M_x and M_y values are for 190° wind angle. These magnitudes are somewhat higher than the 180° values.

Table f contains comparative values of the model forces and moments for configurations E-2_2 and E-2. As is expected, configuration E-2_2 has higher values than those of E-2. This is due, of course, to the fact that E-2_2 are measurements on the orbiter and tanks connected and E-2 was on the orbiter only. The reduction appears to be about a third. Note that the ratios of coefficients shown in Table 2 do not reflect a true difference in loads because of differing values of A and H used in the two coefficients (see section 4.4).

COMPARISON OF MODEL VALUES FOR CONFIGURATIONS E-2_2 AND E-2

E-2_2 = measurements on shuttle and tanks
E-2 = measurements on shuttle only
} MST and PCR in place

Table f

Wind Angle	U_H	E-2_2					E-2				
	ft/sec	F_x lbs	F_y lbs	M_x in/lbs	M_y in/lbs	M_z in/lbs	F_x lbs	F_y lbs	M_x in/lbs	M_y in/lbs	M_z in/lbs
90	27	-.00	-.01	.09	-.07	.01	-.01	-.00	.02	.02	.00
135	27	.01	-.01	.13	.07	.00	.00	-.01	.06	-.06	.00
180	27	-.12	-.09	1.83	-2.09	.20	-.10	-.07	.78	-1.50	-.02
225	27	-.13	-.02	.08	-2.46	.21	-.09	.01	.15	-1.17	-.02
270	27	-.02	.06	-.52	-.33	.03	-.01	.06	-.80	-.11	.01

Note: these are values measured in the model studies with similar reference velocities

The highest values in Table 2 correspond to configuration C which is that for the orbiter and tanks not enclosed by the MST and PCR. The largest value is 1.55 for a wind angle of 90° and - 1.46 for a 270° wind.

Configurations A, B and E-2_2 (have similar reference areas and lengths to configuration C) indicate the significant protection that the surrounding MST and PCR give to the orbiter and tanks.

Configuration D-2 represents measurements on the external tank only without the orbiter in place. If there were no surrounding buildings and this tank was positioned in boundary layer flow, a drag coefficient of about 1.2 might be expected. However, due to the protection given the external tank by the surrounding buildings, Table 2 gives a maximum drag of 0.20.

The magnitude of coefficients in Table 2, for configuration E-2, seems high at a first glance. However, as inspection of these numbers and the corresponding reference area (the frontal projection of SSV only) sheds light. If there were no surrounding structures to inhibit the flow, the SSV on its own might behave in a manner not dissimilar to that of a two-dimensional flat plate (drag coefficient of 1.3). The area adjoining the wings and the body of the orbiter appear to receive much wind load, especially in the vicinity of quartering winds of 225°. The maximum drag (C_{F_y}) of -0.73 with corresponding lateral force (C_{F_x}) of -1.04, thus appears reasonable.

REFERENCES

1. Cermak, J. E. "Laboratory simulation of the Atmospheric Boundary Layer," AIAA J1., Vol. 9, Sept. 1971.

2. Cermak, J. E. "Application of Fluid Mechanics to Wind Engineering," A Freeman Scholar Lecture, ASME J1 of Fluid Engineering, Vol. 97, No. 1, March 1975.

3. Cermak, J. E. "Aerodynamics of Buildings," Annual Review of Fluid Mechanics, Vol. 8, pp. 75-106, 1976.

4. American National Standard Institute, "American National Standard Building Code Requirements for Minimum Design Loads in Buildings and Other Structures," ANSI Standard A58-1, 1972.

5. Velozzi, J. and Cohen, C., "Gust Response Factors," J1 Structural Div., ASCE, Proc. Paper No. 5980, Vol. 94, No. ST6, 1968.

FIGURES

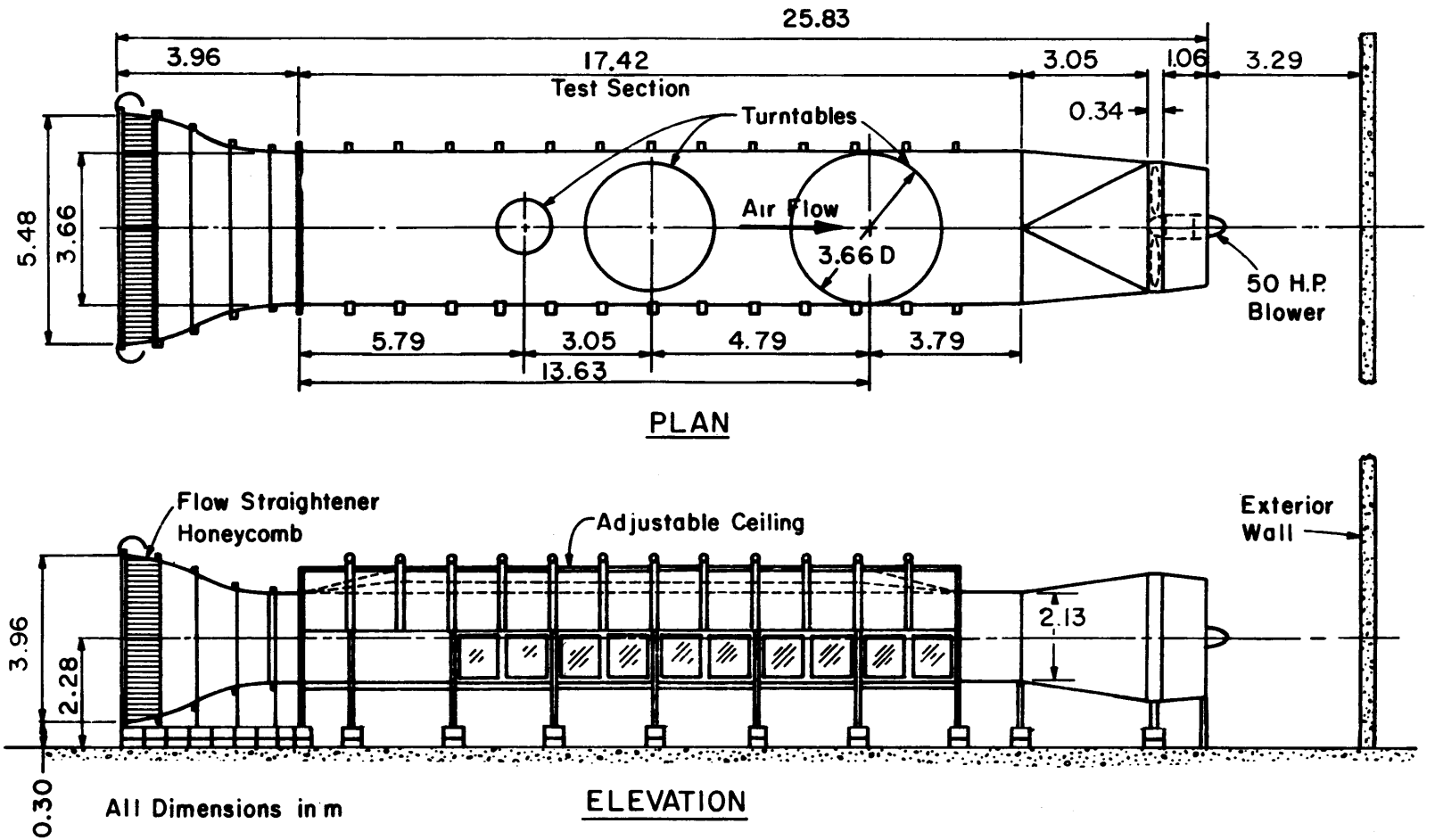

Figure 1. Environmental Wind Tunnel
Fluid Dynamics and Diffusion Laboratory
Colorado State University

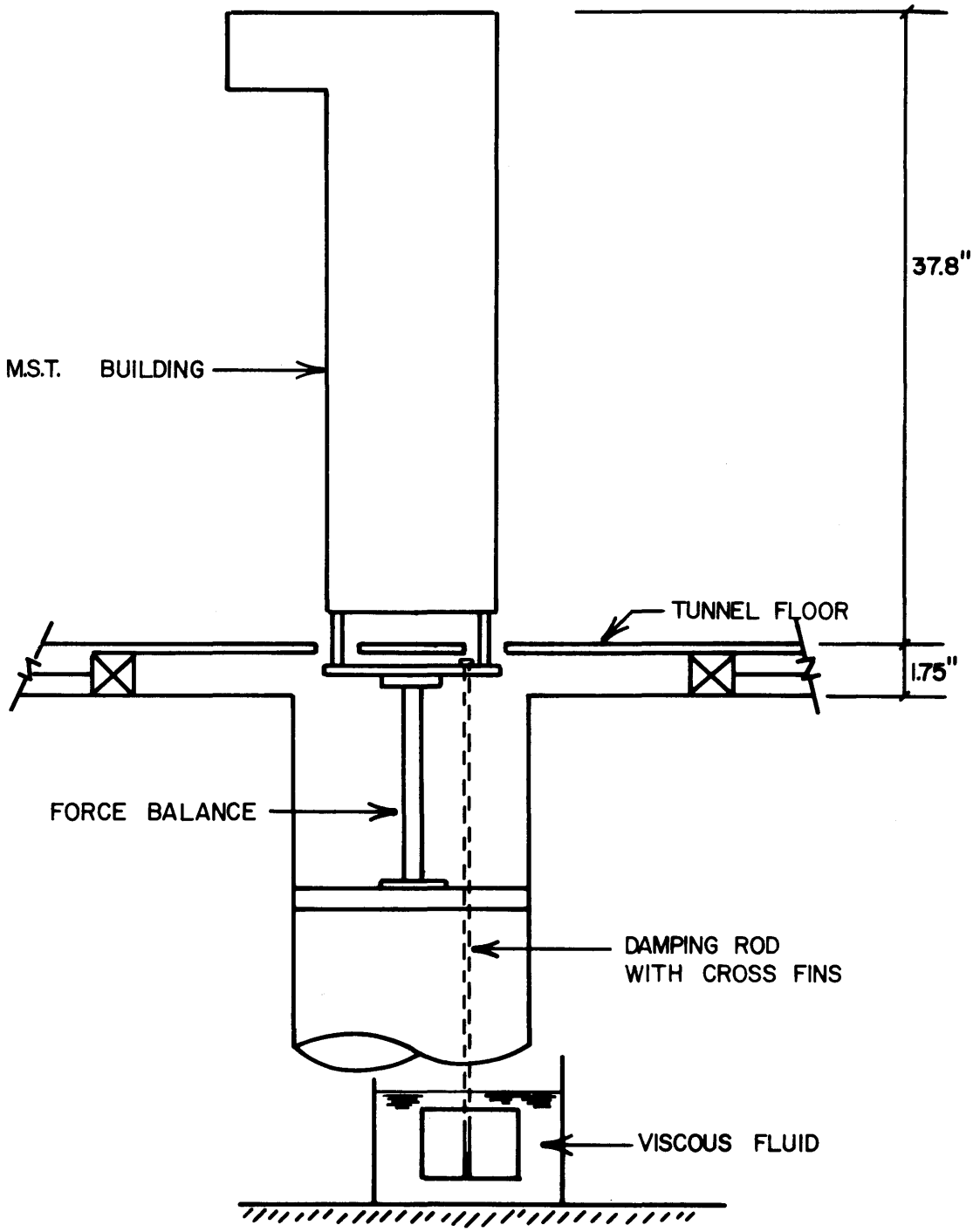

Figure 2. Tunnel Setup of MST

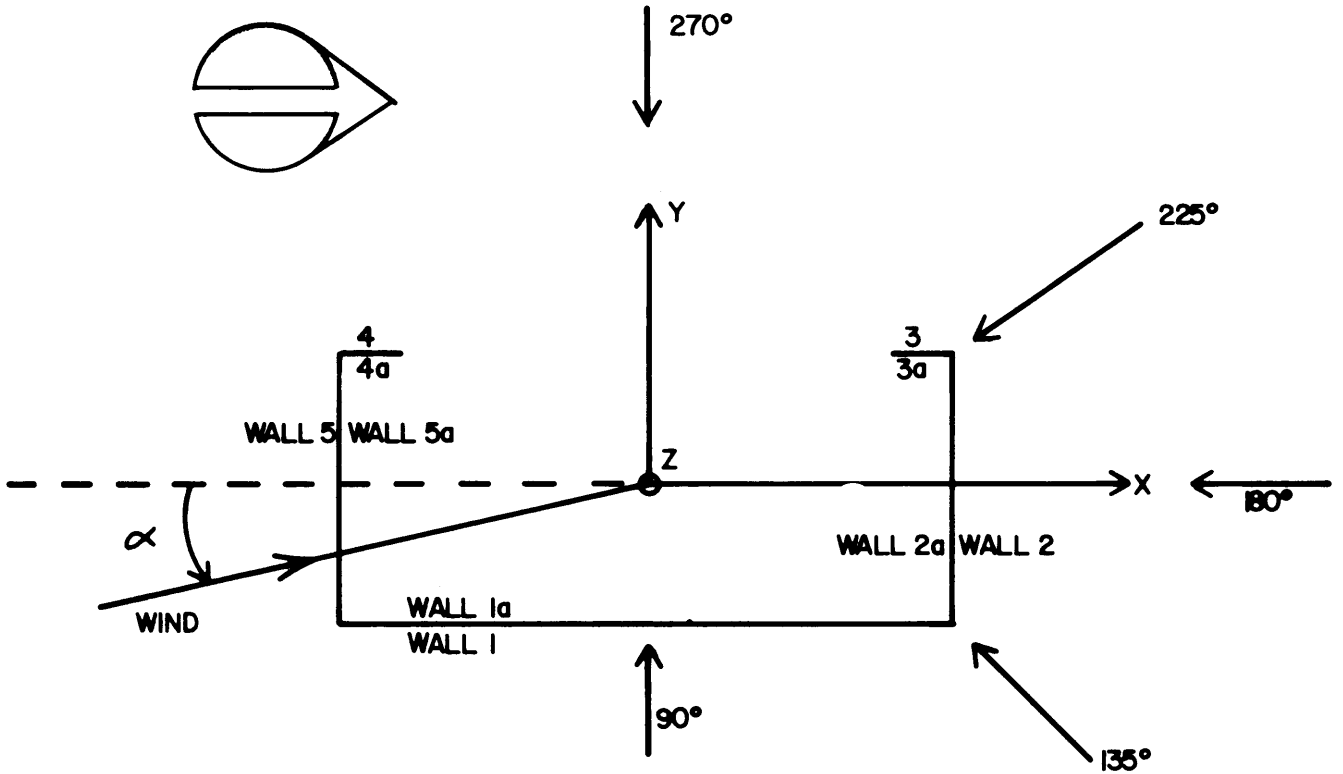

WIND ANGLE: α.

ORIGIN: MST--GROUND LEVEL
SSV--TOP OF LAUNCH MOUNT

MODEL SCALE - 1/100
TOTAL TAPS = 156

Figure 3. Coordinate System - MST

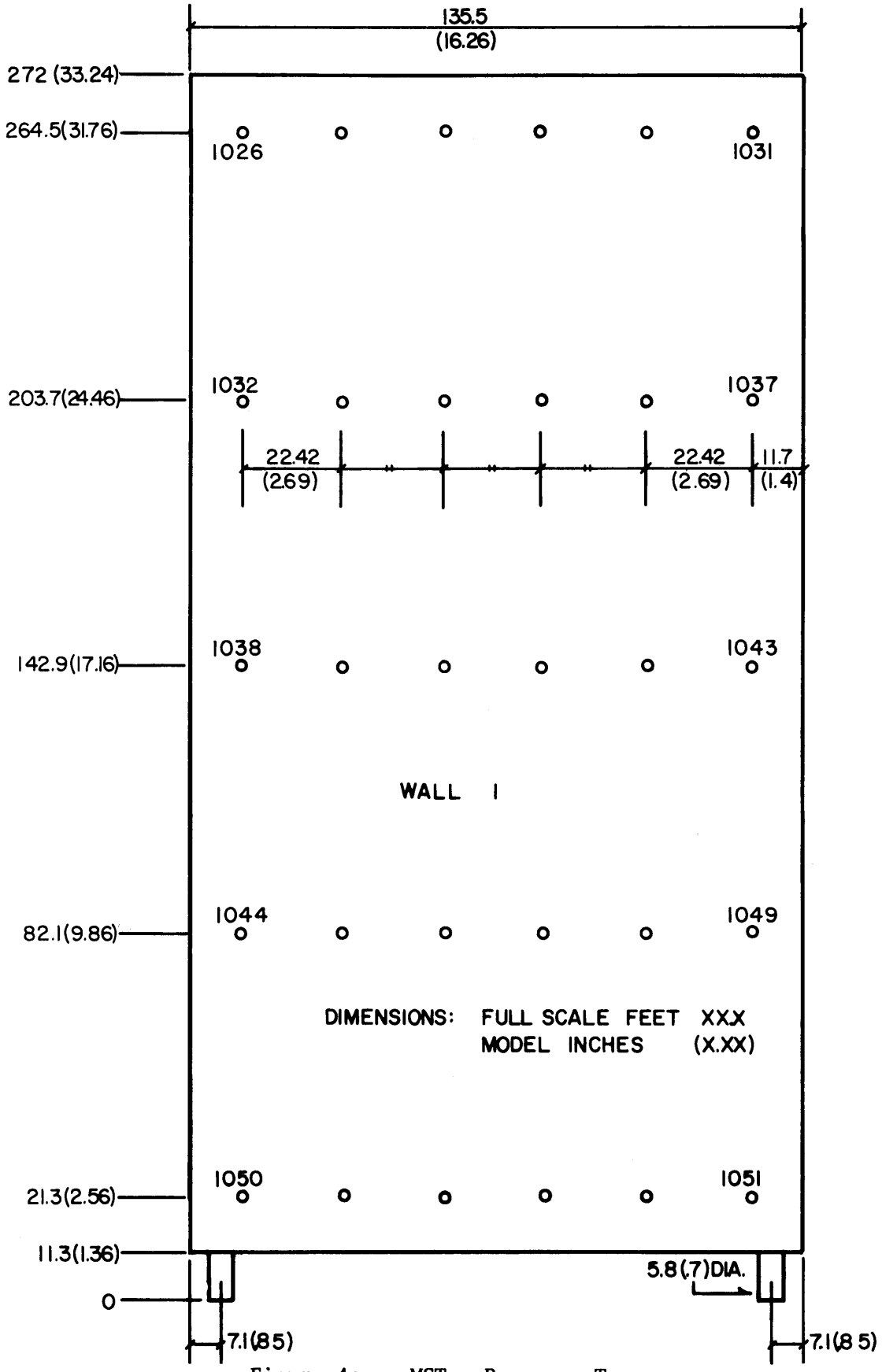

Figure 4a. MST - Pressure Taps

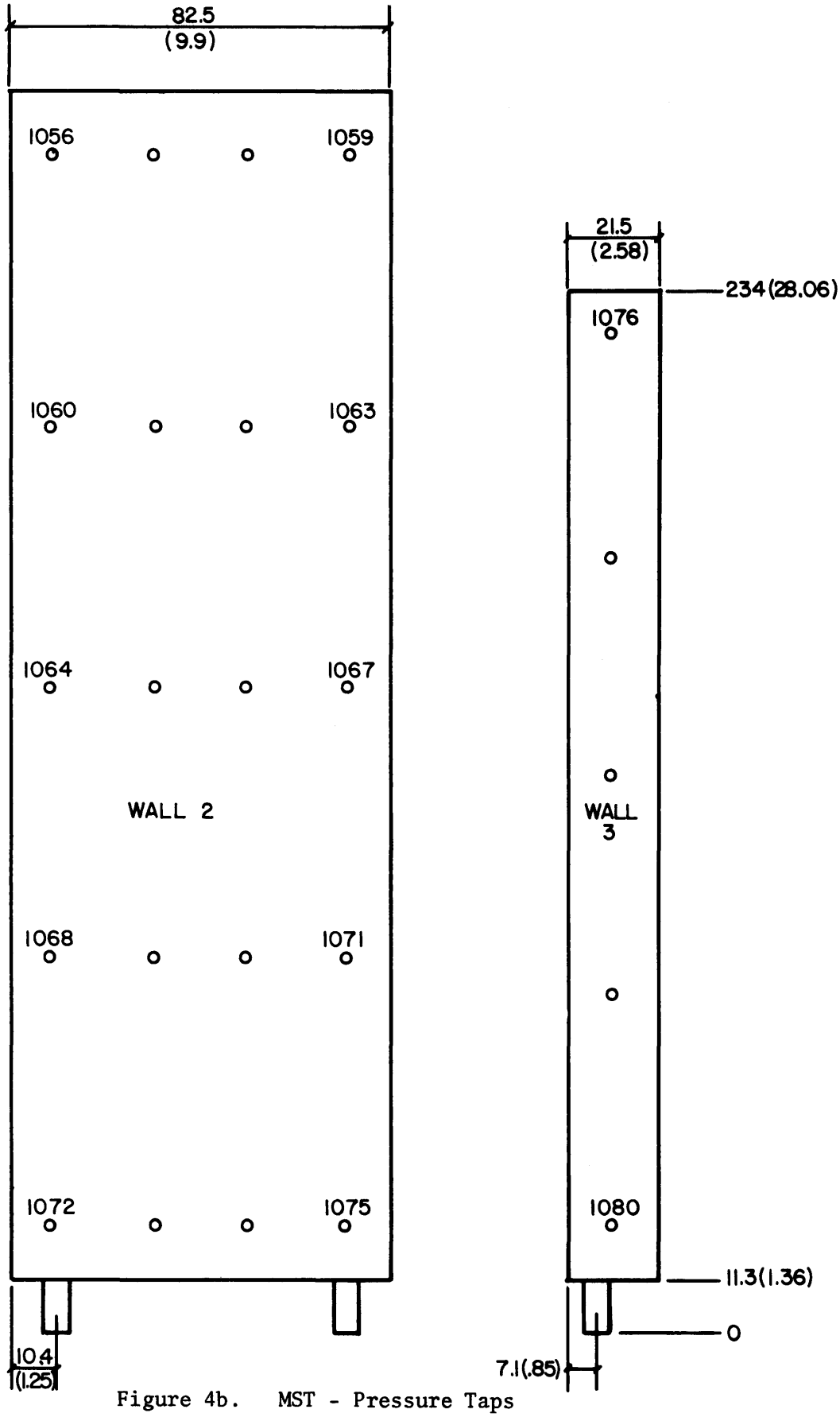

Figure 4b. MST - Pressure Taps

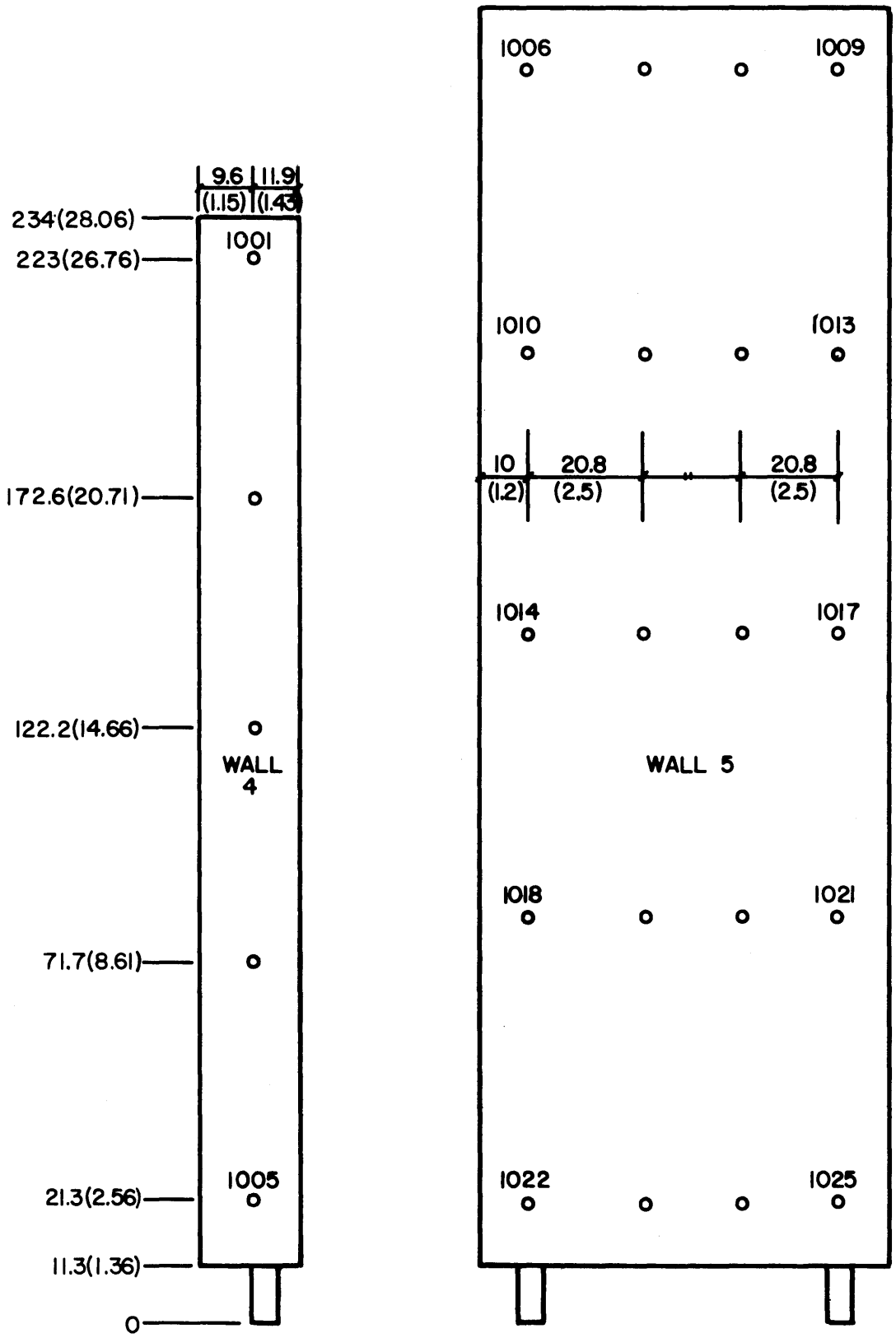

Figure 4c. MST - Pressure Taps

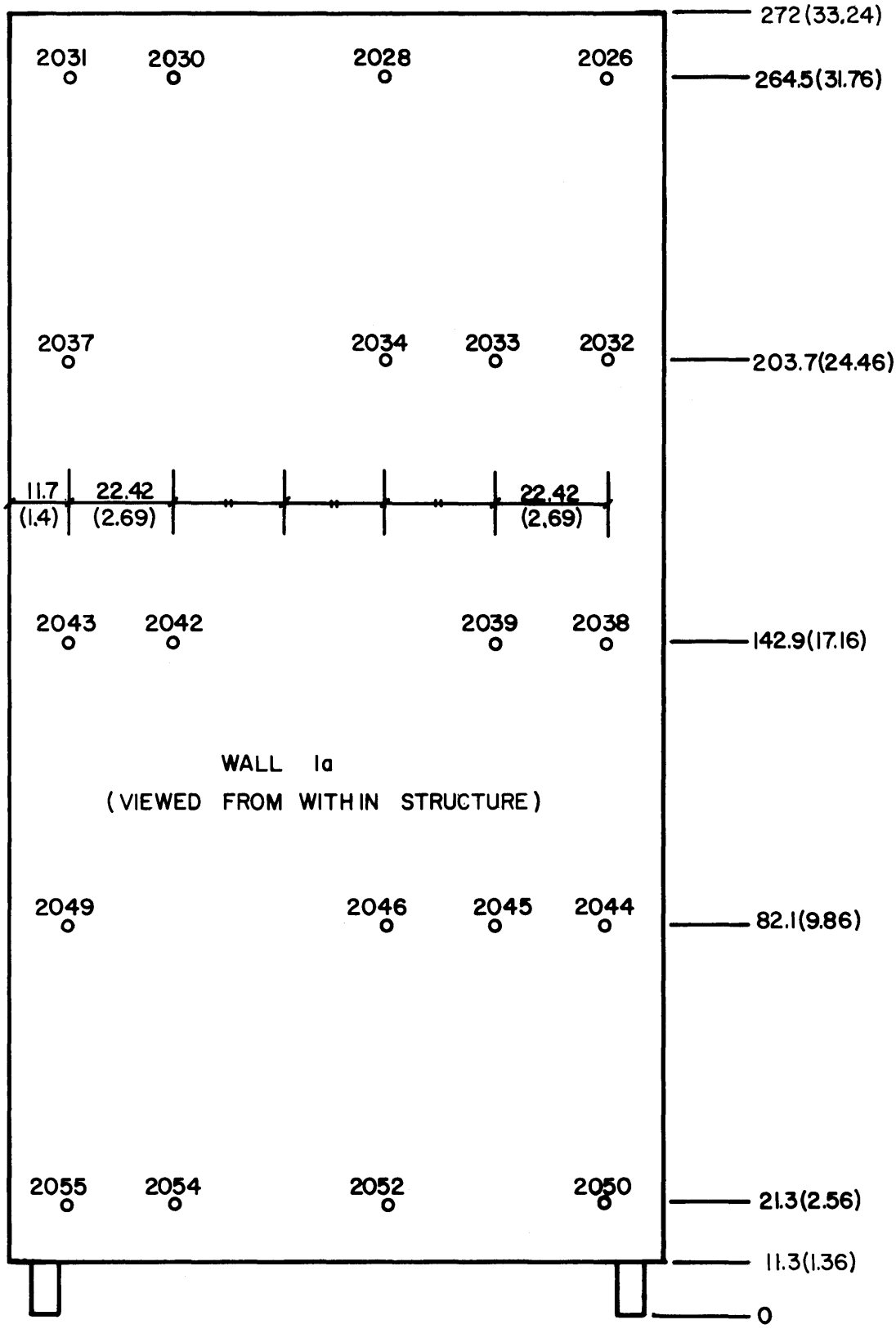

Figure 4d. MST - Pressure Taps

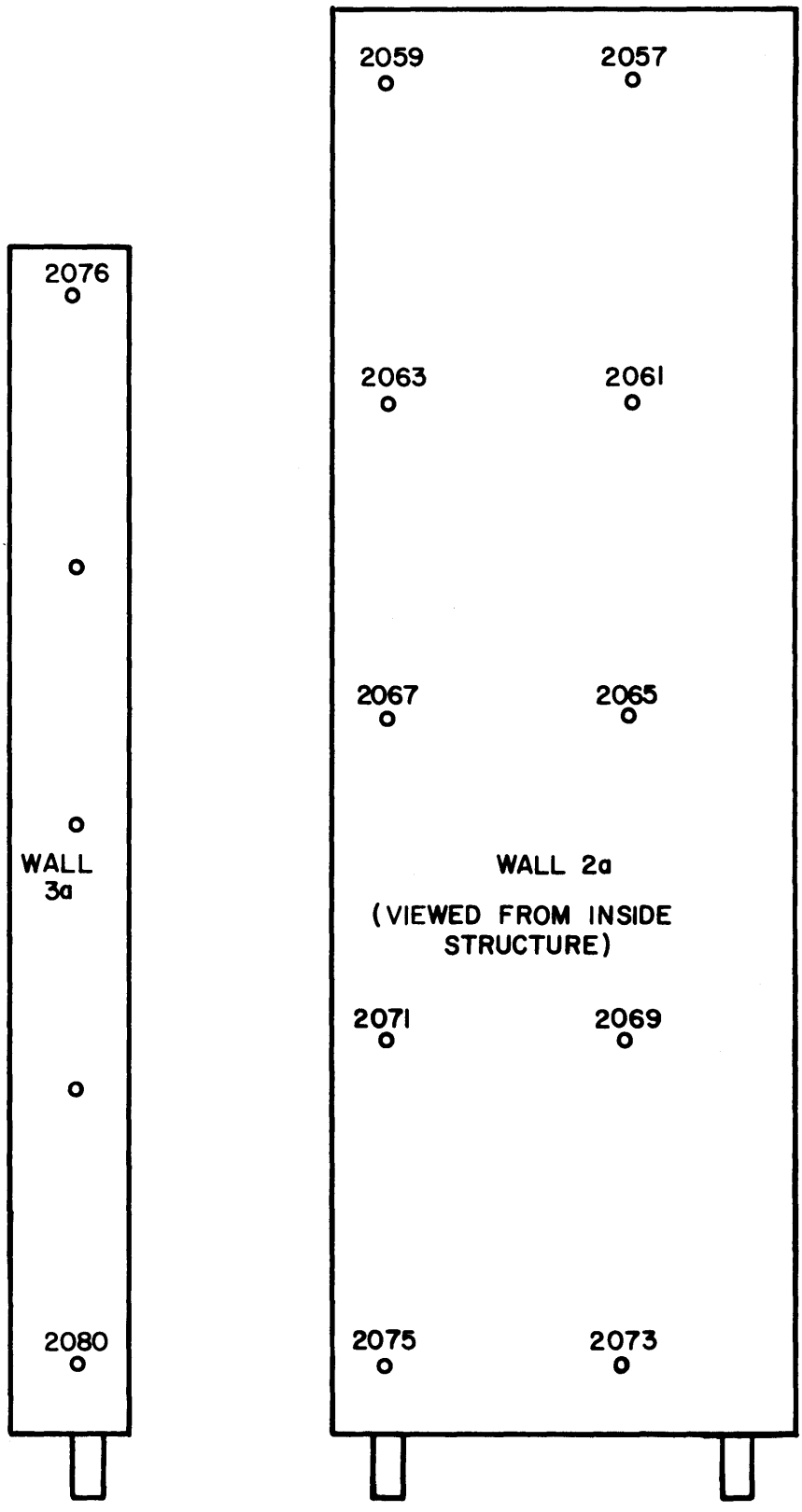

Figure 4e. MST - Pressure Taps

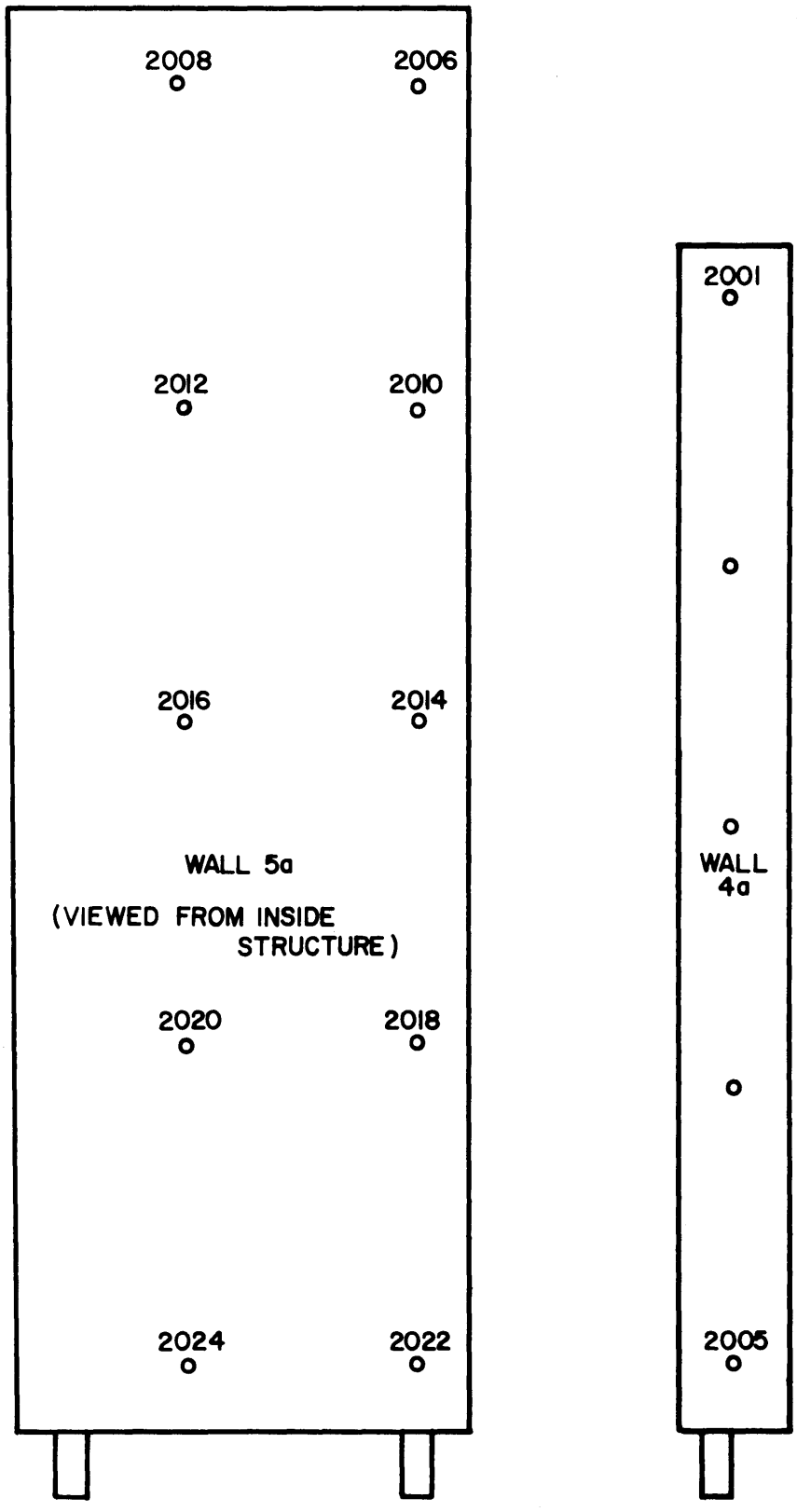

Figure 4f. MST - Pressure Taps

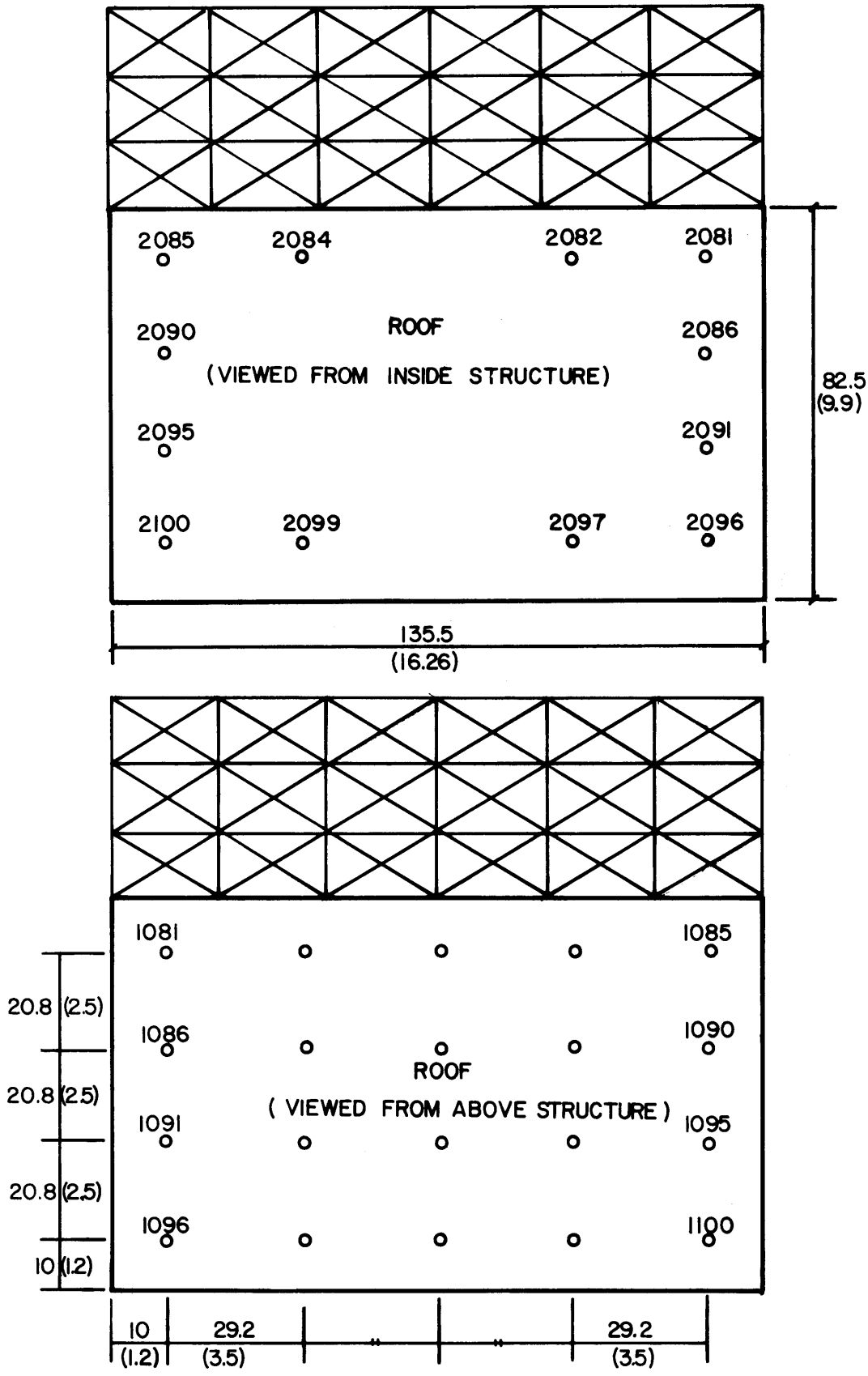

Figure 4g. MST- Pressure Taps

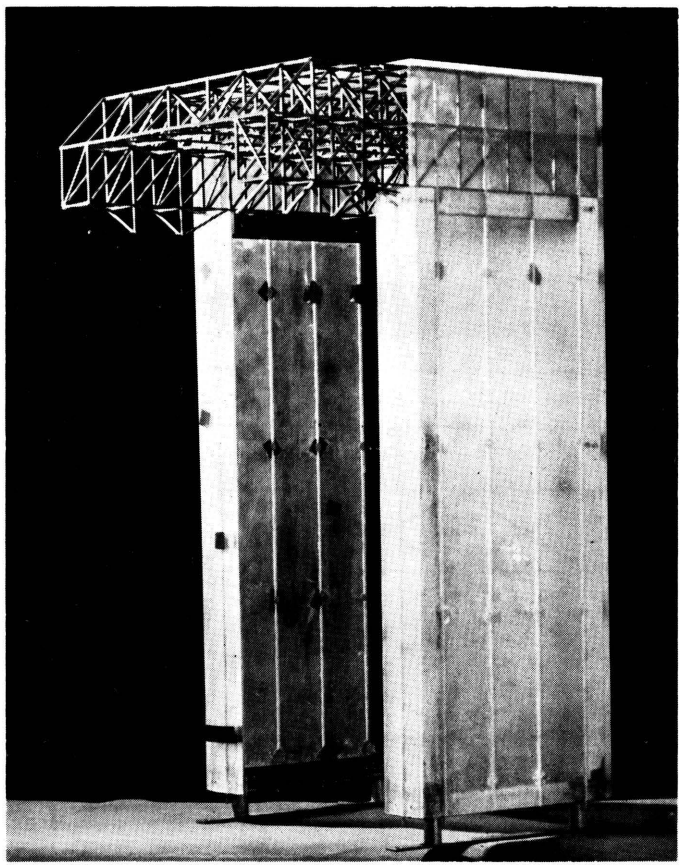

Figure 4h. MST - Pressure Model

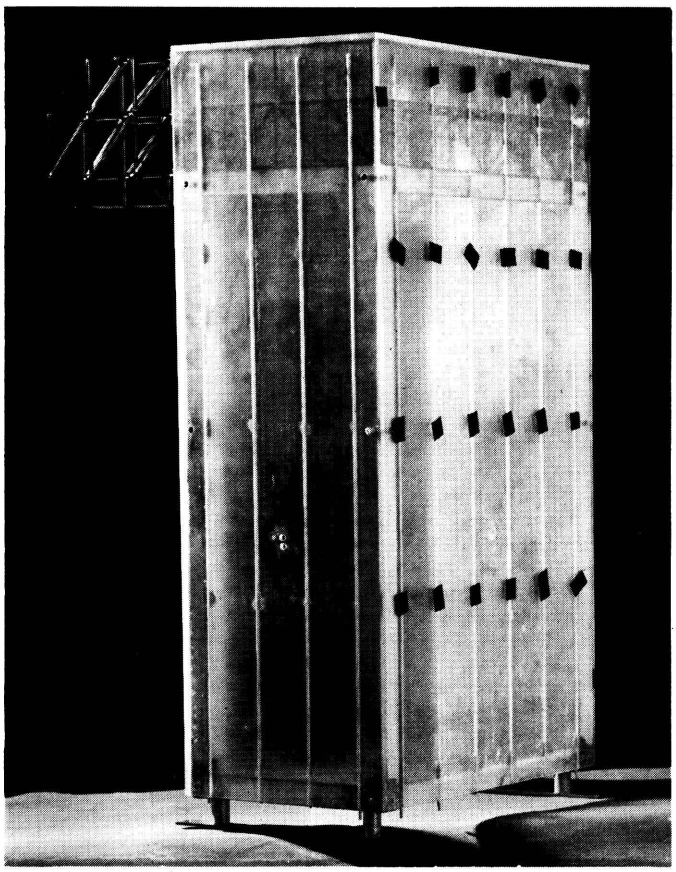

Figure 4j. MST - Pressure Model

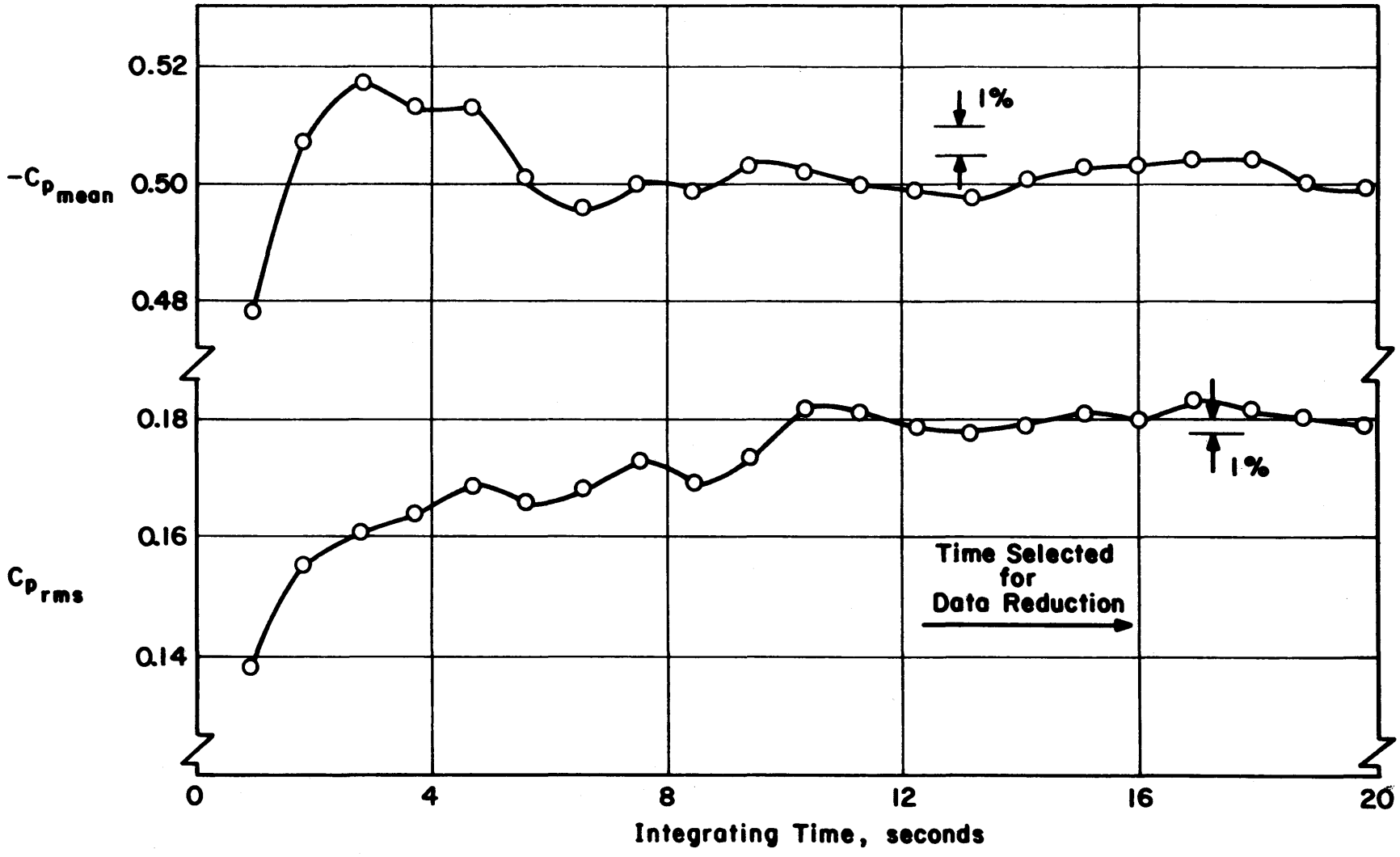

Figure 4k. Data Sampling Time Verification

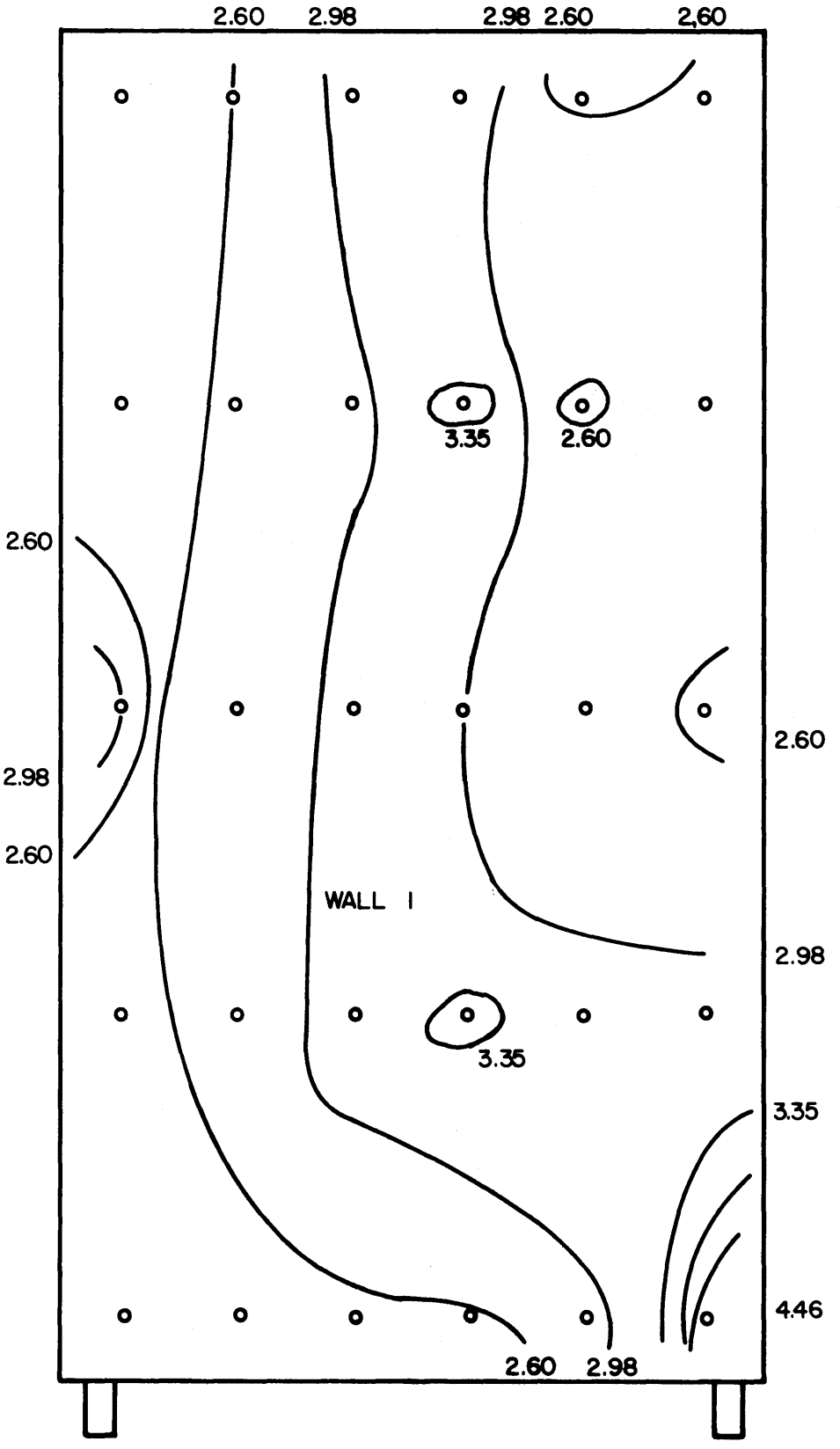

Figure 41. Peak Pressure Contours - External

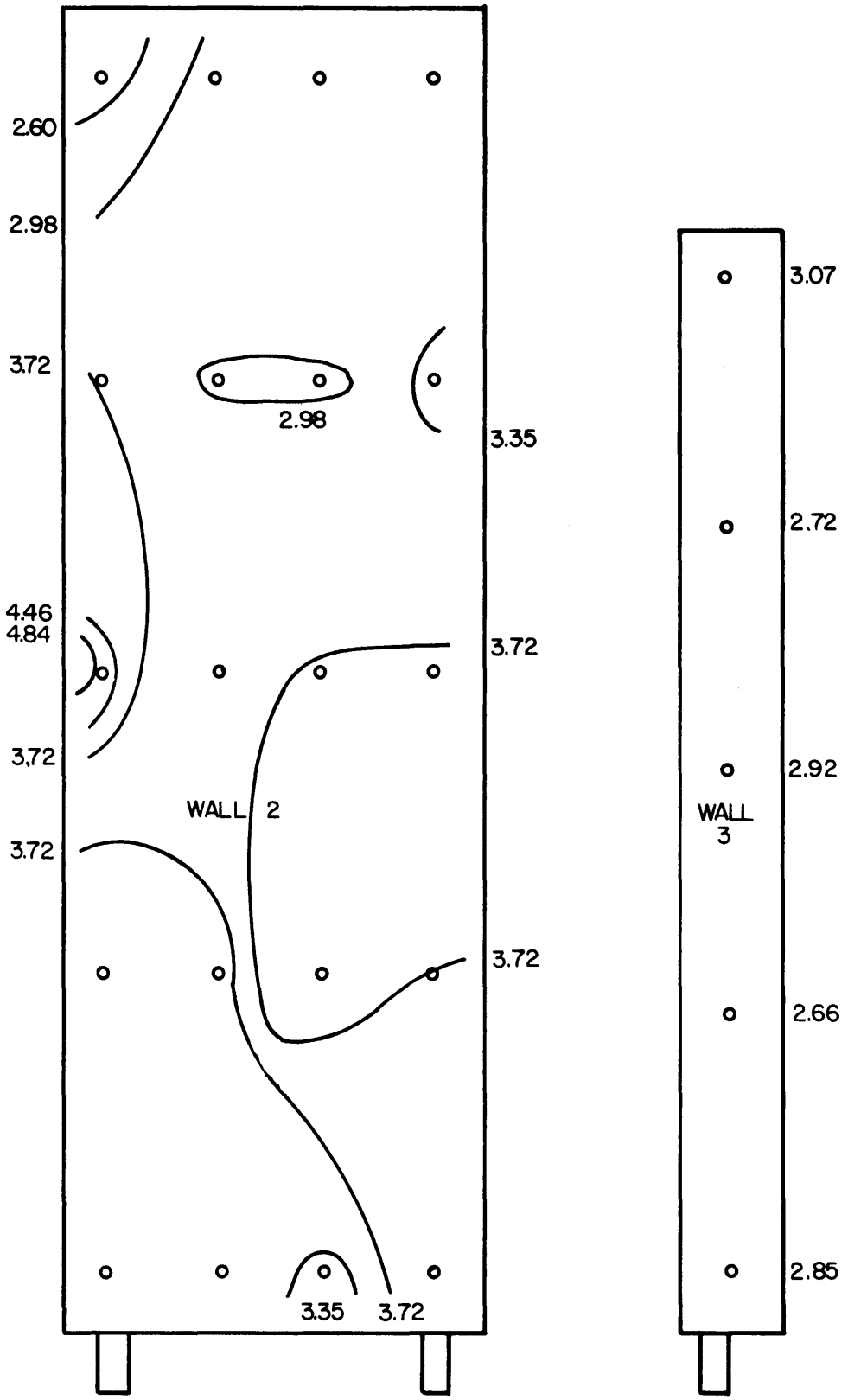

Figure 4m. Peak Pressure Contours - External

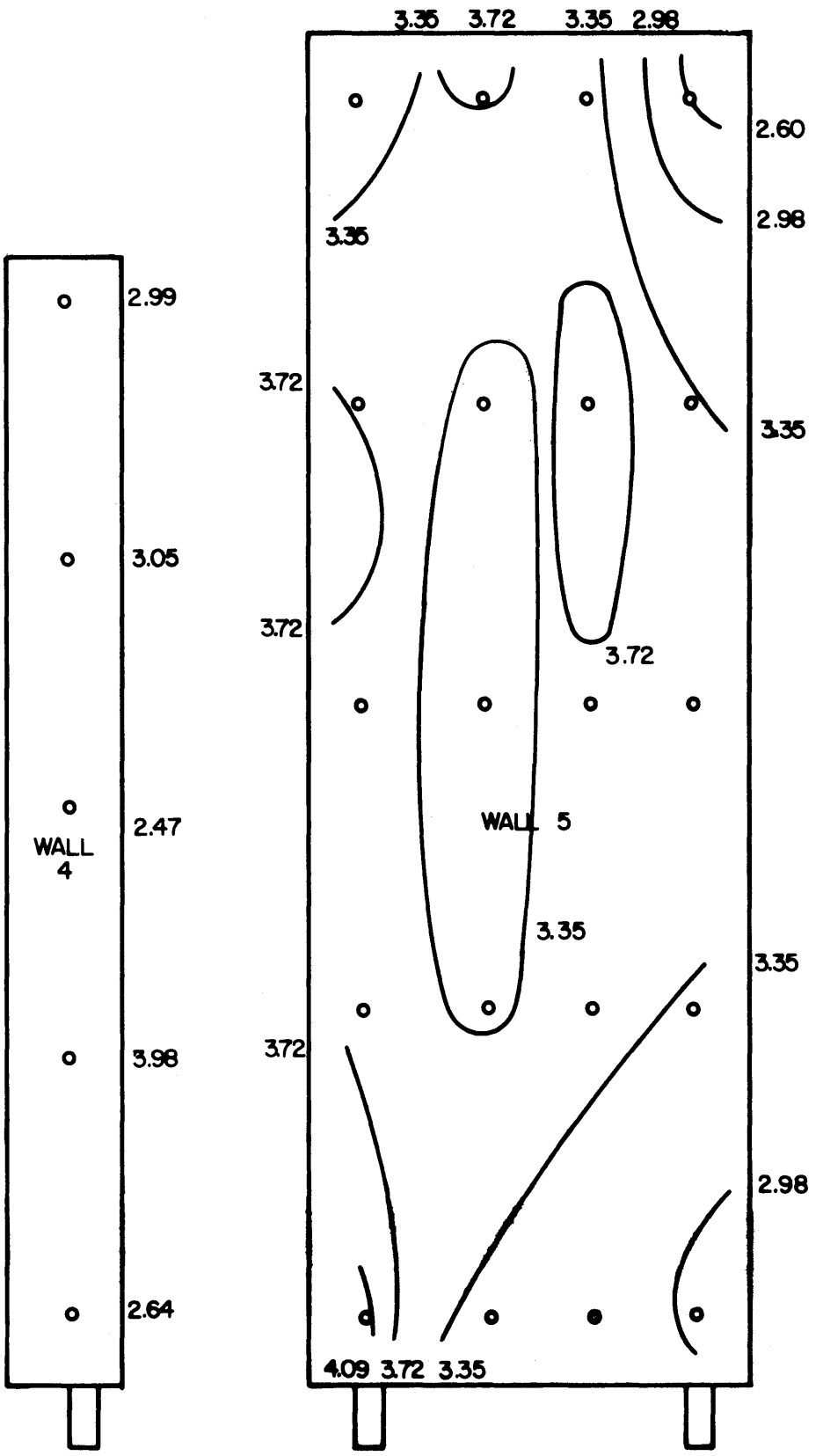

Figure 4n. Peak Pressure Contours - External

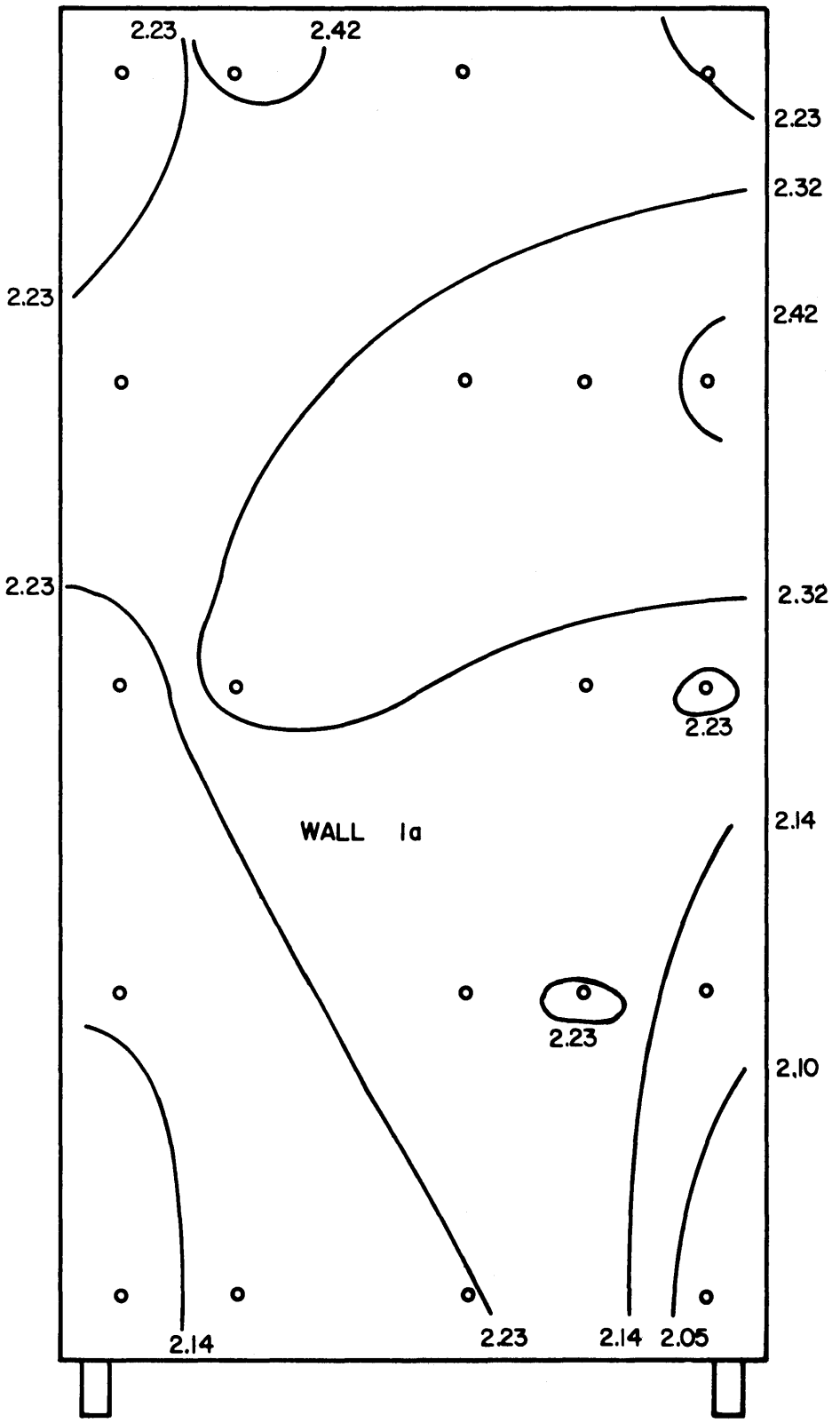

Figure 4p. Peak Pressure Contours - Internal

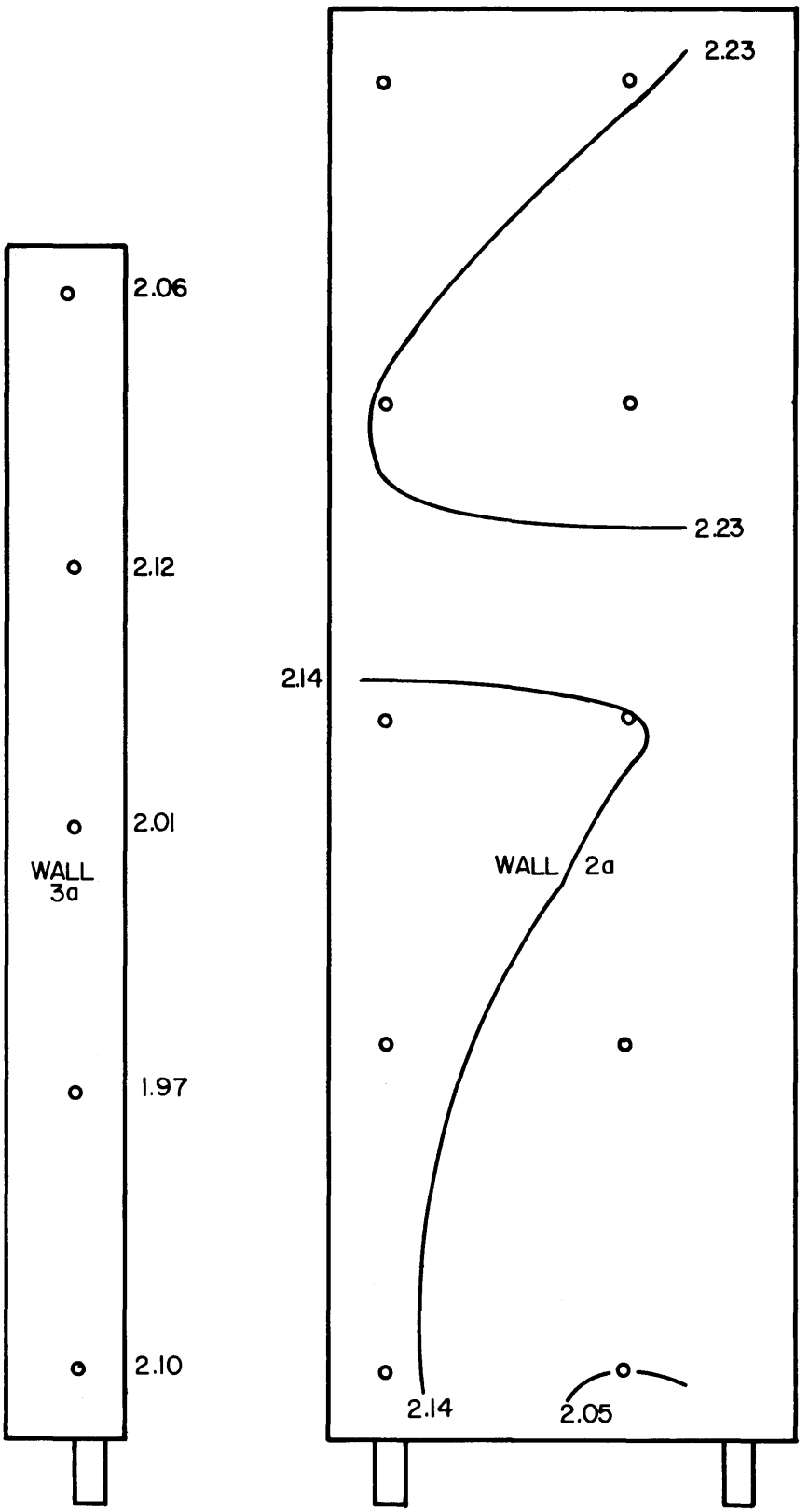

Figure 4q. Peak Pressure Contours - Internal

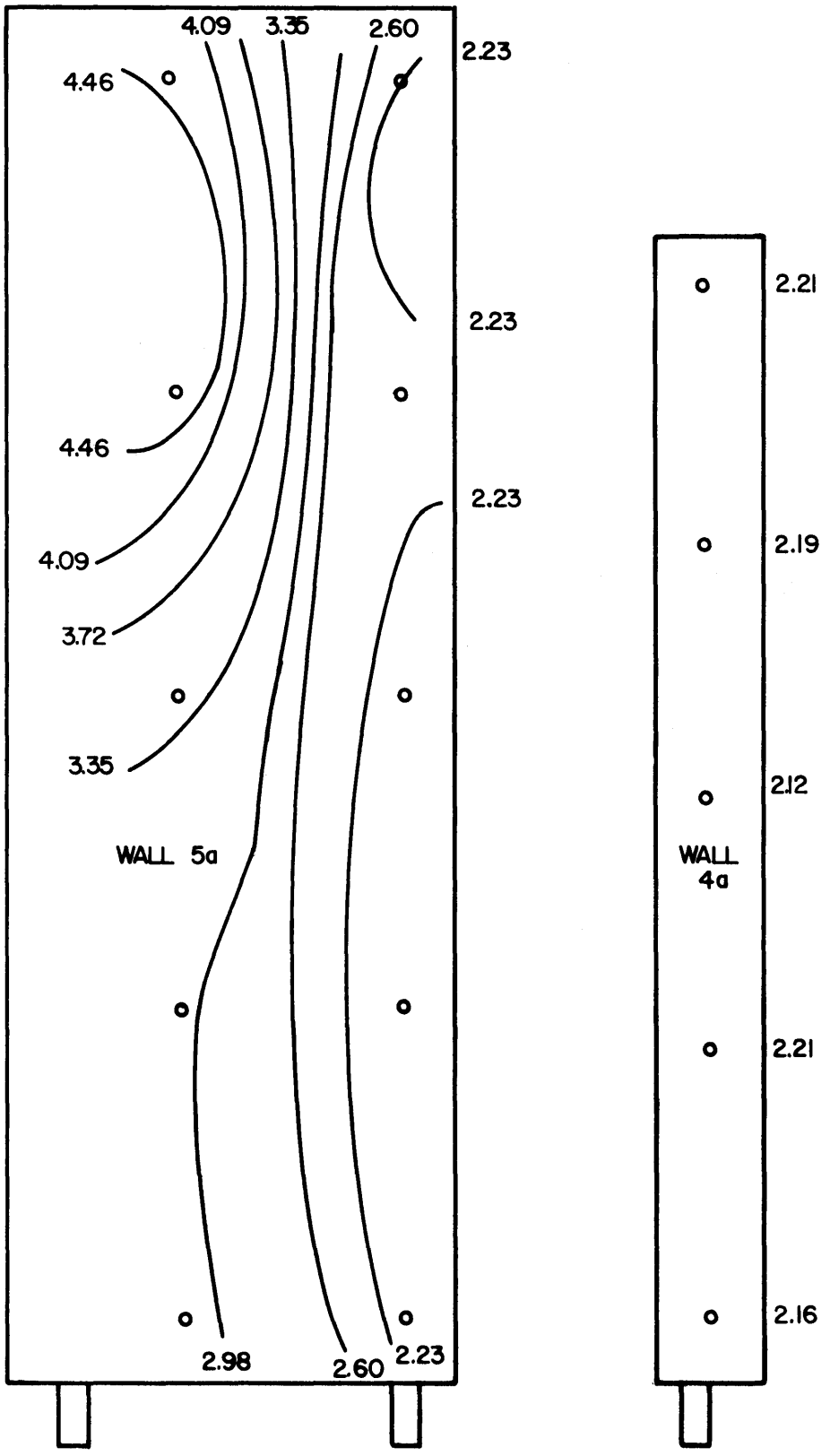

Figure 4r. Peak Pressure Contours - Internal

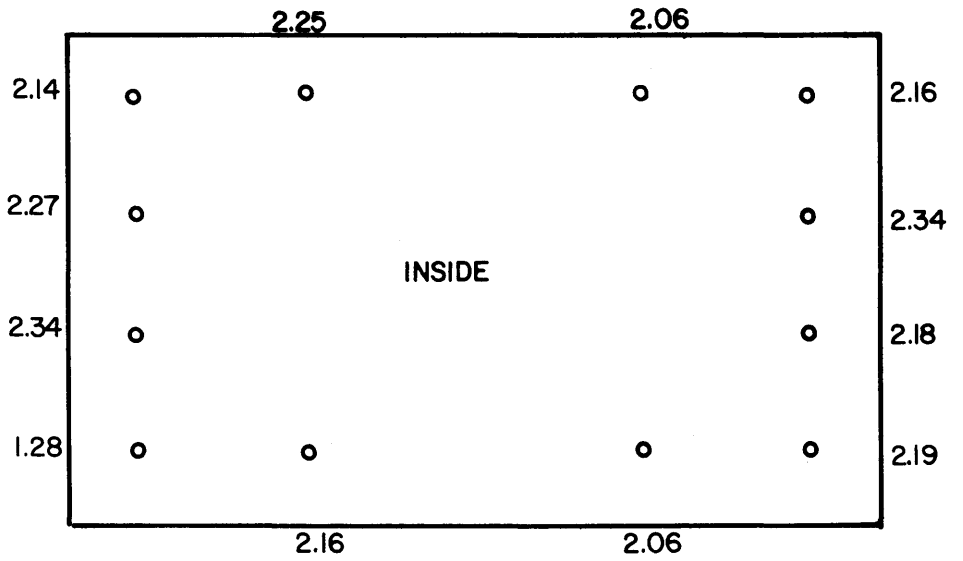

ROOF

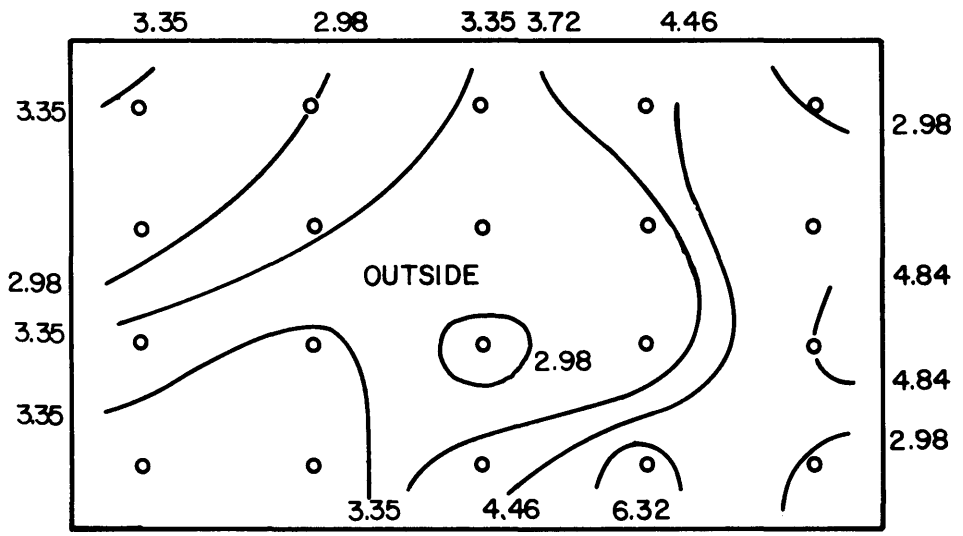

Figure 4s. Peak Pressure Contours - Roof

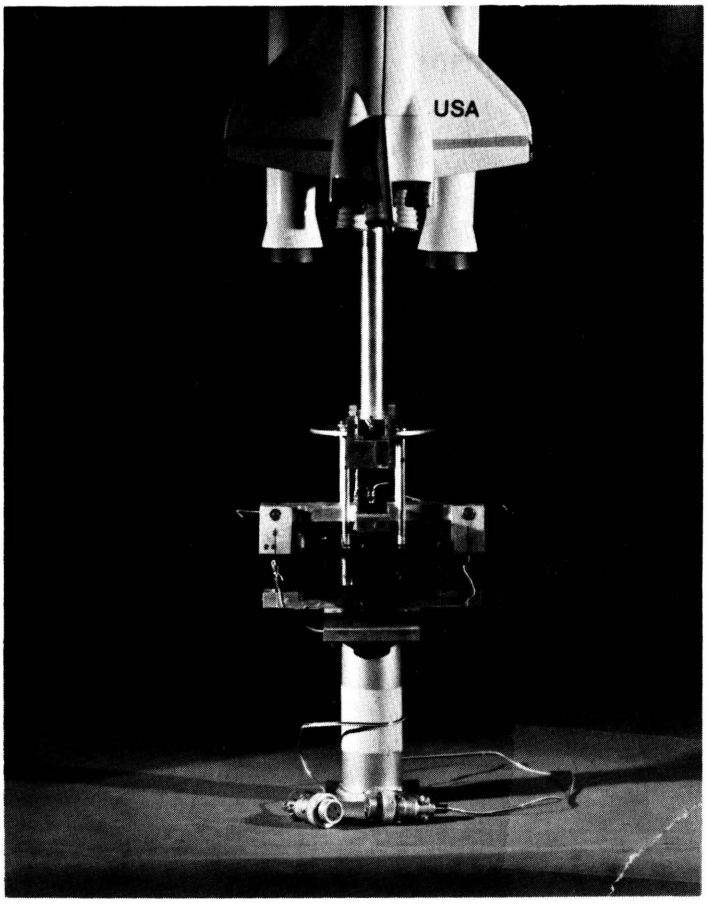

Figure 5a. Two-Component Force Balance

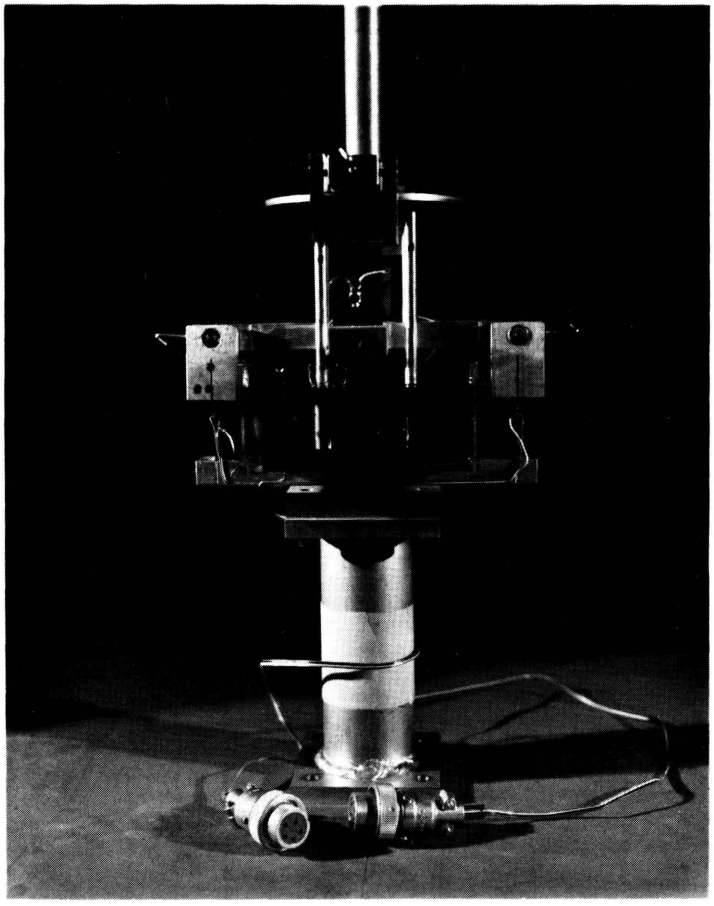

Figure 5b. Two-Component Force Balance

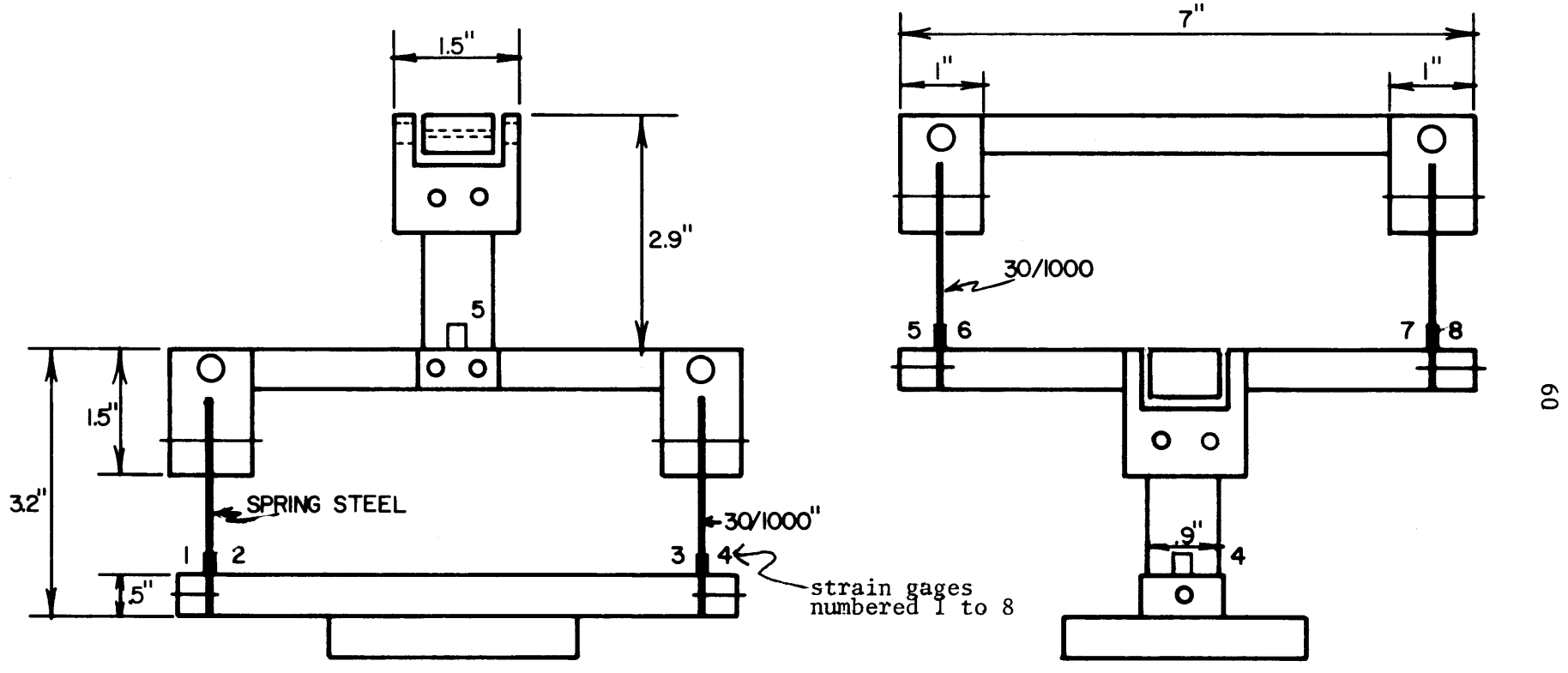

Figure 5c. Two-Component Force Balance

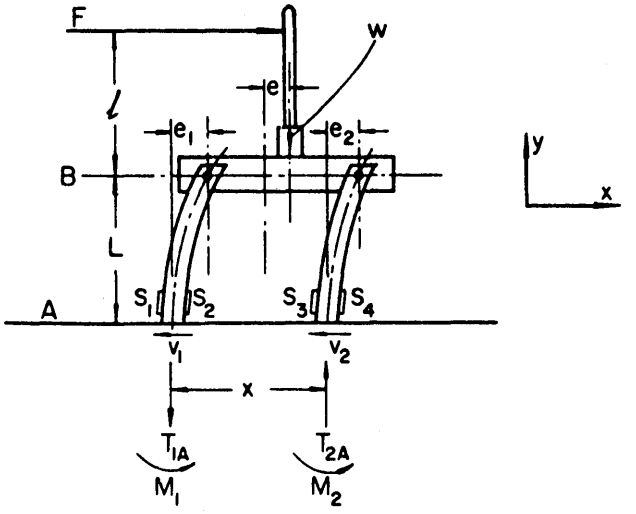

Figure 5d. The Force Diagram of the Dynamometer

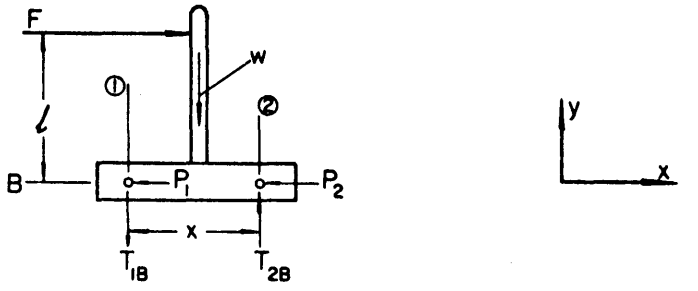

Figure 5e. Free Body Diagram 1

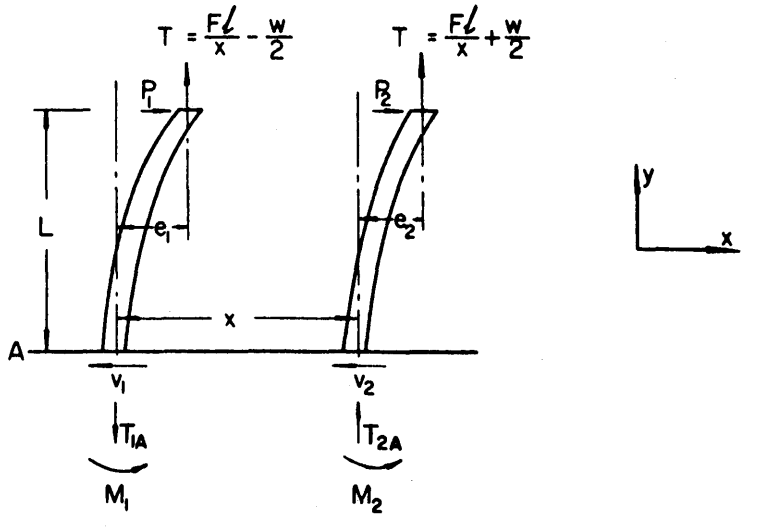

Figure 5f. Free Body Diagram 2

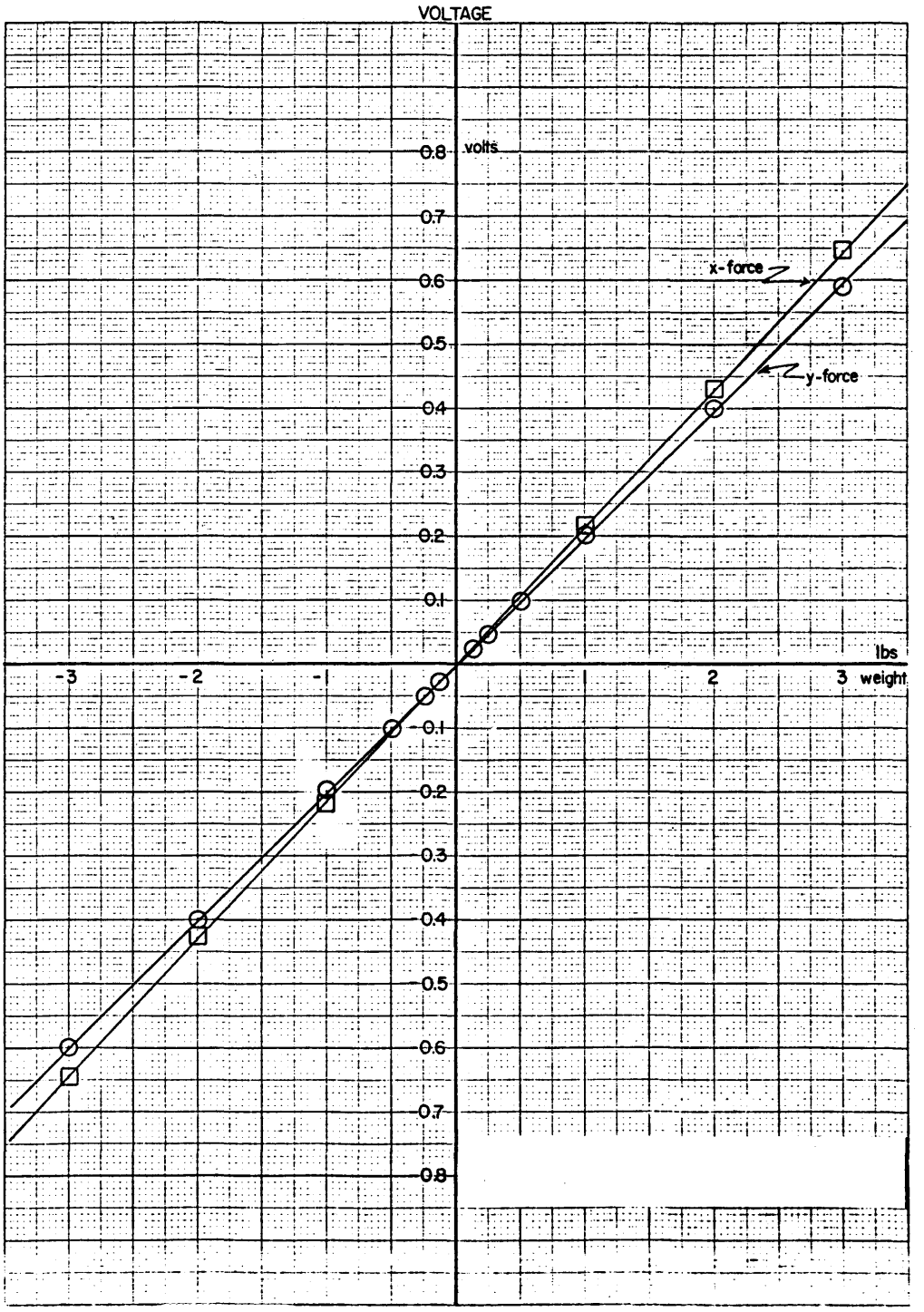

Figure 5g. Two-Component Force Balance Calibration

Figure 6a. Three-Component Moment Balance

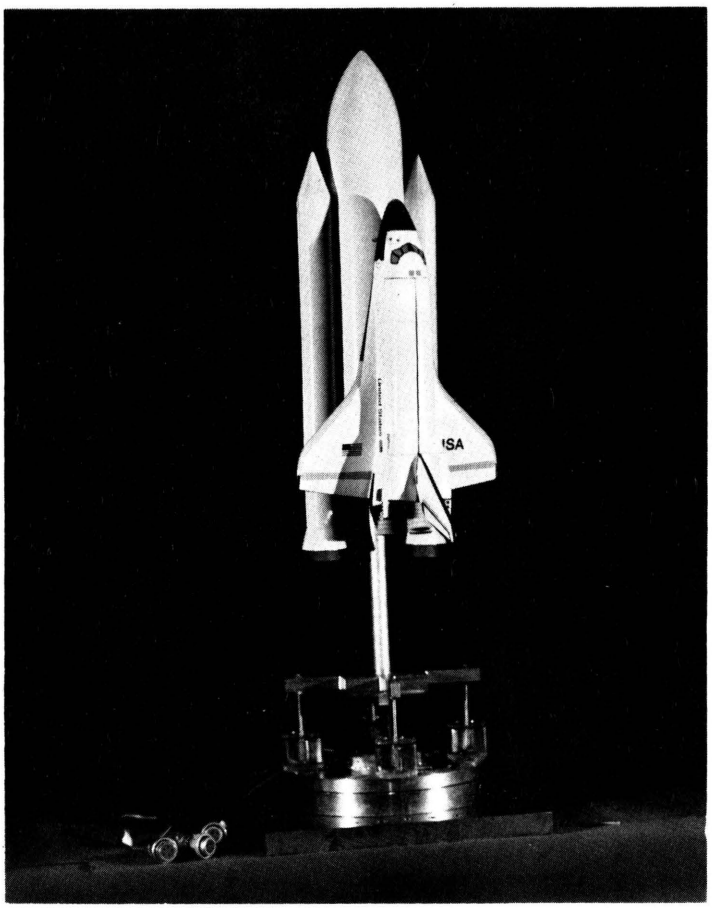

Figure 6b. Three-Component Moment Balance

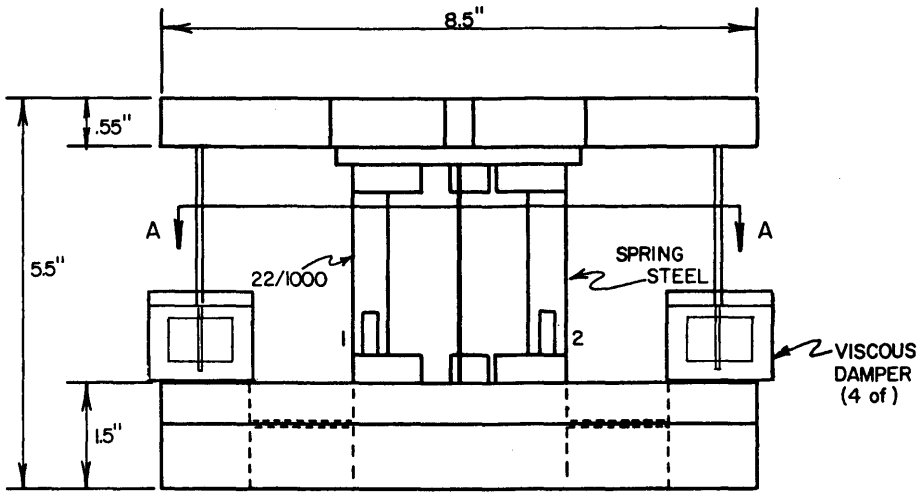

Notes

All spring steel plates are 1/2" wide. Horizontal strain gages used to measure M_x and M_y are numbered 5-10. Vertical strain gages used to measure M_z are numbered 1-4.

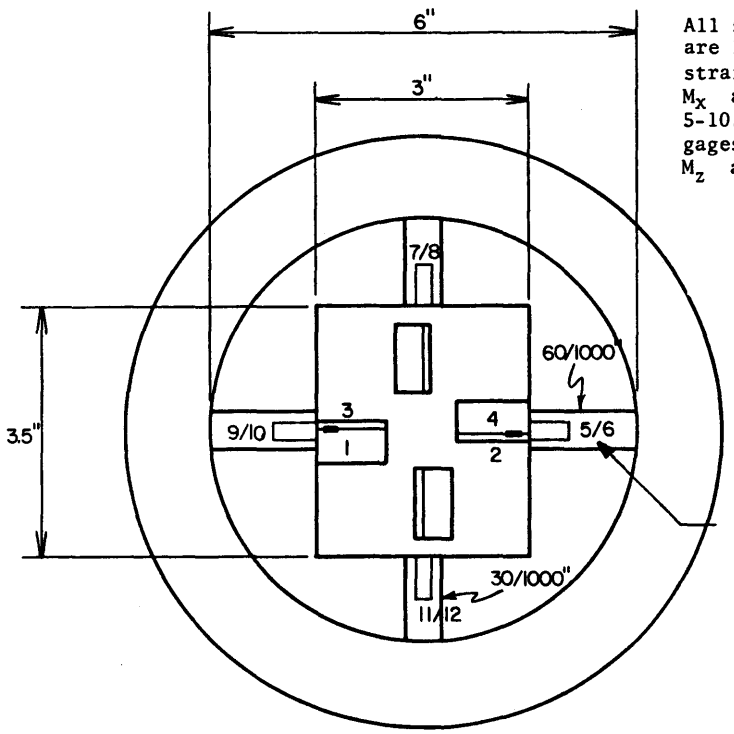

Horizontal spring steel plates on which the strain gages are mounted.

SECTION AA

Figure 6c. Three-Component Moment Balance

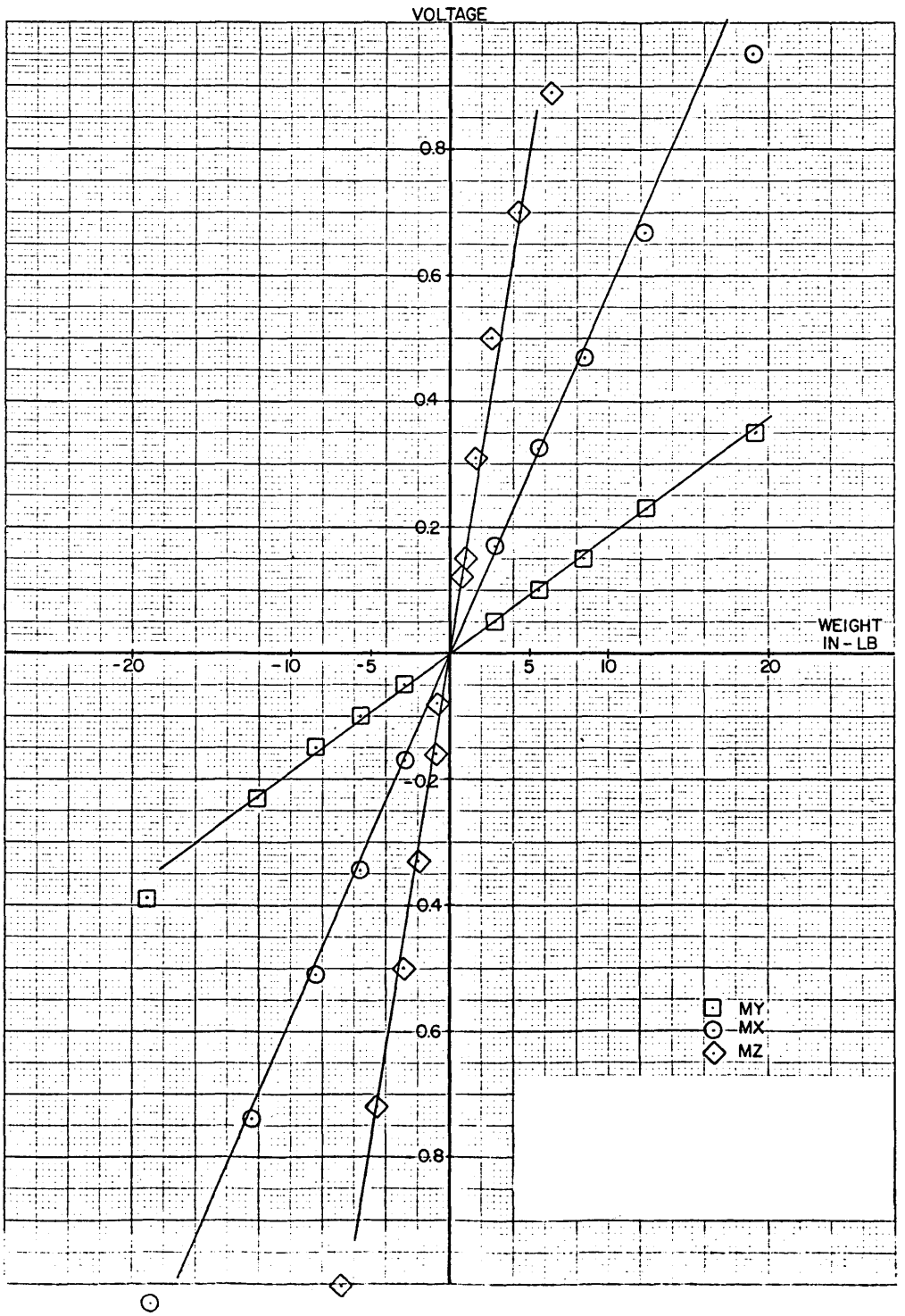

Figure 6d. Three-Component Moment Balance Calibration

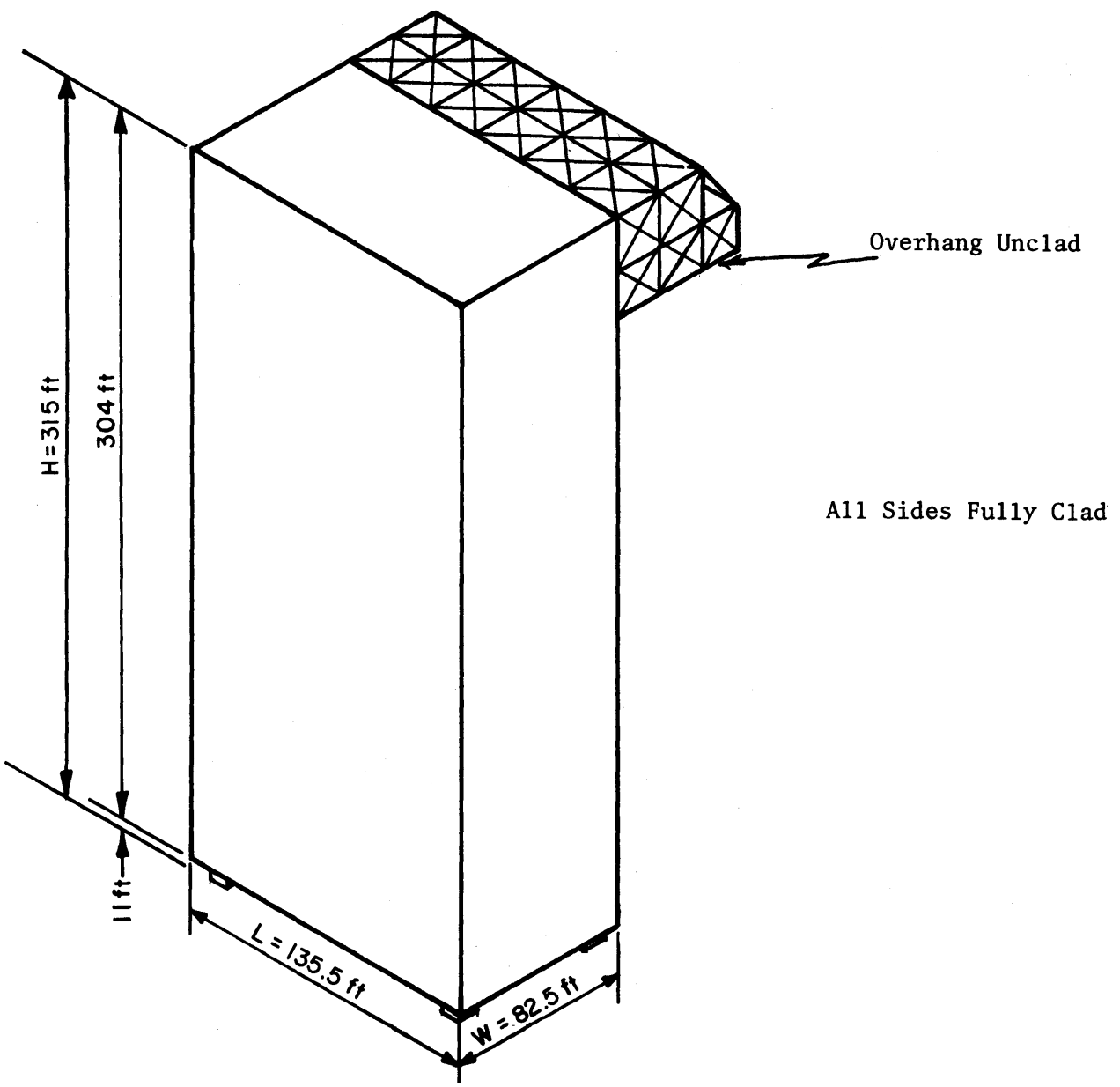

Figure 7a. Configuration 1 - MST

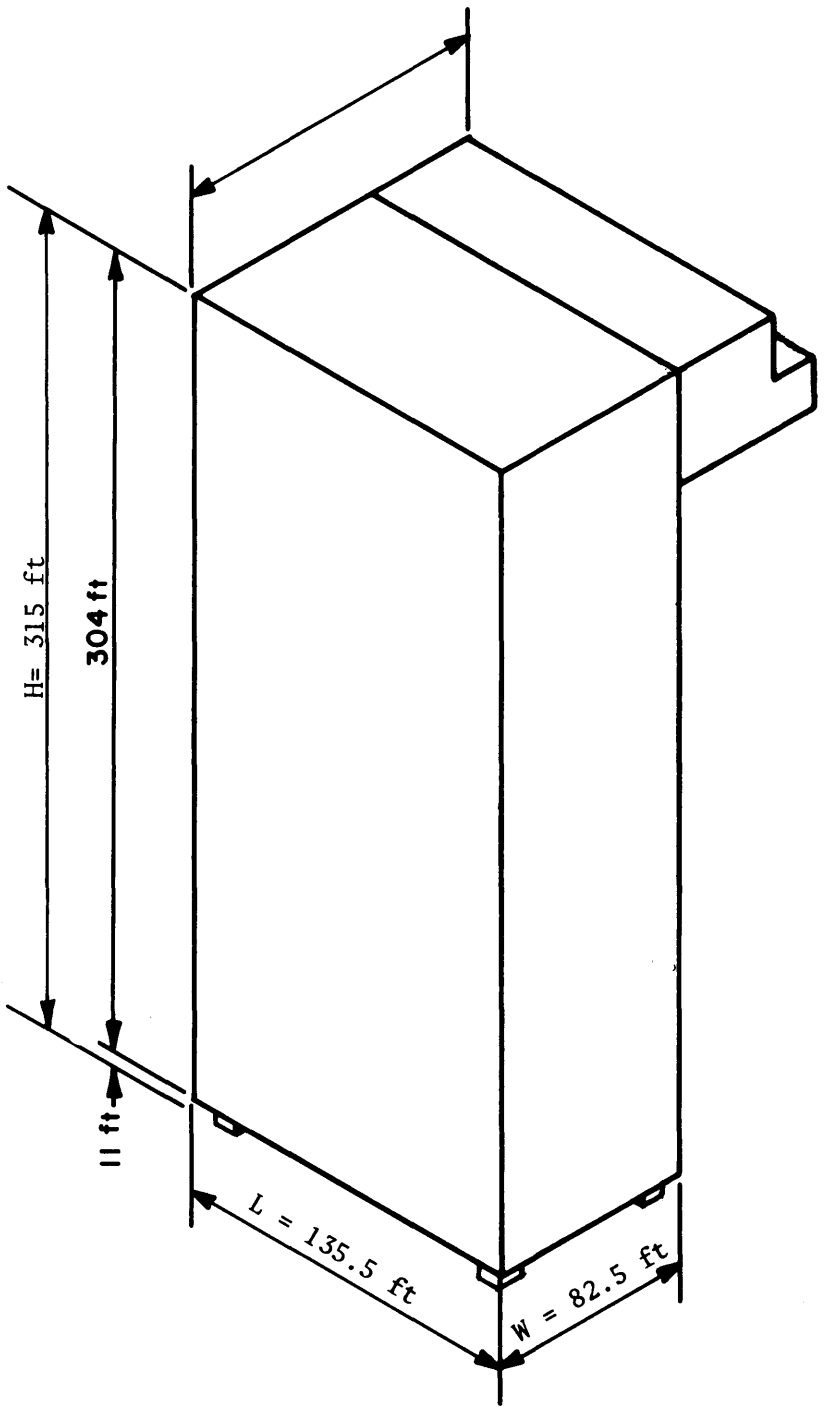

Figure 7b. Configuration 1A - MST

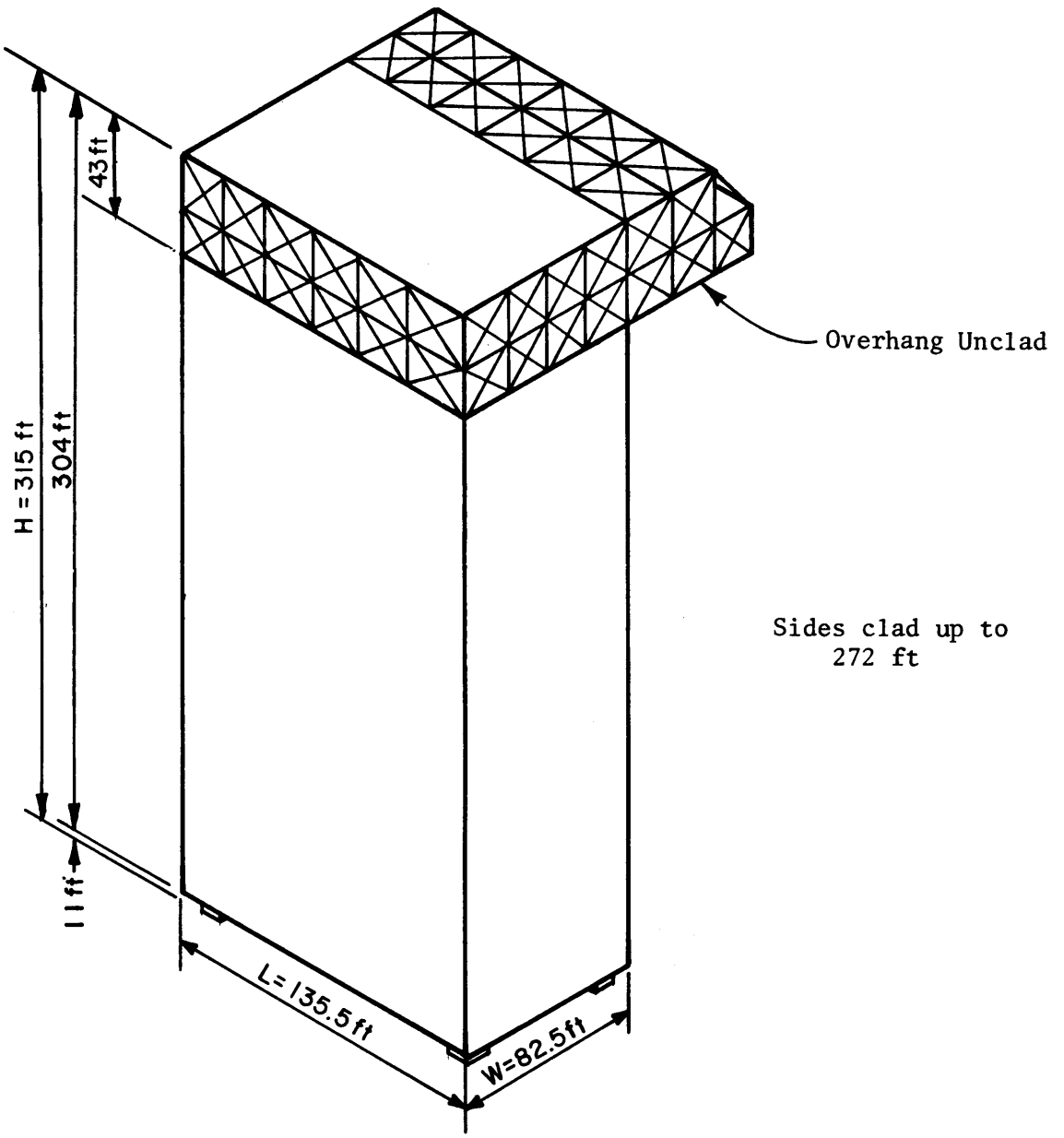

Figure 7c. Configuration 2 - MST

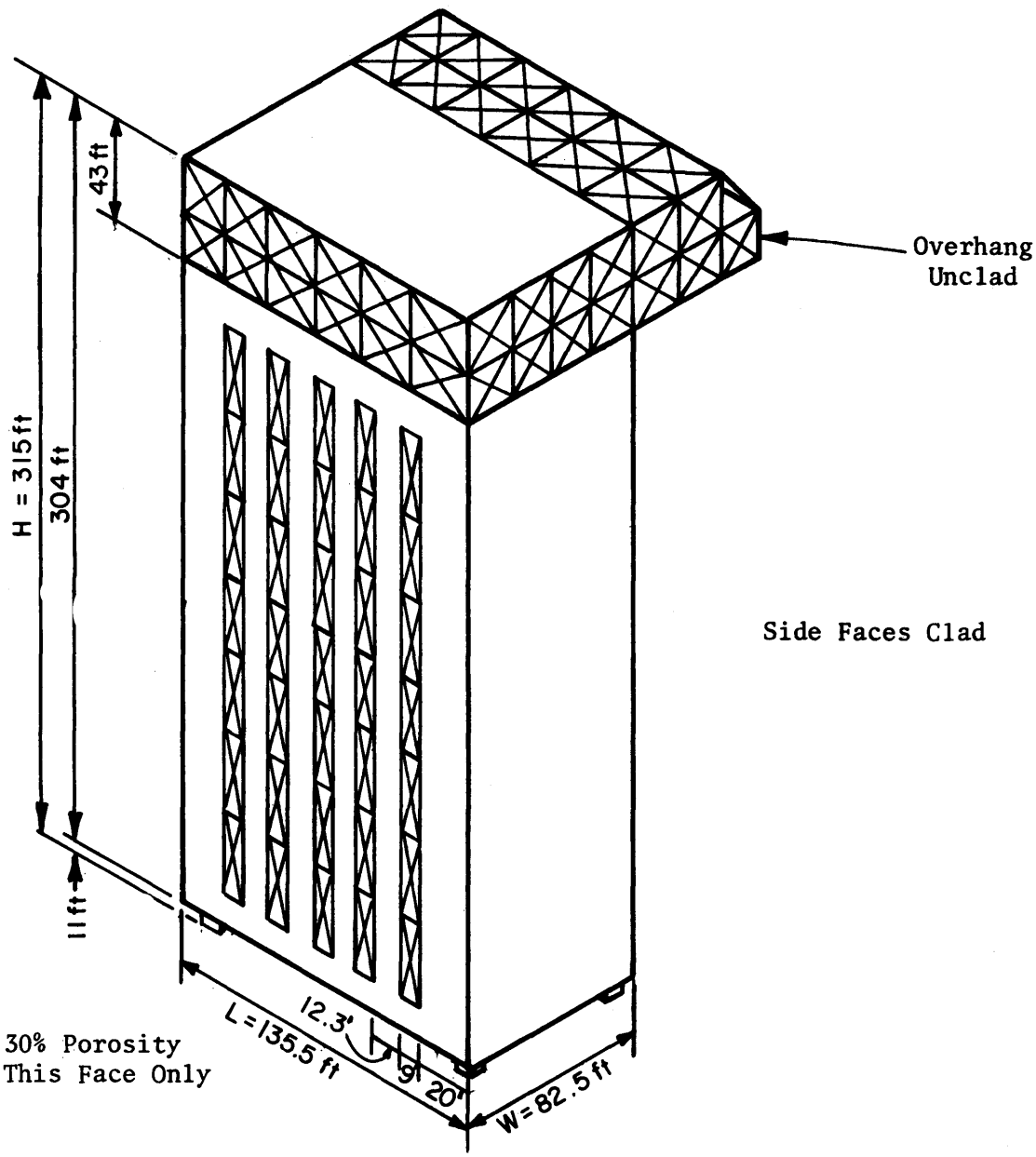

Figure 7d. Configuration 3 - MST

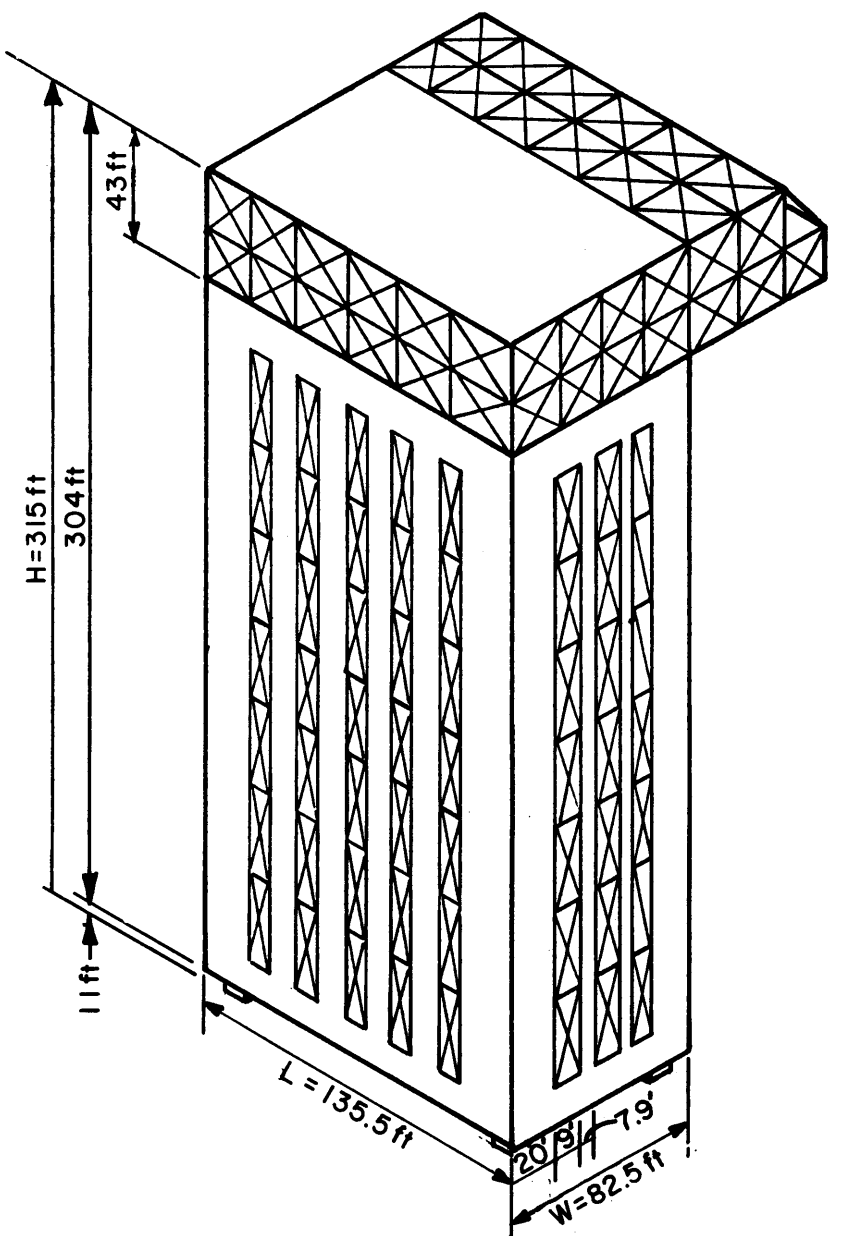

30% Porosity
Each Of Two Side Faces

Figure 7e. Configuration 4 - MST

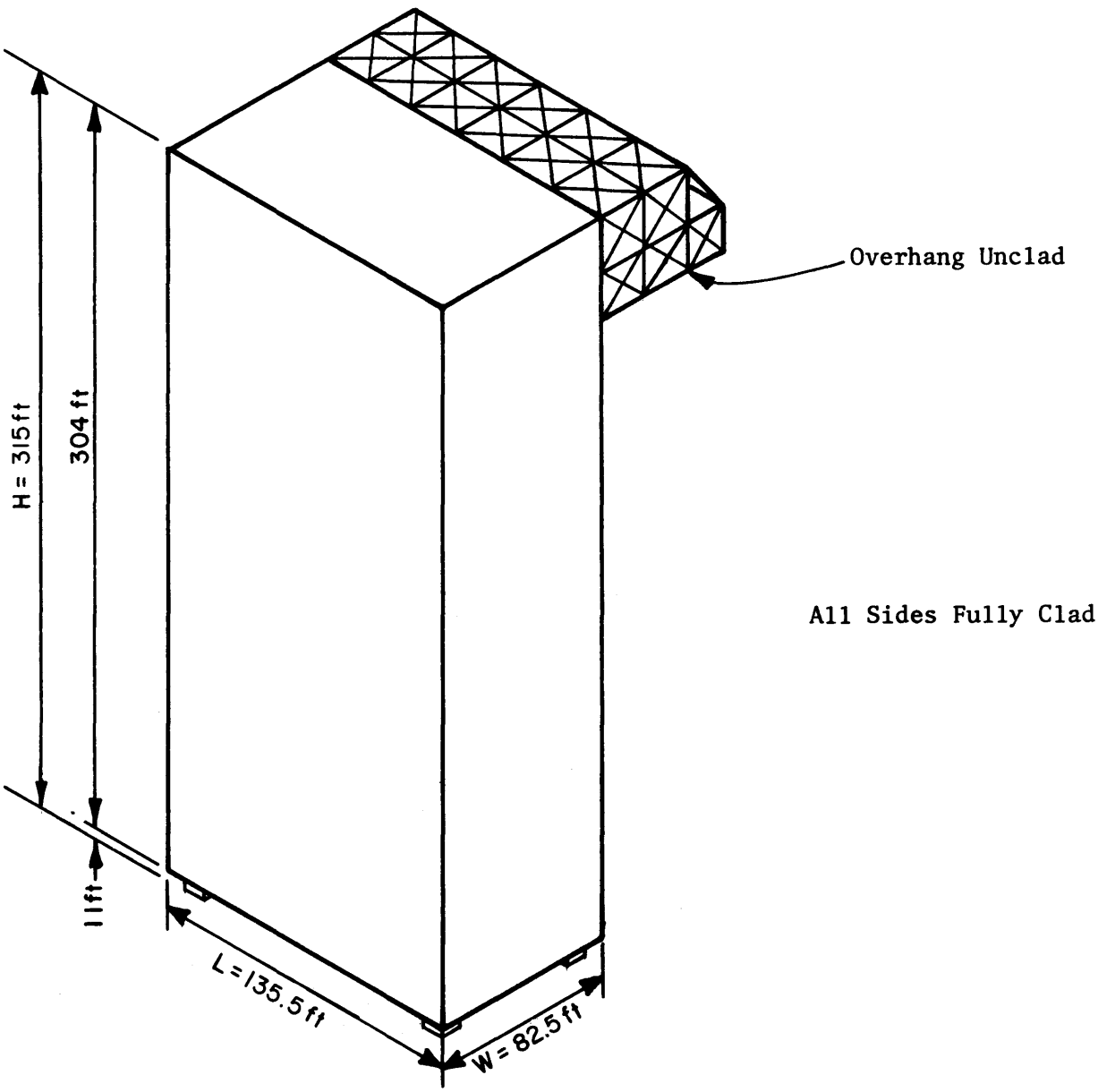

Figure 7f. Configuration 5 - MST

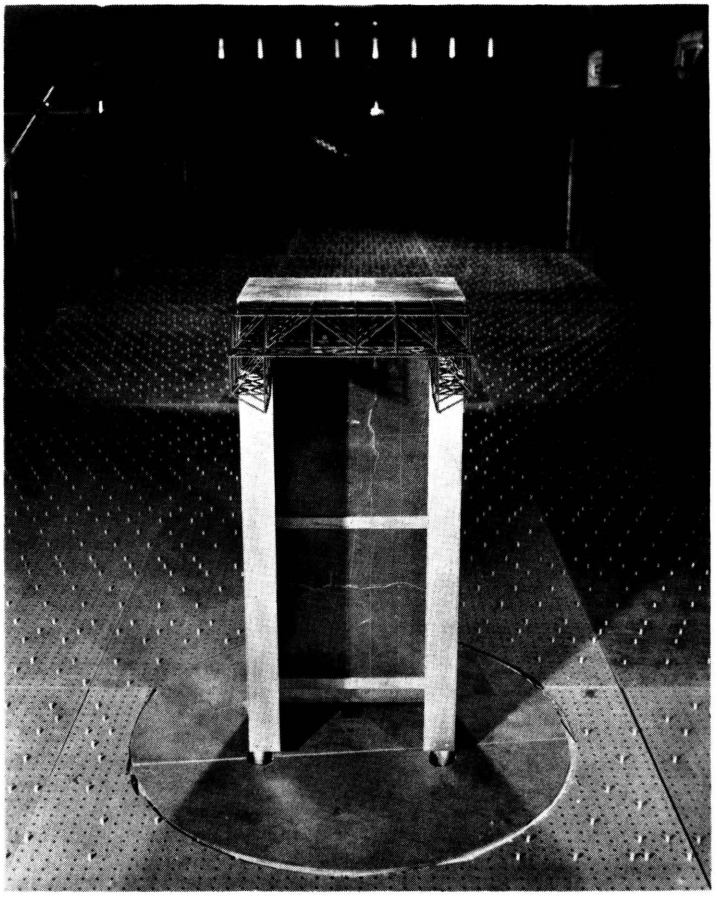

Figure 7g. MST in Wind Tunnel (looking upstream)

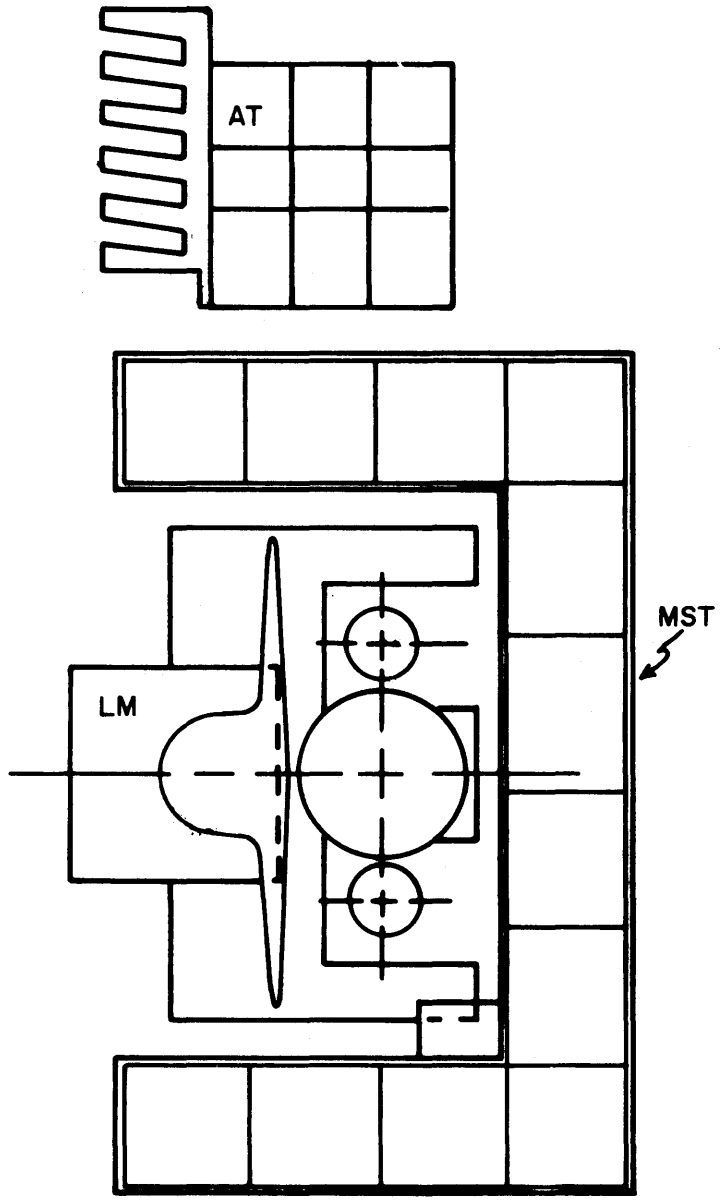

Figure 8a. Configuration A - SSV

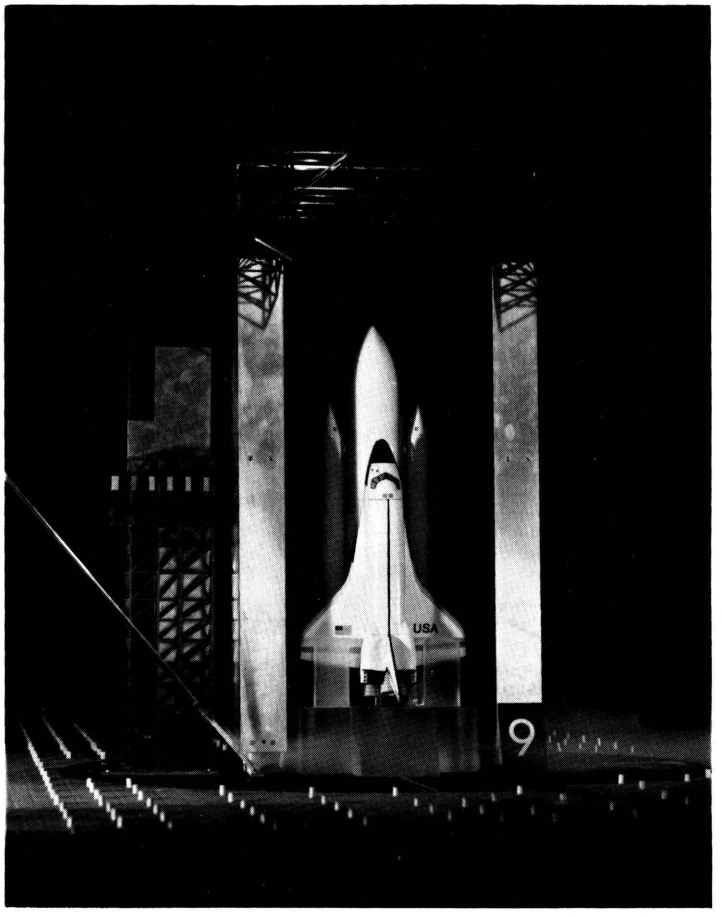

Figure 8aa. Configuration A - SSV

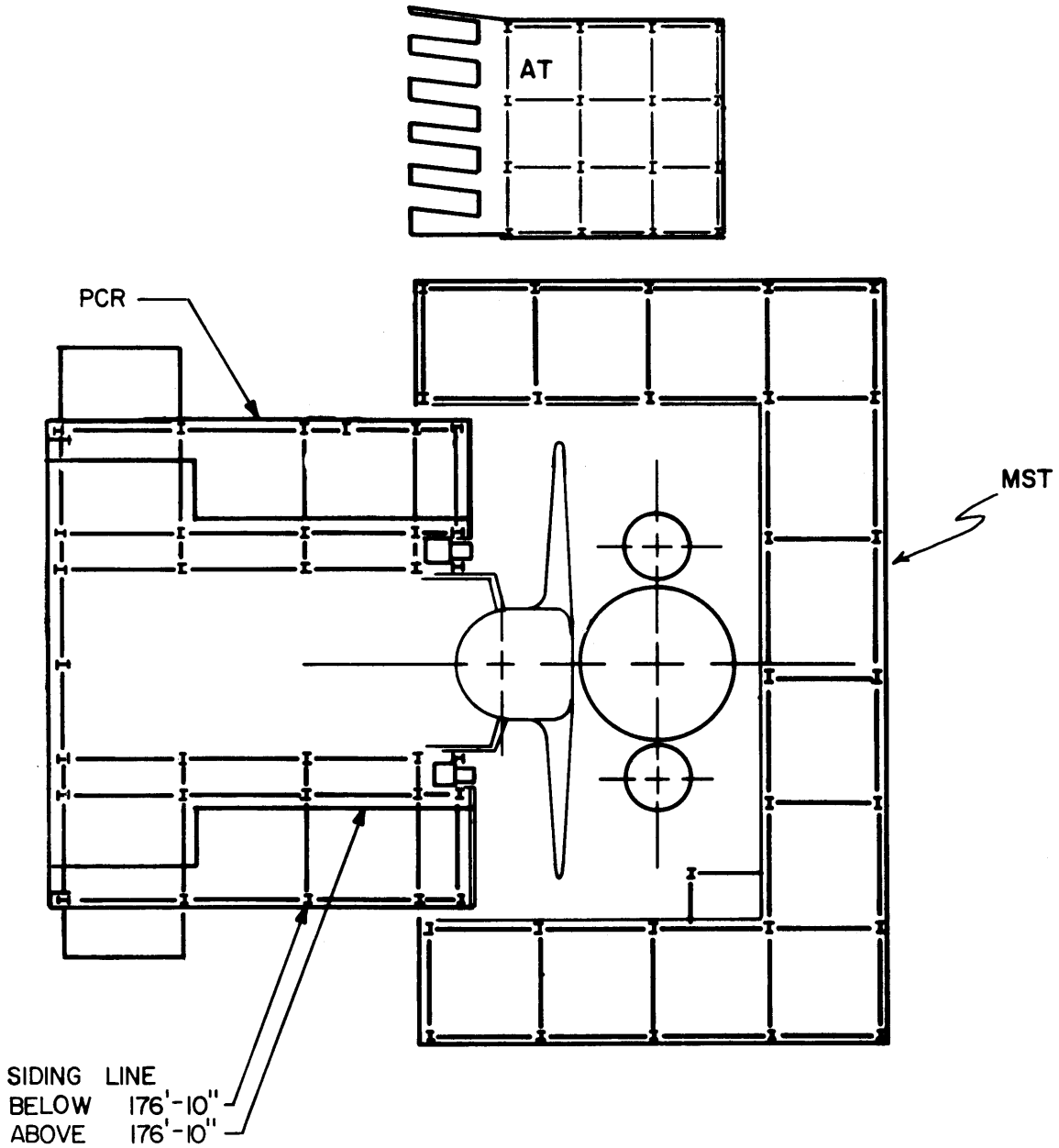

Figure 8b. Configuration B - SSV

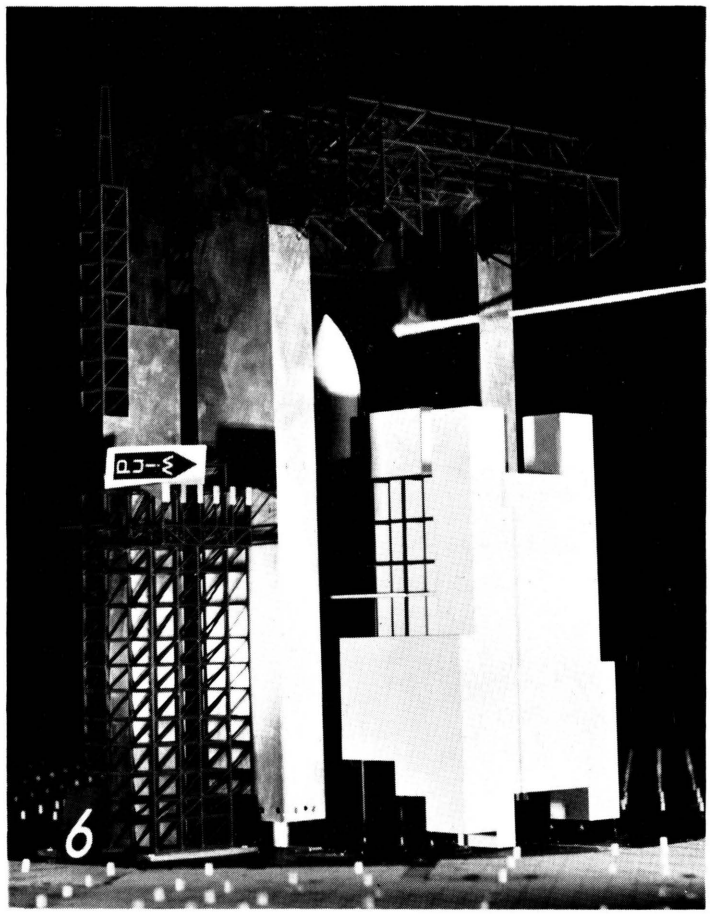

Figure 8bb. Configuration B - SSV
Note: Configuration E similar except PCR Building moved further back 16 ft, 4 in. (away from launch pad).

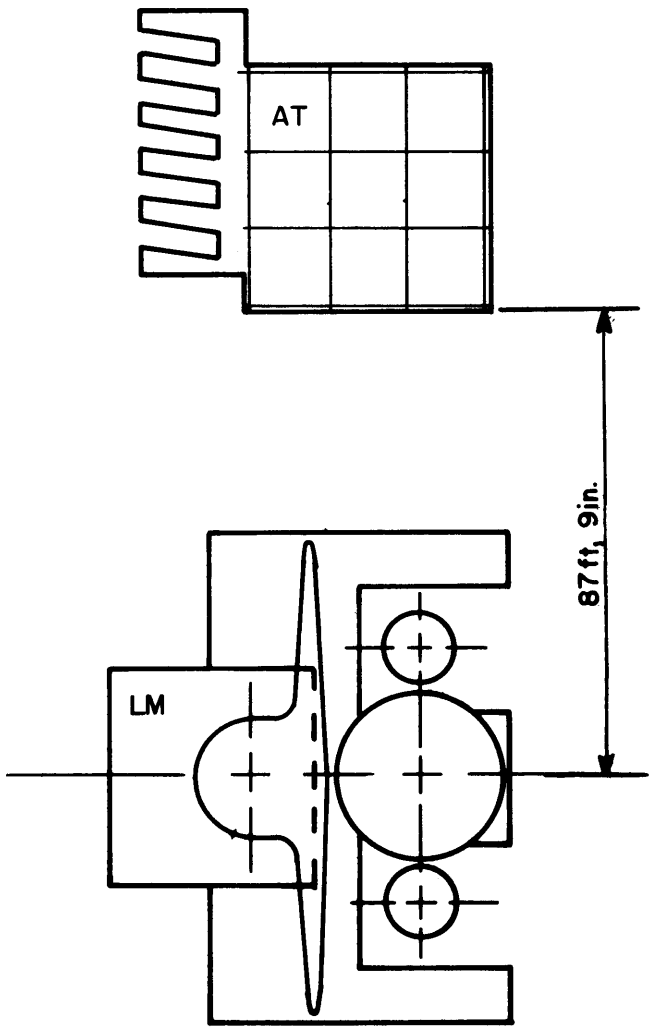

Figure 8c. Configuration C - SSV

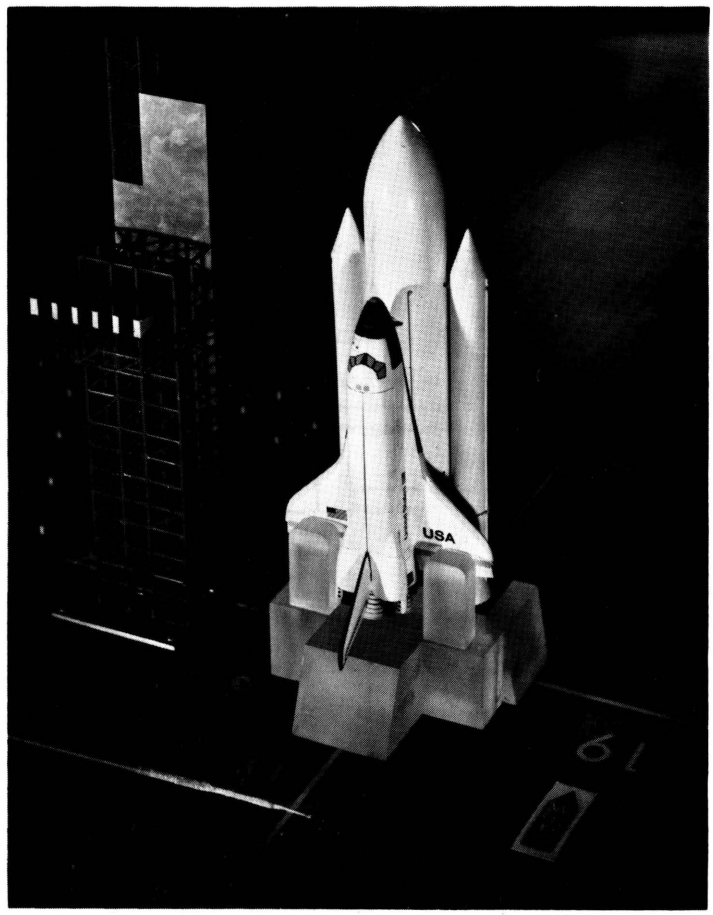

Figure 8cc. Configuration C - SSV

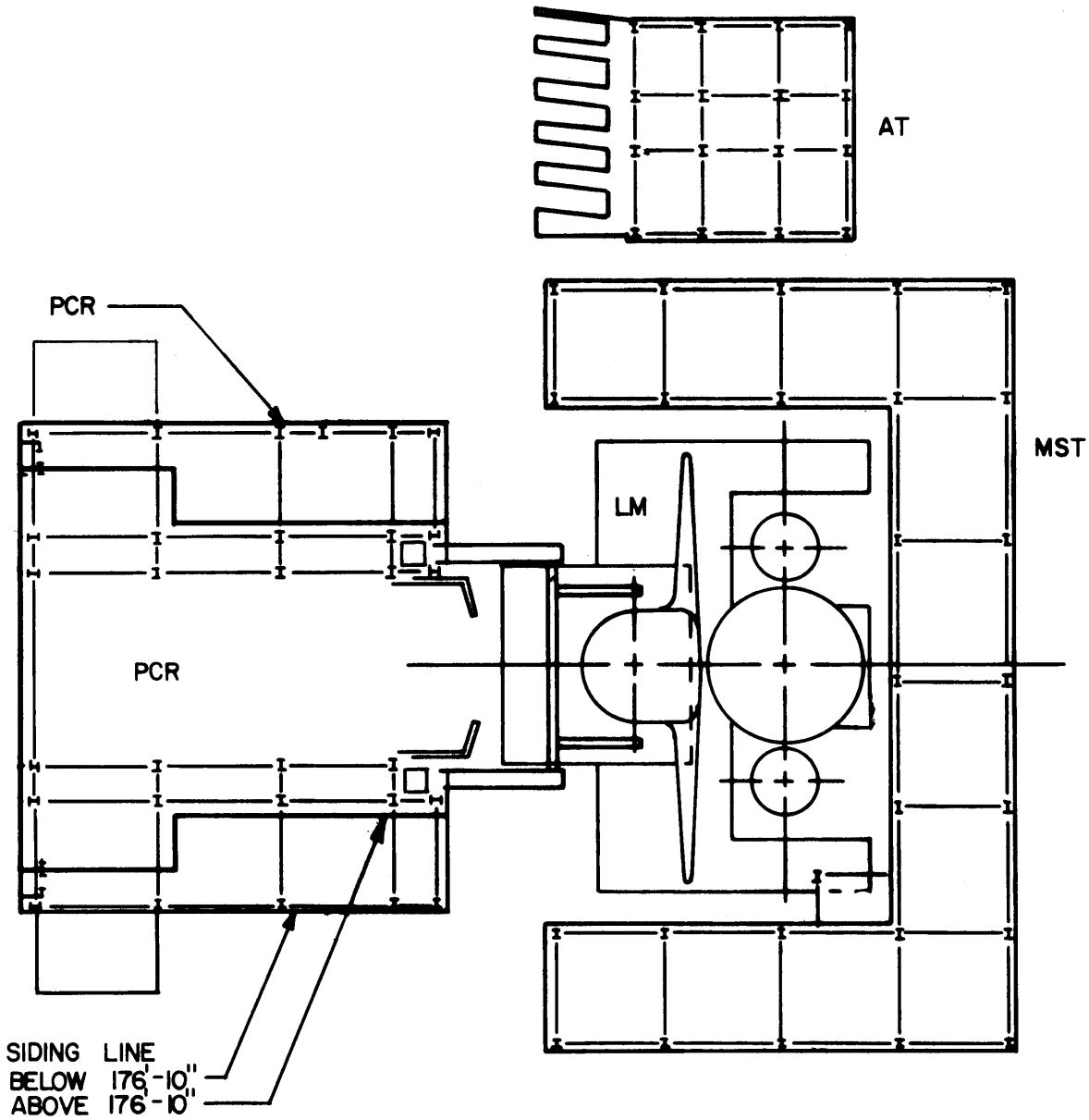

Figure 8d. Configuration E-2_2 - SSV
(Orbiter and tanks connected)

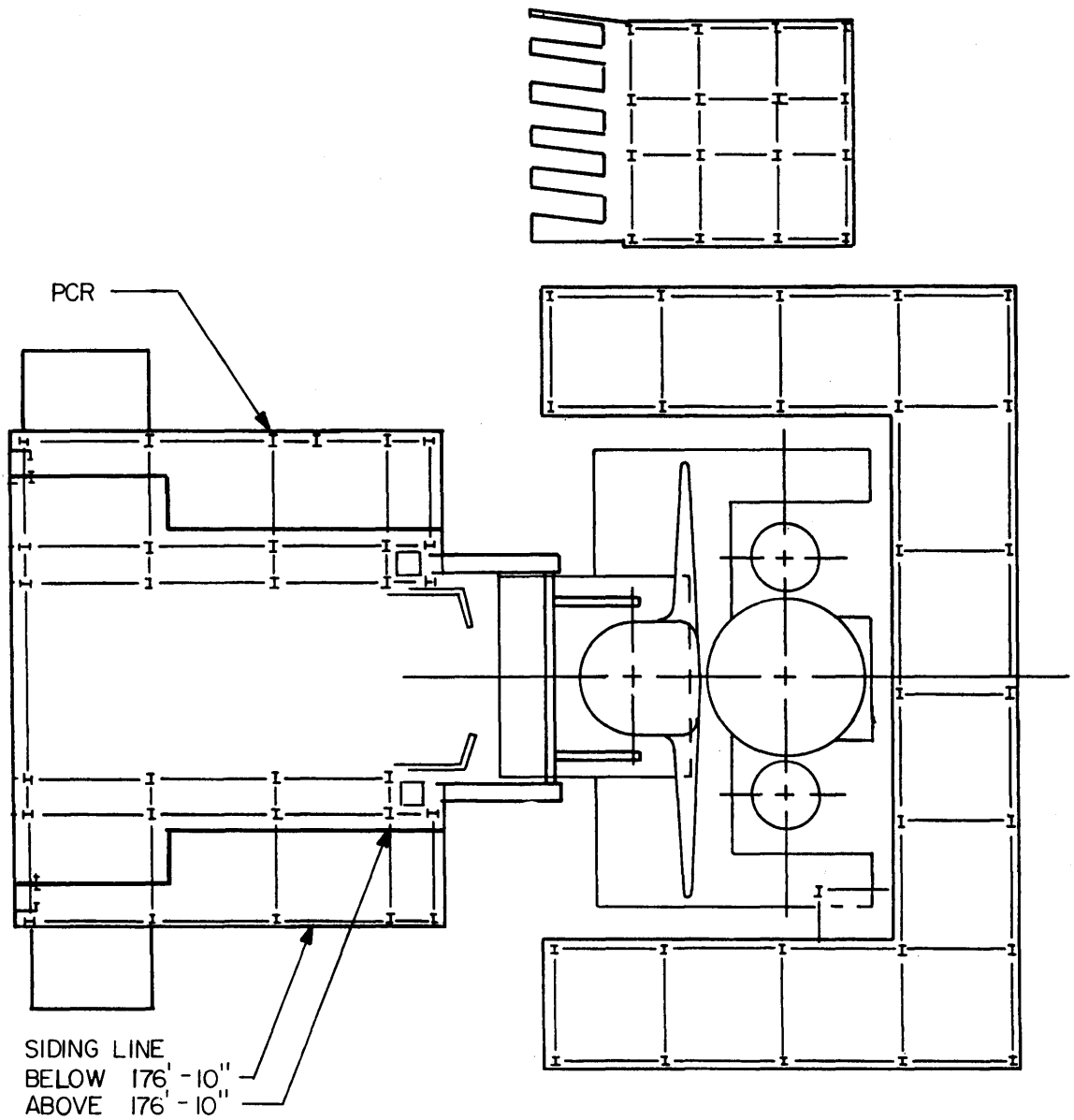

Figure 8e. Configuration E-2 - SSV
(Orbiter disconnected from tanks)

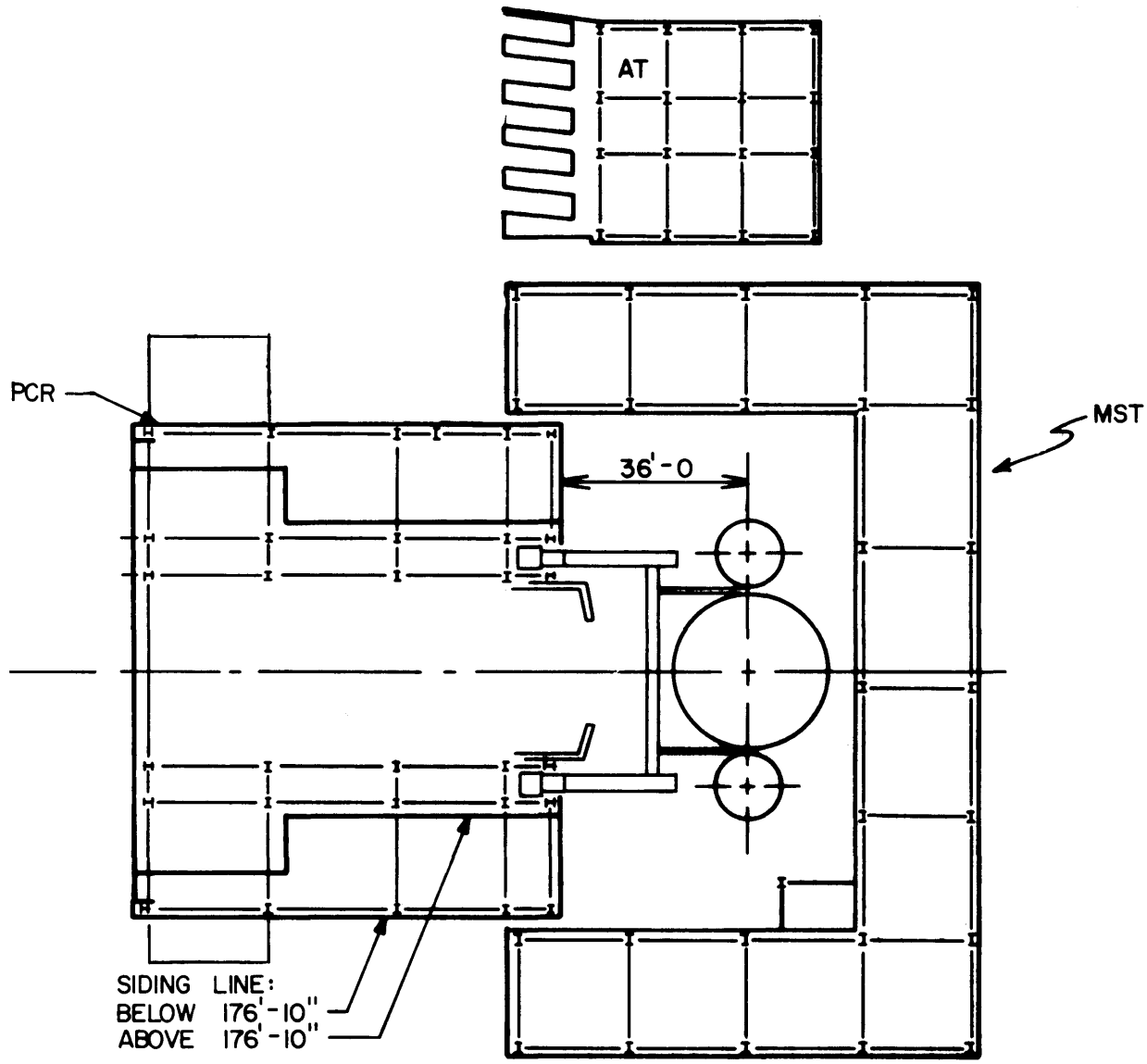

Figure 8f. Configuration D-2 - SSV

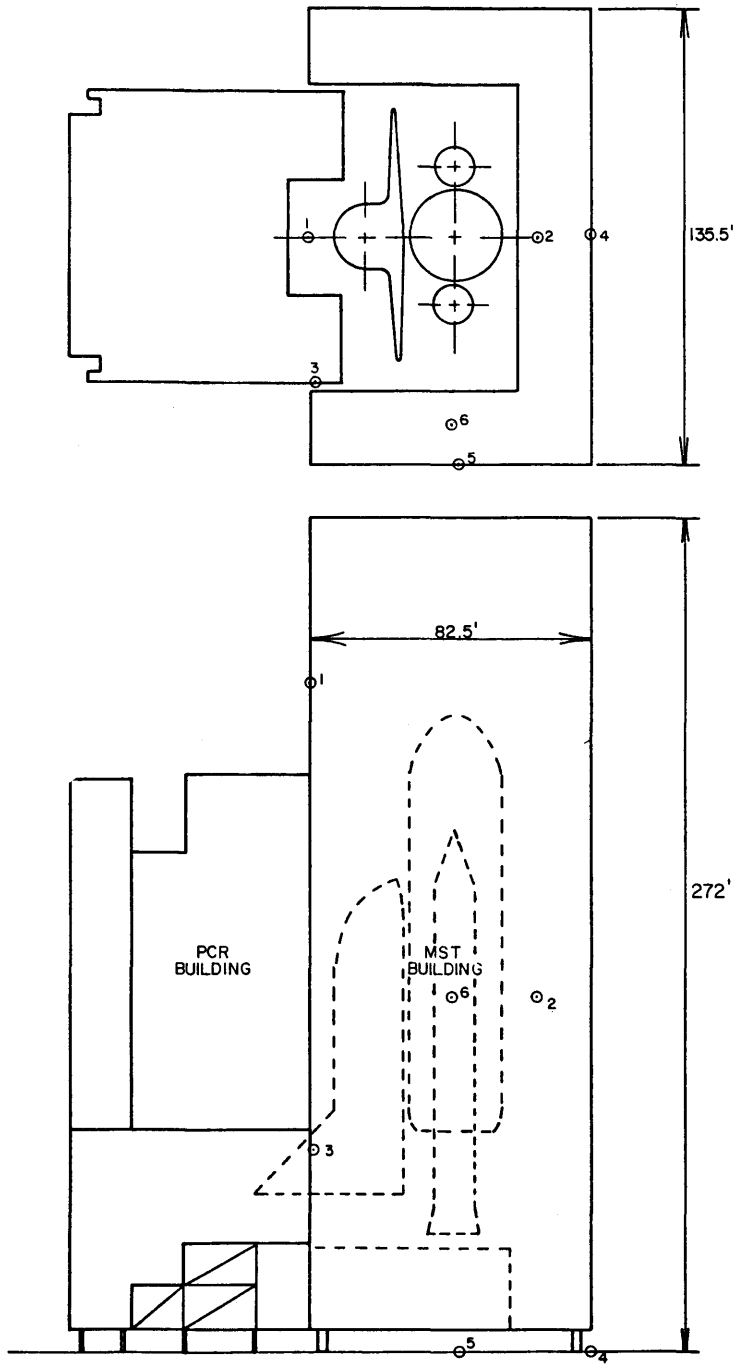

Figure 9. Strategic Velocity Positions

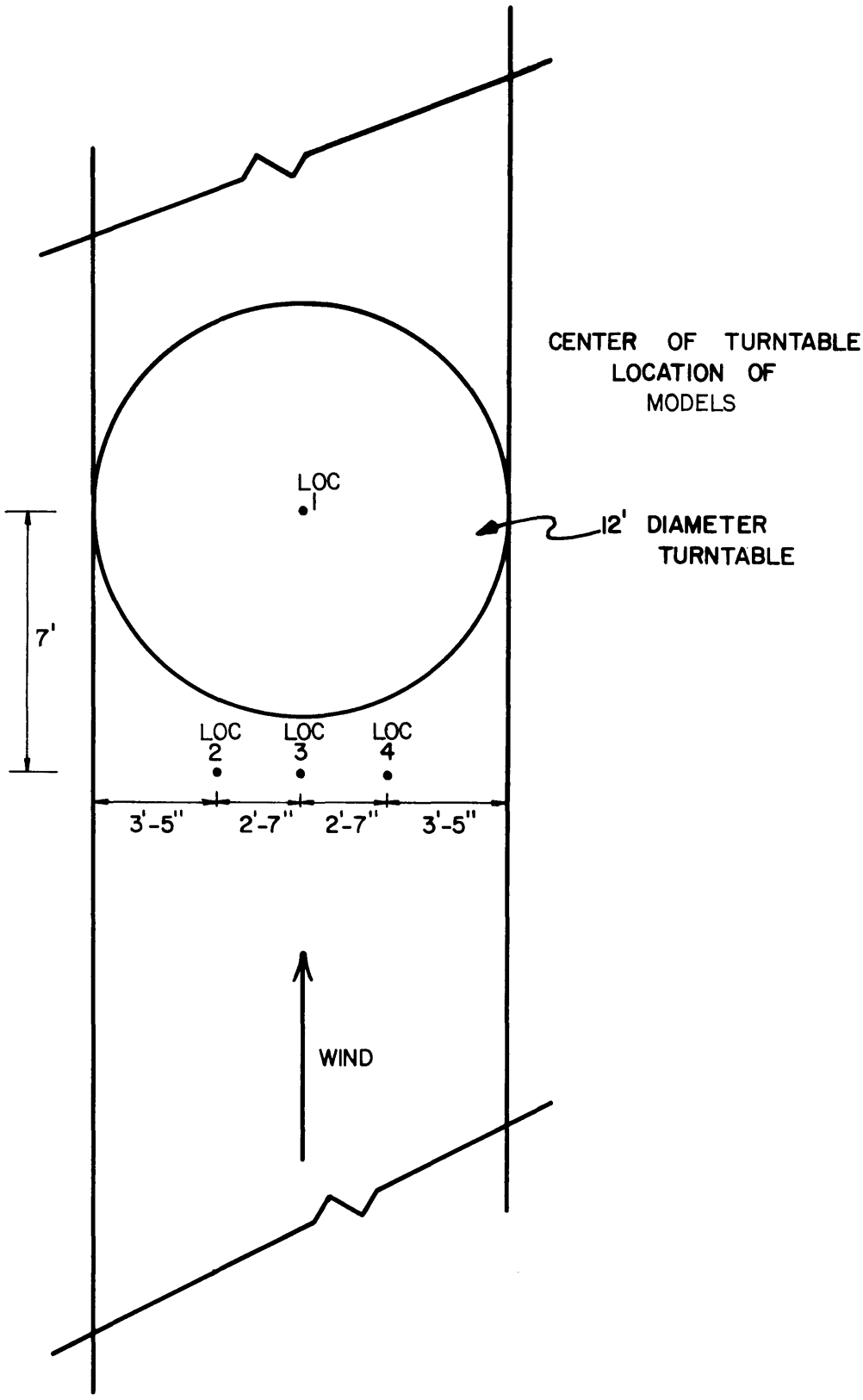

Figure 10. Locations for Velocity Profiles

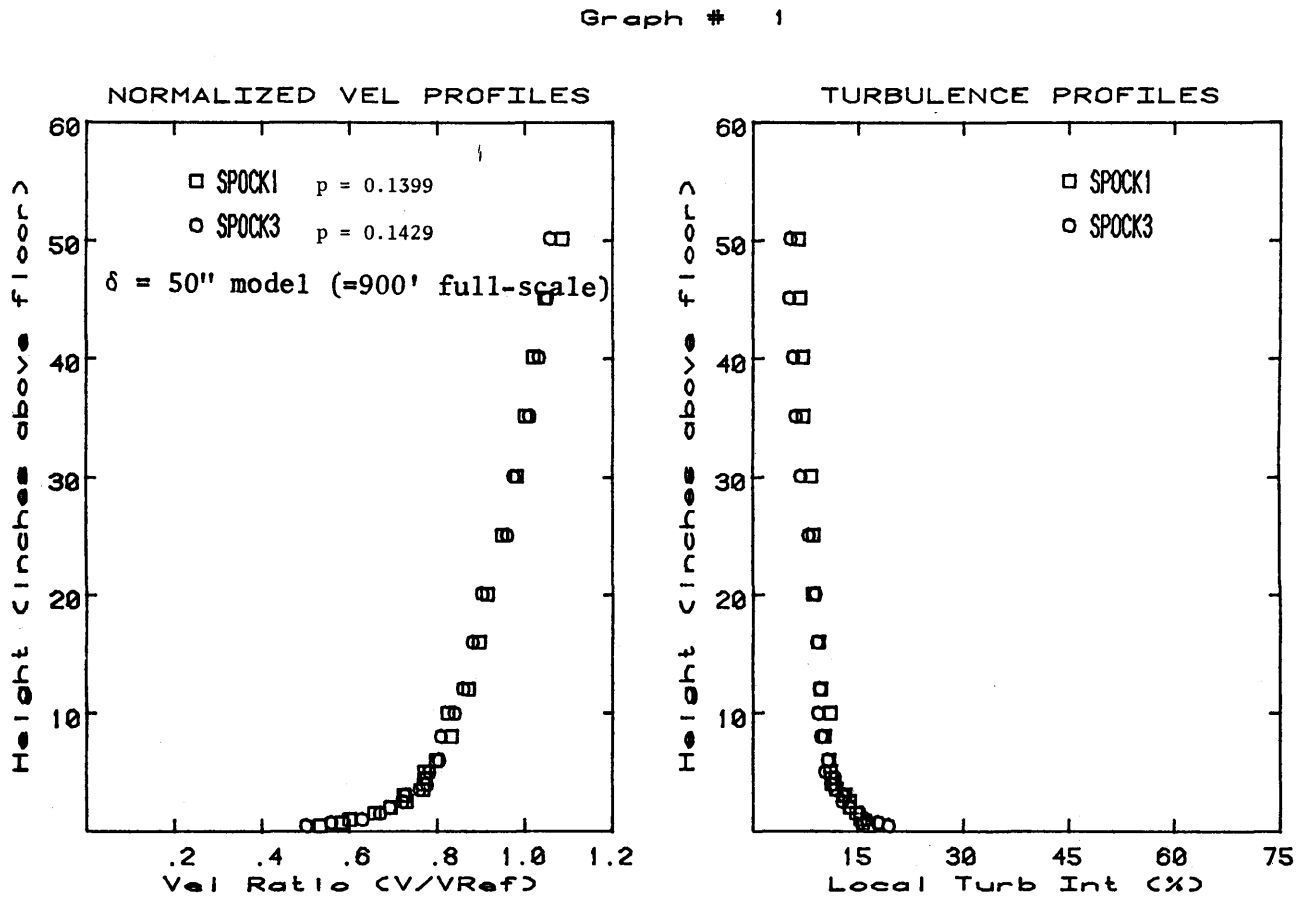

Figure 11. Velocity and Turbulence Profiles

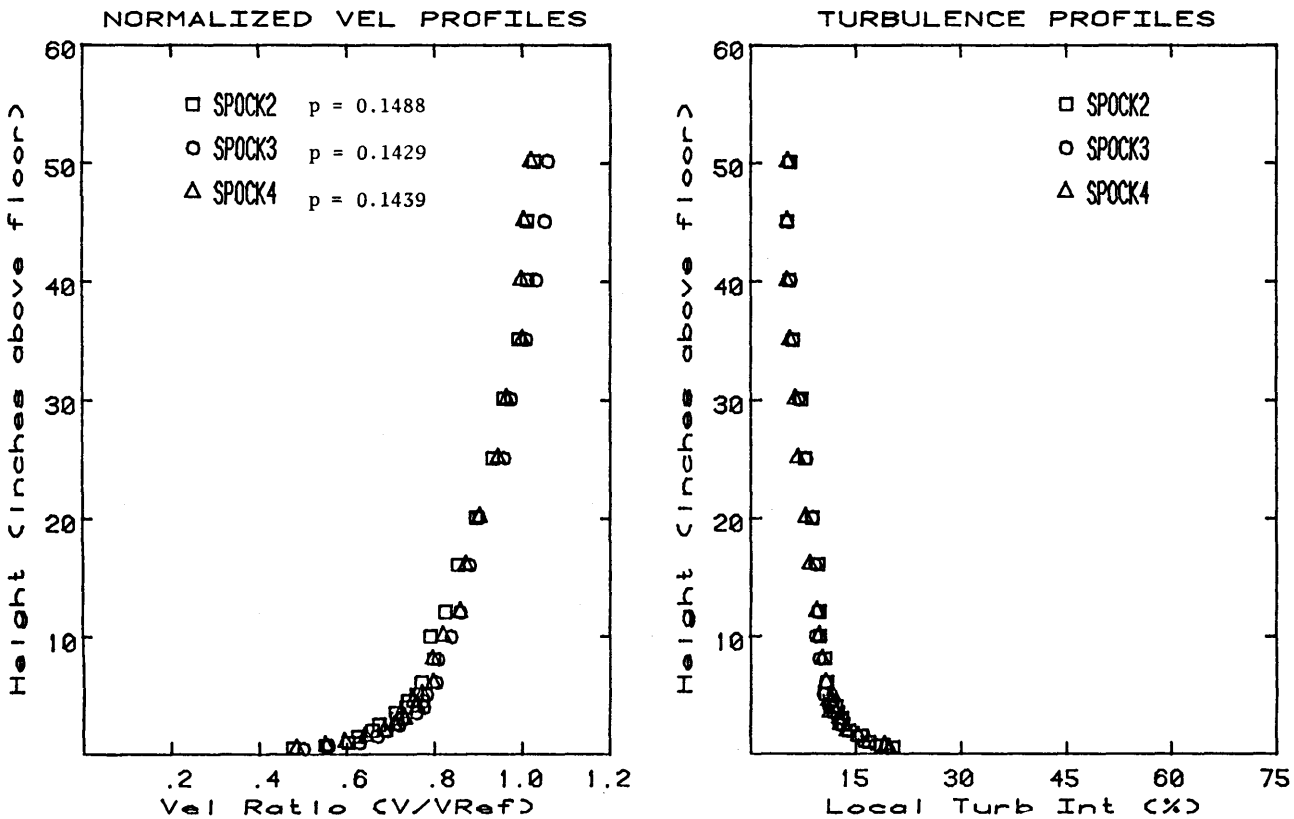

Figure 12. Velocity and Turbulence Profiles

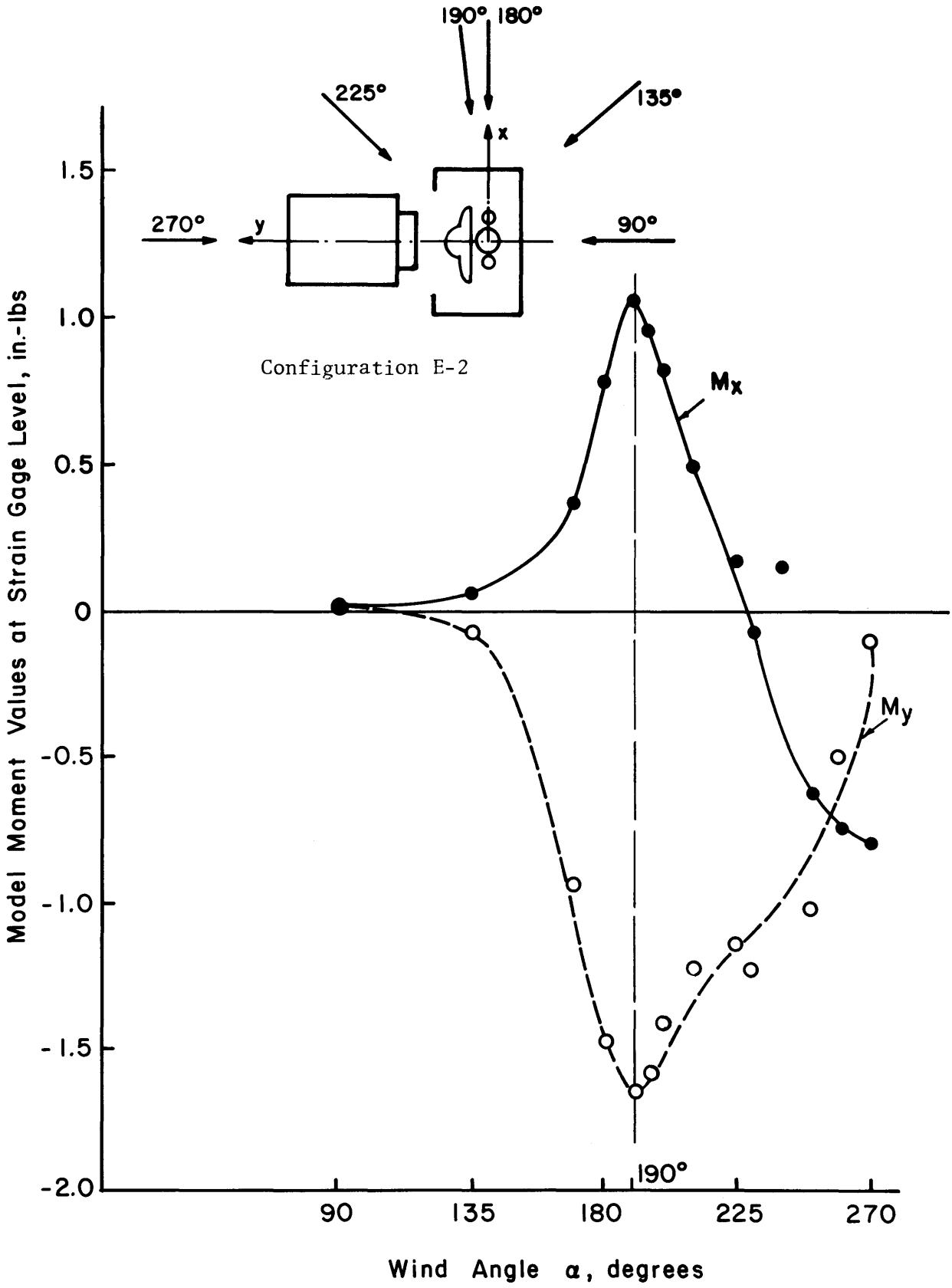

Figure 13. Location of Wind Angle to Give Maximum Moments on SSV

TABLES

Table 1. MST Cladding Loads - Configuration 5 - Mobile Service Tower (MST) Largest Value of ABS(CPMAX) or ABS(CPMAX), Peak Load Reference Pressure = 1 PSF

TAP	AZI-MUTH	PRESS COEFF	PEAK LOAD (PSF)
1001	90	3.00	3.0
1002	90	3.04	3.0
1003	90	2.48	2.5
1004	90	3.97	4.0
1005	90	2.63	2.6
1006	270	3.22	3.2
1007	270	3.75	3.8
1008	270	3.40	3.4
1009	90	2.60	2.6
1010	90	3.68	3.7
1011	270	3.29	3.3
1012	270	3.88	3.9
1013	270	3.30	3.3
1014	90	3.90	3.9
1015	270	3.05	3.0
1016	270	3.64	3.6
1017	270	3.87	3.9
1018	90	3.57	3.6
1019	270	3.31	3.3
1020	270	3.70	3.7
1021	270	3.30	3.3
1022	270	4.11	4.1
1023	270	3.28	3.3
1024	270	3.18	3.2
1025	270	2.86	2.9
1026	270	2.26	2.3
1027	180	2.60	2.6
1028	180	3.20	3.2
1029	180	3.12	3.1
1030	180	2.59	2.6
1031	180	2.66	2.7
1032	180	2.34	2.3
1033	180	2.64	2.6
1034	180	2.95	2.9
1035	180	3.45	3.5
1036	180	2.58	2.6
1037	180	2.68	2.7
1038	270	2.95	2.9
1039	270	2.71	2.7
1040	180	3.00	3.0
1041	180	2.96	3.0
1042	180	2.78	2.8
1043	180	2.47	2.5
1044	270	2.53	2.5
1045	180	2.77	2.8
1046	180	3.15	3.2
1047	180	3.68	3.7
1048	180	3.03	3.0
1049	180	3.12	3.1
1050	270	2.47	2.5
2081	270	2.15	2.2
2082	270	2.06	2.1
2084	270	2.25	2.2
2085	270	2.14	2.1
1051	270	2.42	2.4
1052	270	2.59	2.6
1053	180	2.45	2.5
1054	180	2.92	2.9
1055	180	4.16	4.2
1056	270	2.50	2.5
1057	270	3.22	3.2
1058	90	3.18	3.2
1059	90	3.19	3.2
1060	270	3.68	3.7
1061	270	2.93	2.9
1062	90	2.94	2.9
1063	90	3.49	3.5
1064	270	4.80	4.8
1065	270	3.26	3.3
1066	90	3.79	3.8
1067	90	3.86	3.9
1068	270	3.36	3.4
1069	270	3.42	3.4
1070	270	3.88	3.9
1071	270	3.65	3.7
1072	90	3.63	3.6
1073	90	3.46	3.5
1074	90	3.23	3.2
1075	270	4.00	4.0
1076	90	3.06	3.1
1077	90	2.72	2.7
1078	90	2.93	2.9
1079	90	2.66	2.7
1080	90	2.84	2.8
1081	90	3.31	3.3
1082	90	2.97	3.0
1083	225	3.38	3.4
1084	225	4.38	4.4
1085	270	2.94	2.9
1086	90	3.14	3.1
1087	270	3.32	3.3
1088	90	3.43	3.4
1089	270	3.81	3.8
1090	225	4.73	4.7
1091	270	3.90	3.9
1092	270	3.22	3.2
1093	270	2.83	2.8
1094	270	3.30	3.3
1095	135	4.85	4.9
1096	90	3.09	3.1
1097	270	3.24	3.2
1098	135	4.19	4.2
1099	135	6.56	6.6
1100	270	2.95	2.9
2086	270	2.34	2.3
2090	270	2.27	2.3
2091	270	2.18	2.2
2095	270	2.35	2.3
2001	270	2.21	2.2
2002	180	2.20	2.2
2003	180	2.12	2.1
2004	180	2.21	2.2
2005	180	2.15	2.1
2006	90	2.22	2.2
2008	90	4.42	4.4
2010	225	2.39	2.4
2012	90	4.52	4.5
2014	270	2.07	2.1
2016	90	3.40	3.4
2018	180	2.12	2.1
2020	90	3.00	3.0
2022	180	2.08	2.1
2024	90	3.03	3.0
2026	270	2.23	2.2
2027	270	2.29	2.3
2029	270	2.42	2.4
2031	270	2.16	2.2
2032	225	2.46	2.5
2035	180	2.36	2.4
2036	270	2.40	2.4
2037	270	2.29	2.3
2038	225	2.24	2.2
2039	180	2.18	2.2
2041	270	2.32	2.3
2043	270	2.19	2.2
2044	270	2.06	2.1
2047	180	2.27	2.3
2048	270	2.22	2.2
2049	135	2.16	2.2
2050	90	1.97	2.0
2051	180	2.21	2.2
2053	180	2.19	2.2
2055	180	2.13	2.1
2057	270	2.21	2.2
2059	270	2.18	2.2
2061	270	2.34	2.3
2063	270	2.26	2.3
2065	270	2.11	2.1
2067	135	2.12	2.1
2069	270	2.20	2.2
2071	180	2.13	2.1
2073	270	2.04	2.0
2075	90	2.12	2.1
2076	270	2.06	2.1
2077	180	2.22	2.2
2078	180	2.01	2.0
2079	270	1.97	2.0
2080	270	2.11	2.1
2096	270	2.19	2.2
2097	180	2.07	2.1
2099	270	2.16	2.2
2100	270	2.38	2.4

Table 2. Forces and Moments on Space Shuttle (SSV)

Configuration		Wind Angle	C_{F_x}	C_{F_y}	C_{M_x}	C_{M_y}	C_{M_z}
MST and AT	A	90	.00	.00	.00	.00	.00
	A	135	.03	.00	.00	.00	-.04
	A	180	.00	.00	.00	.00	.07
	A	225	-.26	-.03	+.04	-.08	.29
	A	270	-.03	.03	-.01	.01	.02
MST AT and PCR (close)	B	90	-.03	-.03	+.01	-.01	.02
	B	135	.03	-.03	+.01	-.01	-.02
	B	180	-.18	-.34	+.15	-.08	-.16
	B	225	.49	.03	-.01	.21	.35
	B	270	-.06	.13	-.03	-.04	.06
AT only	C	90	-.07	1.55	-.66	-.05	.13
	C	135	.52	1.02	-.31	-.35	.82
	C	180	-.53	-.29	+.20	-.29	.41
	C	225	-.93	-.80	+.46	-.49	.45
	C	270	-.29	-1.46	+.75	-.09	-.09
MST AT and PCR (moved back from SSV)	$E\text{-}2_2$	90	.00	.03	+.01	-.01	.02
	$E\text{-}2_2$	135	.03	-.03	+.01	.00	.00
	$E\text{-}2_2$	180	-.47	-.34	+.18	-.17	.50
	$E\text{-}2_2$	225	-.50	.06	+.01	-.23	.52
	$E\text{-}2_2$	270	-.06	.19	-.05	-.03	.06

Table 2 (continued)

Configuration	Wind Angle	C_{F_x}	C_{F_y}	C_{M_x}	C_{M_y}	C_{M_z}
E-2	90	-.10	-.03	.02	.02	.00
Shuttle Not Connected to External Tanks	135	.03	-.10	.05	-.05	.00
	170	---	---	.08	-.31	.14
	180	-1.04	-.73	.10	-.48	-.14
Measurements on Shuttle Only	190	---	---	.13	-.53	-.28
	200	---	---	.10	-.45	-.21
	225	-.93	.10	.05	-.29	-.14
	270	-.10	.62	-.21	-.02	-.07
D-2	90	-.05	-.04	.01	.01	.00
Measurements on External Tank Only	135	.03	-.04	.01	.01	.00
	180	-.10	-.11	.02	.07	.00
	225	-.20	.12	.04	.06	.00
	270	-.04	.06	.01	.01	.00

--- No measurement

Note: Where the coefficients listed in Table 2, page 90 are less than about 0.03, the corresponding voltage readings were less than about 5-10 mV. Any voltage readings below these are considered to be at the lower bounds of probable values and hence such coefficients given are to be used only as approximate estimates of true values.

Table 3. Wind Velocites and Turbulence Intensities
SSV - Configuration B

Key: 1V means the y-z plane velocity components at location 1
1H means the horizontal velocity components at location 2
U_H = velocity at building height = U_{272} (full scale)

WIND AZIMUTH	U_{mean}/U_H (percent)	U_{rms}/U_H (percent)	U_{peak}/U_H (percent)
Location 1V			
90.00	15.6	5.4	31.8
135.00	19.8	5.2	35.4
180.00	18.4	5.0	33.4
225.00	33.8	4.1	46.1
270.00	49.9	6.8	70.3
Location 1H			
90.00	20.7	8.6	46.5
135.00	26.5	8.4	51.7
180.00	29.8	8.1	54.1
225.00	85.8	7.5	108.3
270.00	54.5	7.3	76.5
Location 2V			
90.00	29.5	8.8	55.9
135.00	17.0	5.4	33.2
180.00	29.2	8.9	55.9
225.00	39.0	14.2	81.6
270.00	55.7	7.2	77.3
Location 2H			
90.00	20.8	4.2	33.4
135.00	15.4	4.2	28.0
180.00	33.3	11.2	66.9
225.00	29.0	9.8	58.4
270.00	24.5	3.5	35.0
Location 3V			
90.00	18.8	8.0	42.8
135.00	26.9	6.8	47.3
180.00	21.5	8.3	46.4
225.00	80.1	14.9	124.8
270.00	74.2	15.5	120.7
Location 3H			

Table 3 (continued)

WIND AZIMUTH	U_{mean}/U_H (percent)	U_{rms}/U_H (percent)	U_{peak}/U_H (percent)
Location 3H			
90.00	18.7	7.3	40.6
135.00	25.3	7.5	47.8
180.00	23.7	8.0	47.7
225.00	73.4	17.5	125.9
270.00	64.0	17.1	115.3
Location 4V			
90.00	71.2	6.0	89.2
135.00	55.0	4.1	67.3
180.00	27.6	11.8	63.0
225.00	82.1	10.7	114.2
270.00	102.5	9.4	130.7
Location 4H			
90.00	52.3	3.6	63.1
135.00	50.0	4.2	62.6
180.00	15.7	6.2	34.3
225.00	44.2	7.2	65.8
270.00	55.9	5.6	72.7
Location 5V			
90.00	63.5	19.2	121.1
135.00	63.8	16.2	112.4
180.00	15.2	5.3	31.1
225.00	58.2	18.6	114.0
270.00	82.0	23.9	153.7
Location 5H			
90.00	51.8	12.5	89.3
135.00	49.4	9.6	78.2
180.00	9.0	2.7	17.1
225.00	27.7	10.9	60.4
270.00	40.1	15.7	87.2
Location 6V			
90.00	12.7	3.3	22.6
135.00	20.4	6.2	39.0
180.00	16.8	4.9	31.5
225.00	27.7	10.2	58.3
270.00	39.6	12.8	78.0

Table 3 (continued)

WIND AZIMUTH	U_{mean}/U_H (percent)	U_{rms}/U_H (percent)	U_{peak}/U_H (percent)
Location 6H			
90.00	12.2	3.1	21.5
135.00	16.8	4.4	30.0
180.00	18.2	5.2	33.8
225.00	24.0	8.0	48.0
270.00	24.8	6.5	44.3

APPENDIX A

APPENDIX A

FORCE AND MOMENT COEFFICIENTS FOR M.S.T. BUILDING CONFIG ONE

---COEFFICIENTS TO BE USED WITH FULL SCALE WIND VELOCITY AT 30 FEET---

WIND DIRECTION = 90

CFX	CFY	CMX	CMY	CMZ
-.05	2.25	-1.04	-.07	-.00

WIND DIRECTION = 135

CFX	CFY	CMX	CMY	CMZ
1.19	1.95	-.87	1.01	-.04

WIND DIRECTION = 180

CFX	CFY	CMX	CMY	CMZ
1.86	.02	.21	1.41	-.01

WIND DIRECTION = 225

CFX	CFY	CMX	CMY	CMZ
1.92	-1.53	1.09	1.42	-.00

WIND DIRECTION = 270

CFX	CFY	CMX	CMY	CMZ
.13	-2.36	1.48	.05	-.00

APPENDIX A

FORCE AND MOMENT COEFFICIENTS FOR M.S.T. BUILDING CONFIG ONE A

---COEFFICIENTS TO BE USED WITH FULL SCALE WIND VELOCITY AT 30 FEET---

WIND DIRECTION = 90

CFX	CFY	CMX	CMY	CMZ
-.02	2.26	-1.01	-.03	.00

WIND DIRECTION = 135

CFX	CFY	CMX	CMY	CMZ
1.41	1.98	-.85	1.14	-.04

WIND DIRECTION = 180

CFX	CFY	CMX	CMY	CMZ
1.86	-.06	.27	1.48	-.02

WIND DIRECTION = 225

CFX	CFY	CMX	CMY	CMZ
1.95	-1.43	1.11	1.52	-.01

WIND DIRECTION = 270

CFX	CFY	CMX	CMY	CMZ
.10	-1.97	1.35	.05	-.01

APPENDIX A

FORCE AND MOMENT COEFFICIENTS FOR M.S.T. BUILDING CONFIG TWO

---COEFFICIENTS TO BE USED WITH FULL SCALE WIND VELOCITY AT 30 FEET---

WIND DIRECTION = 90

CFX	CFY	CMX	CMY	CMZ
.01	2.08	-.93	-.01	.00

WIND DIRECTION = 135

CFX	CFY	CMX	CMY	CMZ
1.25	1.90	-.80	1.00	-.04

WIND DIRECTION = 180

CFX	CFY	CMX	CMY	CMZ
1.87	.06	-.06	1.41	-.01

WIND DIRECTION = 225

CFX	CFY	CMX	CMY	CMZ
1.83	-1.34	.87	1.42	-.02

WIND DIRECTION = 270

CFX	CFY	CMX	CMY	CMZ
-.05	-1.96	1.12	.04	-.01

APPENDIX A

FORCE AND MOMENT COEFFICIENTS FOR M.S.T. BUILDING CONFIG THREE

---COEFFICIENTS TO BE USED WITH FULL SCALE WIND VELOCITY AT 30 FEET---

WIND DIRECTION = 90

CFX	CFY	CMX	CMY	CMZ
.03	1.72	-.74	.01	.00

WIND DIRECTION = 135

CFX	CFY	CMX	CMY	CMZ
2.02	1.44	-.56	1.41	-.00

WIND DIRECTION = 180

CFX	CFY	CMX	CMY	CMZ
1.77	.17	.12	1.43	-.02

WIND DIRECTION = 225

CFX	CFY	CMX	CMY	CMZ
2.44	-.90	.72	1.73	-.04

WIND DIRECTION = 270

CFX	CFY	CMX	CMY	CMZ
-.01	-1.41	.98	.09	-.00

APPENDIX A

FORCE AND MOMENT COEFFICIENTS FOR M.S.T. BUILDING CONFIG FOUR

---COEFFICIENTS TO BE USED WITH FULL SCALE WIND VELOCITY AT 30 FEET---

WIND DIRECTION = 90

CFX	CFY	CMX	CMY	CMZ
.03	1.78	-.77	.00	.00

WIND DIRECTION = 135

CFX	CFY	CMX	CMY	CMZ
1.57	1.60	-.59	1.23	-.03

WIND DIRECTION = 180

CFX	CFY	CMX	CMY	CMZ
1.83	.13	.13	1.41	-.02

WIND DIRECTION = 225

CFX	CFY	CMX	CMY	CMZ
1.93	-.87	.66	1.40	-.03

WIND DIRECTION = 270

CFX	CFY	CMX	CMY	CMZ
-.05	-1.71	1.04	.03	-.00

APPENDIX A

FORCE AND MOMENT COEFFICIENTS FOR M.S.T. BUILDING CONFIG FIVE

---COEFFICIENTS TO BE USED WITH FULL SCALE WIND VELOCITY AT 30 FEET---

WIND DIRECTION = 90

CFX	CFY	CMX	CMY	CMZ
-.01	1.94	-.87	-.01	.00

WIND DIRECTION = 135

CFX	CFY	CMX	CMY	CMZ
1.17	1.59	-.75	.87	-.04

WIND DIRECTION = 180

CFX	CFY	CMX	CMY	CMZ
1.67	-.14	.19	1.20	-.00

WIND DIRECTION = 225

CFX	CFY	CMX	CMY	CMZ
1.75	-1.50	1.01	1.31	-.01

WIND DIRECTION = 270

CFX	CFY	CMX	CMY	CMZ
-.05	-1.98	1.37	.07	-.01

APPENDIX B

APPENDIX B -- PRESSURE DATA: MOBILE SERVICE TOWER (M.S.T.)

WD	TAP	CPMEAN	CPRMS	CPMAX	CPMIN
90	1001	-1.471	.303	-.395	-2.998
90	1002	-1.334	.288	-.515	-3.044
90	1003	-1.298	.318	-.440	-2.476
90	1004	-1.440	.356	-.386	-3.974
90	1005	-1.499	.261	-.588	-2.633
90	1006	-1.604	.338	-.263	-2.999
90	1007	-1.750	.341	-.524	-3.326
90	1008	-1.846	.335	-.855	-3.242
90	1009	-1.609	.275	-.754	-2.597
90	1010	-1.651	.377	-.675	-3.676
90	1011	-1.578	.312	-.611	-2.833
90	1012	-1.587	.307	-.755	-2.818
90	1013	-1.445	.285	-.571	-3.561
90	1014	-1.681	.410	-.561	-3.903
90	1015	-1.588	.323	-.612	-2.967
90	1016	-1.644	.293	-.757	-2.577
90	1017	-1.389	.265	-.620	-2.314
90	1018	-1.654	.373	-.613	-3.570
90	1019	-1.640	.319	-.583	-2.958
90	1020	-1.725	.308	-.710	-2.848
90	1021	-1.460	.276	-.459	-2.414
90	1022	-1.428	.275	-.519	-2.653
90	1023	-1.624	.302	-.653	-2.838
90	1024	-1.683	.306	-.759	-2.889
90	1025	-1.580	.303	-.605	-2.687
90	1026	.724	.280	1.552	-.372
90	1027	.869	.290	1.787	-.356
90	1028	.872	.299	1.834	-.280
90	1029	.941	.282	1.918	-.113
90	1030	.933	.283	1.795	-.006
90	1031	.768	.286	1.647	-.160
90	1032	.823	.259	1.700	-.061
90	1033	1.227	.266	2.033	.303
90	1034	1.340	.268	2.269	.333
90	1035	1.359	.260	2.240	.344
90	1036	1.255	.278	2.082	.281
90	1037	.844	.271	1.808	-.020
90	1038	.733	.240	1.604	-.385
90	1039	1.148	.250	1.996	.008
90	1040	1.279	.260	2.175	.109
90	1041	1.307	.249	2.009	.248
90	1042	1.217	.255	2.051	.373
90	1043	.769	.257	1.700	-.077
90	1044	.596	.228	1.407	-.125
90	1045	.969	.242	1.793	.282
90	1046	1.077	.258	2.090	.303
90	1047	1.131	.245	2.027	.396
90	1048	1.045	.263	2.001	.232
90	1049	.608	.277	1.807	-.253
90	1050	.401	.254	1.338	-.505

WD	TAP	CPMEAN	CPRMS	CPMAX	CPMIN
90	1051	.724	.258	1.675	-.136
90	1052	.827	.265	1.755	-.006
90	1053	.878	.259	1.791	.089
90	1054	.778	.253	1.532	-.048
90	1055	.381	.266	1.287	-.481
90	1056	-1.717	.188	-1.214	-2.394
90	1057	-1.566	.274	-.714	-2.437
90	1058	-1.601	.310	-.737	-3.175
90	1059	-1.627	.335	-.020	-3.186
90	1060	-1.596	.318	-.614	-2.790
90	1061	-1.582	.323	-.571	-2.816
90	1062	-1.545	.328	-.634	-2.939
90	1063	-1.759	.399	-.625	-3.494
90	1064	-1.691	.308	-.685	-3.054
90	1065	-1.556	.306	-.646	-2.767
90	1066	-1.600	.382	-.561	-3.795
90	1067	-1.874	.472	-.260	-3.855
90	1068	-1.823	.381	-.822	-3.313
90	1069	-1.679	.375	-.601	-3.203
90	1070	-1.615	.346	-.600	-3.028
90	1071	-1.781	.394	-.281	-3.576
90	1072	-1.855	.374	-.489	-3.627
90	1073	-1.742	.350	-.455	-3.463
90	1074	-1.571	.347	-.740	-3.235
90	1075	-1.524	.318	-.509	-2.795
90	1076	-1.329	.316	-.447	-3.065
90	1077	-1.261	.293	-.463	-2.722
90	1078	-1.175	.343	-.326	-2.928
90	1079	-1.284	.292	-.355	-2.660
90	1080	-1.428	.267	-.537	-2.837
90	1081	-1.801	.335	-.596	-3.314
90	1082	-1.747	.320	-.656	-2.974
90	1083	-1.917	.357	-.570	-3.285
90	1084	-1.786	.307	-.653	-2.933
90	1085	-1.753	.312	-.631	-2.860
90	1086	-1.718	.325	-.807	-3.145
90	1087	-1.710	.301	-.745	-2.803
90	1088	-1.741	.311	-.780	-3.435
90	1089	-1.681	.303	-.757	-3.178
90	1090	-1.793	.356	-.714	-3.314
90	1091	-1.778	.337	-.805	-3.541
90	1092	-1.640	.278	-.838	-2.748
90	1093	-1.658	.277	-.804	-2.685
90	1094	-1.648	.271	-.890	-3.068
90	1095	-1.684	.264	-.810	-3.041
90	1096	-1.840	.296	-.917	-3.088
90	1097	-1.682	.251	-.948	-2.594
90	1098	-1.713	.252	-.965	-2.741
90	1099	-1.709	.261	-.981	-3.824
90	1100	-1.760	.253	-.725	-2.507

WD	TAP	CPMEAN	CPRMS	CPMAX	CPMIN
90	2001	-1.196	.230	-.458	-2.116
90	2002	-1.198	.205	-.540	-1.882
90	2003	-1.149	.211	-.428	-1.957
90	2004	-1.210	.197	-.612	-1.930
90	2005	-1.173	.237	-.256	-1.957
90	2006	-1.319	.242	-.609	-2.216
90	2008	-1.601	.383	-.664	-4.418
90	2010	-1.155	.206	-.489	-1.880
90	2012	-1.555	.334	-.699	-4.523
90	2014	-1.074	.205	-.414	-1.961
90	2016	-1.411	.320	-.565	-3.398
90	2018	-1.129	.221	-.454	-1.903
90	2020	-1.512	.324	-.691	-2.997
90	2022	-1.120	.228	-.262	-1.901
90	2024	-1.476	.302	-.571	-3.034
90	2026	-1.045	.221	-.234	-1.894
90	2027	-1.135	.228	-.219	-2.007
90	2029	-1.081	.225	-.271	-1.861
90	2031	-1.182	.203	-.531	-1.837
90	2032	-1.067	.221	-.333	-1.809
90	2035	-1.157	.227	-.402	-1.901
90	2036	-1.063	.216	-.318	-1.880
90	2037	-1.139	.210	-.449	-1.882
90	2038	-.988	.205	-.117	-1.800
90	2039	-1.099	.218	-.173	-1.863
90	2041	-.998	.209	-.090	-1.780
90	2043	-1.066	.216	-.354	-1.927
90	2044	-1.086	.231	-.403	-1.826
90	2047	-1.136	.229	-.258	-1.887
90	2048	-1.062	.236	-.249	-1.903
90	2049	-1.208	.232	-.438	-2.026
90	2050	-1.040	.214	-.339	-1.965
90	2051	-1.157	.229	-.380	-2.160
90	2053	-1.090	.220	-.397	-2.079
90	2055	-1.105	.235	-.327	-1.906
90	2057	-1.130	.222	-.417	-1.848
90	2059	-1.290	.237	-.475	-2.121
90	2061	-1.164	.226	-.430	-1.972
90	2063	-1.220	.222	-.420	-1.970
90	2065	-1.065	.215	-.358	-1.889
90	2067	-1.157	.220	-.341	-1.901
90	2069	-1.128	.236	-.283	-1.937
90	2071	-1.245	.232	-.475	-1.934
90	2073	-1.093	.221	-.372	-1.801
90	2075	-1.151	.235	-.434	-2.120
90	2076	-1.108	.226	-.297	-1.781
90	2077	-1.220	.212	-.529	-1.887
90	2078	-1.118	.208	-.479	-1.962
90	2079	-1.144	.186	-.561	-1.861
90	2080	-1.088	.227	-.410	-1.839

APPENDIX B -- PRESSURE DATA: MOBILE SERVICE TOWER (M.S.T.)

WD	TAP	CPMEAN	CPRMS	CPMAX	CPMIN
90	2081	-1.302	.210	-.623	-2.075
90	2082	-1.239	.207	-.483	-1.853
90	2084	-1.214	.210	-.599	-1.824
90	2085	-1.202	.207	-.520	-1.996
90	2086	-1.152	.234	-.297	-1.993
90	2090	-1.053	.222	-.359	-1.940
90	2091	-1.053	.215	-.354	-1.747
90	2095	-1.024	.208	-.364	-1.709
90	2096	-1.123	.224	-.404	-1.823
90	2097	-1.182	.203	-.509	-1.897
90	2099	-1.120	.191	-.542	-1.827
90	2100	-1.102	.217	-.421	-1.799
135	1001	-1.303	.196	-.604	-2.063
135	1002	-1.322	.200	-.621	-2.101
135	1003	-1.334	.217	-.438	-2.050
135	1004	-1.404	.268	-.292	-2.267
135	1005	-1.460	.216	-.794	-2.232
135	1006	-1.126	.195	-.493	-1.757
135	1007	-1.162	.191	-.577	-1.802
135	1008	-1.252	.215	-.534	-2.021
135	1009	-1.092	.189	-.473	-1.795
135	1010	-1.143	.190	-.425	-1.804
135	1011	-1.196	.185	-.552	-1.867
135	1012	-1.204	.209	-.439	-1.920
135	1013	-1.111	.203	-.326	-1.793
135	1014	-1.047	.191	-.395	-1.725
135	1015	-1.135	.206	-.441	-1.915
135	1016	-1.222	.208	-.496	-1.891
135	1017	-1.028	.198	-.366	-1.727
135	1018	-.995	.215	-.342	-1.725
135	1019	-1.077	.211	-.356	-1.825
135	1020	-1.149	.215	-.450	-1.880
135	1021	-.923	.198	-.296	-1.603
135	1022	-1.236	.245	-.460	-2.276
135	1023	-1.182	.258	-.200	-2.213
135	1024	-1.089	.232	-.144	-1.928
135	1025	-.952	.211	-.032	-1.636
135	1026	-.193	.196	.455	-.756
135	1027	.040	.208	.688	-.605
135	1028	.114	.214	.842	-.590
135	1029	.257	.201	1.149	-.408
135	1030	.425	.243	1.232	-.388
135	1031	.702	.250	1.531	-.060
135	1032	-.214	.193	.508	-.885
135	1033	.205	.201	.931	-.468
135	1034	.426	.194	1.209	-.230
135	1035	.668	.196	1.408	.088
135	1036	.894	.242	1.738	-.155
135	1037	1.145	.264	1.910	-.006
135	1038	-.189	.188	.397	-.906
135	1039	.183	.199	.808	-.624
135	1040	.370	.198	1.030	-.366
135	1041	.648	.195	1.368	-.006
135	1042	.882	.231	1.619	-.046
135	1043	1.100	.265	1.987	.134
135	1044	-.158	.193	.585	-.825
135	1045	.178	.201	.876	-.524
135	1046	.345	.197	1.038	-.378
135	1047	.608	.196	1.394	-.032
135	1048	.791	.232	1.498	-.127
135	1049	.975	.261	1.911	.008
135	1050	-.169	.189	.475	-.754
135	1051	.064	.193	.730	-.547
135	1052	.219	.194	.920	-.393
135	1053	.389	.186	1.059	-.164
135	1054	.546	.211	1.236	-.219
135	1055	.661	.236	1.451	-.228
135	1056	.614	.201	1.411	-.145
135	1057	.395	.256	1.369	-.434
135	1058	.227	.223	.889	-.572
135	1059	-.133	.206	.525	-.904
135	1060	1.069	.274	1.824	.203
135	1061	.750	.236	1.435	-.019
135	1062	.445	.232	1.171	-.398
135	1063	-.118	.212	.581	-.859
135	1064	.953	.295	2.008	.109
135	1065	.689	.250	1.622	-.086
135	1066	.383	.221	1.189	-.355
135	1067	-.168	.223	.696	-.848
135	1068	.767	.284	1.854	-.121
135	1069	.567	.241	1.526	-.125
135	1070	.279	.220	1.041	-.556
135	1071	-.255	.210	.372	-.972
135	1072	.501	.240	1.625	-.255
135	1073	.316	.212	1.256	-.321
135	1074	.148	.207	.889	-.593
135	1075	-.280	.201	.494	-1.033
135	1076	-1.088	.197	-.317	-1.757
135	1077	-1.141	.201	-.393	-1.740
135	1078	-1.136	.209	-.486	-1.753
135	1079	-1.305	.205	-.389	-2.026
135	1080	-1.215	.190	-.611	-1.978
135	1081	-1.062	.237	-.117	-2.118
135	1082	-.998	.196	-.369	-1.752
135	1083	-1.041	.206	-.352	-1.819
135	1084	-1.037	.246	-.292	-2.109
135	1085	-1.585	.209	-.932	-2.246
135	1086	-1.270	.317	-.213	-2.535
135	1087	-.738	.232	-.059	-1.687
135	1088	-.797	.205	-.059	-1.513
135	1089	-.762	.214	.034	-1.432
135	1090	-2.250	.315	-1.110	-3.332
135	1091	-1.482	.267	-.638	-2.428
135	1092	-1.905	.335	-.641	-2.994
135	1093	-.877	.311	.155	-2.248
135	1094	-.904	.183	-.274	-1.577
135	1095	-3.283	.436	-1.621	-4.853
135	1096	-1.294	.223	-.564	-2.305
135	1097	-1.958	.309	-.929	-2.930
135	1098	-2.991	.413	-1.241	-4.188
135	1099	-4.459	.657	-1.713	-6.555
135	1100	-1.515	.220	-.825	-2.185
135	2001	-1.343	.194	-.648	-1.988
135	2002	-1.235	.190	-.591	-1.835
135	2003	-1.207	.190	-.598	-1.965
135	2004	-1.210	.209	-.395	-2.004
135	2005	-.905	.244	-.110	-1.822
135	2006	-1.215	.199	-.595	-1.898
135	2008	-1.254	.250	-.263	-2.016
135	2010	-1.246	.190	-.567	-1.890
135	2012	-1.190	.242	-.299	-2.098
135	2014	-1.097	.196	-.498	-1.767
135	2016	-1.098	.240	-.229	-2.071
135	2018	-1.129	.200	-.434	-1.846
135	2020	-1.183	.235	-.447	-2.056
135	2022	-.926	.226	-.083	-1.632
135	2024	-1.154	.238	-.265	-1.925
135	2026	-1.180	.201	-.527	-1.884
135	2027	-1.248	.207	-.572	-2.023
135	2029	-1.141	.198	-.561	-1.916
135	2031	-1.212	.213	-.413	-1.979
135	2032	-1.164	.208	-.366	-1.804
135	2035	-1.253	.208	-.552	-1.902
135	2036	-1.119	.223	-.337	-1.847
135	2037	-1.169	.219	-.425	-1.843
135	2038	-1.145	.204	-.381	-1.767
135	2039	-1.284	.214	-.494	-2.010
135	2041	-1.261	.207	-.516	-1.920
135	2043	-1.224	.214	-.277	-2.024
135	2044	-1.099	.192	-.409	-1.897
135	2047	-1.228	.190	-.602	-2.019
135	2048	-1.206	.213	-.510	-1.922
135	2049	-1.399	.239	-.663	-2.158
135	2050	-1.123	.209	-.444	-1.890
135	2051	-1.245	.218	-.491	-2.015
135	2053	-1.200	.206	-.476	-1.915
135	2055	-1.263	.243	-.478	-2.110
135	2057	-1.156	.217	-.250	-1.929
135	2059	-1.208	.218	-.427	-1.979
135	2061	-1.196	.229	-.423	-1.959

APPENDIX B -- PRESSURE DATA: MOBILE SERVICE TOWER (M.S.T.)

WD	TAP	CPMEAN	CPRMS	CPMAX	CPMIN
135	2063	-1.241	.213	-.559	-1.993
135	2065	-1.208	.201	-.146	-1.946
135	2067	-1.243	.235	-.412	-2.119
135	2069	-1.249	.210	-.540	-1.945
135	2071	-1.269	.224	-.518	-2.121
135	2073	-1.232	.205	-.502	-1.851
135	2075	-1.297	.208	-.505	-2.110
135	2076	-1.150	.193	-.534	-1.767
135	2077	-1.266	.197	-.595	-1.887
135	2078	-1.230	.194	-.618	-1.908
135	2079	-1.240	.197	-.540	-1.870
135	2080	-1.239	.207	-.629	-2.029
135	2081	-1.232	.197	-.548	-1.973
135	2082	-1.145	.186	-.445	-1.806
135	2084	-1.123	.191	-.525	-1.796
135	2085	-1.107	.181	-.476	-1.756
135	2086	-1.143	.216	-.358	-1.888
135	2090	-1.059	.201	-.387	-1.749
135	2091	-1.069	.185	-.445	-1.692
135	2095	-1.021	.197	-.393	-1.864
135	2096	-1.152	.194	-.529	-1.776
135	2097	-1.197	.185	-.574	-1.814
135	2099	-1.139	.192	-.545	-1.911
135	2100	-1.109	.207	-.424	-1.975
180	1001	-1.240	.368	.036	-2.313
180	1002	-1.175	.343	.239	-2.140
180	1003	-1.124	.336	.192	-2.212
180	1004	-1.003	.332	.391	-2.401
180	1005	-.874	.279	.237	-2.041
180	1006	-.767	.218	-.006	-1.601
180	1007	-.817	.213	.036	-1.630
180	1008	-.915	.247	.093	-1.872
180	1009	-.778	.224	.073	-1.564
180	1010	-.758	.219	.078	-1.472
180	1011	-.774	.198	-.122	-1.480
180	1012	-.807	.225	-.035	-1.679
180	1013	-.815	.236	-.075	-1.687
180	1014	-.684	.250	.167	-1.771
180	1015	-.707	.222	.022	-1.605
180	1016	-.798	.242	-.091	-1.958
180	1017	-.752	.257	.099	-1.679
180	1018	-.685	.249	.141	-1.573
180	1019	-.734	.232	.050	-1.443
180	1020	-.803	.235	.036	-1.579
180	1021	-.713	.250	.086	-1.521
180	1022	-.681	.212	.155	-1.376
180	1023	-.730	.205	.050	-1.452
180	1024	-.856	.230	-.135	-1.769
180	1025	-.715	.241	-.045	-2.071
180	1026	-.829	.347	.302	-2.030
180	1027	-1.210	.404	.160	-2.601
180	1028	-1.658	.391	-.291	-3.196
180	1029	-1.678	.329	-.653	-3.123
180	1030	-1.635	.289	-.743	-2.593
180	1031	-1.652	.260	-.839	-2.656
180	1032	-1.052	.378	.245	-2.338
180	1033	-1.367	.383	.311	-2.635
180	1034	-1.657	.363	.152	-2.948
180	1035	-1.664	.362	-.295	-3.450
180	1036	-1.512	.311	-.537	-2.575
180	1037	-1.502	.288	-.570	-2.679
180	1038	-.944	.383	.605	-2.408
180	1039	-1.265	.377	.228	-2.666
180	1040	-1.634	.354	-.275	-3.004
180	1041	-1.537	.334	-.529	-2.961
180	1042	-1.422	.314	-.497	-2.780
180	1043	-1.425	.295	-.530	-2.473
180	1044	-.873	.373	.476	-2.296
180	1045	-1.262	.400	.747	-2.768
180	1046	-1.698	.382	-.488	-3.152
180	1047	-1.664	.387	-.441	-3.682
180	1048	-1.581	.315	-.635	-3.032
180	1049	-1.631	.308	-.634	-3.116
180	1050	-.734	.279	.196	-1.725
180	1051	-.928	.279	.022	-1.814
180	1052	-1.228	.293	-.236	-2.227
180	1053	-1.337	.289	-.400	-2.452
180	1054	-1.646	.299	-.449	-2.920
180	1055	-1.842	.415	-.785	-4.164
180	1056	.952	.213	1.603	.193
180	1057	1.168	.289	2.160	-.032
180	1058	1.183	.270	1.992	.168
180	1059	1.075	.274	1.909	.091
180	1060	1.039	.260	1.839	.152
180	1061	1.436	.263	2.308	.559
180	1062	1.491	.266	2.424	.511
180	1063	1.177	.268	2.074	.124
180	1064	.827	.277	1.846	-.148
180	1065	1.240	.269	2.256	.452
180	1066	1.299	.266	2.025	.445
180	1067	.960	.268	1.786	.104
180	1068	.665	.259	1.439	-.219
180	1069	1.078	.252	1.839	.271
180	1070	1.142	.258	2.083	.249
180	1071	.817	.261	1.709	-.090
180	1072	.403	.243	1.240	-.379
180	1073	.770	.230	1.507	.060
180	1074	.801	.244	1.552	-.167
180	1075	.573	.255	1.301	-.298
180	1076	-1.206	.235	-.508	-2.027
180	1077	-1.278	.238	-.516	-2.031
180	1078	-1.271	.209	-.555	-2.124
180	1079	-1.347	.230	-.665	-2.140
180	1080	-1.244	.233	-.374	-2.084
180	1081	-1.001	.323	.450	-2.171
180	1082	-1.352	.364	.383	-2.746
180	1083	-1.675	.303	-.572	-2.651
180	1084	-1.896	.298	-1.026	-3.095
180	1085	-1.855	.279	-.938	-2.800
180	1086	-.764	.300	.338	-1.763
180	1087	-1.164	.340	.146	-2.348
180	1088	-1.479	.290	-.359	-2.556
180	1089	-1.652	.289	-.862	-3.432
180	1090	-1.547	.259	-.769	-2.557
180	1091	-.733	.277	.235	-1.641
180	1092	-1.103	.290	.120	-2.017
180	1093	-1.401	.268	-.298	-2.275
180	1094	-1.611	.236	-.836	-2.483
180	1095	-1.509	.212	-.825	-2.208
180	1096	-.785	.272	.133	-1.852
180	1097	-1.150	.312	.196	-2.086
180	1098	-1.510	.291	-.488	-2.542
180	1099	-1.720	.264	-.787	-2.823
180	1100	-1.586	.216	-.938	-2.370
180	2001	-1.200	.238	-.333	-1.913
180	2002	-1.256	.259	-.385	-2.198
180	2003	-1.257	.242	-.531	-2.119
180	2004	-1.350	.258	-.588	-2.207
180	2005	-1.071	.277	-.208	-2.149
180	2006	-1.022	.227	-.293	-1.714
180	2008	-1.028	.296	-.092	-2.311
180	2010	-1.165	.239	-.423	-2.102
180	2012	-.956	.277	-.082	-2.032
180	2014	-1.219	.235	-.415	-1.964
180	2016	-.887	.263	-.134	-1.761
180	2018	-1.241	.236	-.463	-2.117
180	2020	-.888	.249	-.032	-1.780
180	2022	-.764	.301	.231	-2.080
180	2024	-.896	.263	.047	-1.916
180	2026	-1.130	.215	-.334	-1.919
180	2027	-1.173	.220	-.354	-2.037
180	2029	-1.161	.213	-.437	-2.001
180	2031	-1.198	.228	-.499	-1.892
180	2032	-1.159	.251	-.259	-2.161
180	2035	-1.317	.255	-.466	-2.365
180	2036	-1.223	.225	-.556	-2.057
180	2037	-1.291	.217	-.642	-2.051
180	2038	-1.157	.229	-.390	-1.990
180	2039	-1.269	.238	-.487	-2.185
180	2041	-1.185	.224	-.396	-1.985

APPENDIX B -- PRESSURE DATA: MOBILE SERVICE TOWER (M.S.T.)

WD	TAP	CPMEAN	CPRMS	CPMAX	CPMIN
180	2043	-1.260	.243	-.541	-2.011
180	2044	-1.201	.231	-.400	-2.053
180	2047	-1.282	.233	-.555	-2.266
180	2048	-1.215	.233	-.451	-2.117
180	2049	-1.344	.231	-.590	-2.153
180	2050	-1.005	.281	.139	-1.962
180	2051	-1.287	.252	-.512	-2.207
180	2053	-1.291	.240	-.536	-2.192
180	2055	-1.285	.241	-.498	-2.125
180	2057	-1.071	.241	-.370	-1.853
180	2059	-1.198	.245	-.398	-2.037
180	2061	-1.262	.230	-.570	-2.142
180	2063	-1.261	.244	-.425	-2.004
180	2065	-1.191	.235	-.447	-1.909
180	2067	-1.299	.243	-.527	-2.051
180	2069	-1.236	.235	-.468	-2.042
180	2071	-1.272	.255	-.563	-2.127
180	2073	-1.192	.238	-.446	-1.985
180	2075	-1.276	.249	-.512	-2.112
180	2076	-1.121	.227	-.437	-1.799
180	2077	-1.311	.249	-.348	-2.216
180	2078	-1.193	.227	-.447	-2.010
180	2079	-1.197	.223	-.530	-1.967
180	2080	-1.221	.242	-.471	-2.076
180	2081	-1.233	.222	-.476	-1.898
180	2082	-1.237	.220	-.536	-1.941
180	2084	-1.145	.233	-.407	-1.897
180	2085	-1.194	.208	-.532	-1.906
180	2086	-1.125	.241	-.262	-1.934
180	2090	-1.088	.228	-.394	-1.791
180	2091	-1.070	.219	-.348	-1.769
180	2095	-1.069	.222	-.387	-1.818
180	2096	-1.166	.228	-.441	-1.834
180	2097	-1.260	.242	-.316	-2.066
180	2099	-1.118	.218	-.377	-1.835
180	2100	-1.167	.233	-.403	-1.920
225	1001	-.344	.334	.557	-1.740
225	1002	-.234	.353	.670	-2.020
225	1003	-.598	.491	.432	-2.315
225	1004	-.910	.606	.599	-2.768
225	1005	-.870	.457	.402	-2.488
225	1006	-1.256	.178	-.669	-1.874
225	1007	-1.347	.173	-.763	-1.927
225	1008	-1.498	.198	-.729	-2.203
225	1009	-1.320	.169	-.712	-1.830
225	1010	-1.264	.204	-.679	-2.010
225	1011	-1.349	.197	-.792	-2.008
225	1012	-1.384	.219	-.726	-2.108
225	1013	-1.320	.210	-.725	-2.036
225	1014	-1.149	.210	-.373	-1.816
225	1015	-1.265	.225	-.417	-2.017
225	1016	-1.419	.236	-.664	-2.110
225	1017	-1.244	.225	-.491	-1.904
225	1018	-1.045	.233	-.300	-1.893
225	1019	-1.185	.244	-.414	-2.030
225	1020	-1.345	.249	-.574	-2.156
225	1021	-1.150	.231	-.376	-1.992
225	1022	-.990	.242	-.034	-1.916
225	1023	-1.129	.247	-.212	-2.206
225	1024	-1.345	.258	-.445	-2.382
225	1025	-1.160	.232	-.326	-2.133
225	1026	-1.232	.201	-.602	-2.118
225	1027	-1.260	.210	-.511	-2.067
225	1028	-1.319	.225	-.469	-2.116
225	1029	-1.114	.210	-.285	-1.990
225	1030	-1.098	.198	-.439	-1.631
225	1031	-1.165	.188	-.539	-1.717
225	1032	-1.350	.207	-.378	-2.211
225	1033	-1.393	.211	-.540	-2.201
225	1034	-1.375	.213	-.624	-2.108
225	1035	-1.269	.208	-.556	-1.966
225	1036	-1.233	.219	-.450	-2.096
225	1037	-1.295	.215	-.600	-2.171
225	1038	-1.223	.201	-.564	-2.034
225	1039	-1.308	.204	-.658	-2.031
225	1040	-1.407	.213	-.708	-2.125
225	1041	-1.185	.198	-.504	-1.864
225	1042	-1.127	.205	-.305	-1.993
225	1043	-1.188	.214	-.389	-2.116
225	1044	-1.122	.209	-.328	-1.823
225	1045	-1.221	.216	-.501	-2.030
225	1046	-1.331	.224	-.589	-2.081
225	1047	-1.095	.210	-.376	-1.937
225	1048	-1.041	.227	-.370	-1.851
225	1049	-1.085	.237	-.356	-1.957
225	1050	-1.059	.235	-.317	-1.859
225	1051	-1.142	.229	-.402	-1.869
225	1052	-1.297	.239	-.551	-2.216
225	1053	-1.073	.219	-.340	-1.952
225	1054	-1.004	.229	-.176	-1.873
225	1055	-1.040	.241	-.285	-1.913
225	1056	-.252	.140	.225	-.743
225	1057	.150	.219	.993	-.605
225	1058	.328	.231	1.186	-.412
225	1059	.580	.254	1.522	-.174
225	1060	-.241	.232	.478	-1.123
225	1061	.317	.236	.995	-.556
225	1062	.616	.222	1.397	-.064
225	1063	.905	.248	1.773	.157
225	1064	-.342	.229	.490	-1.336
225	1065	.272	.217	1.031	-.544
225	1066	.579	.204	1.274	-.169
225	1067	.822	.234	1.509	.079
225	1068	-.296	.233	.456	-1.096
225	1069	.278	.222	.912	-.499
225	1070	.531	.231	1.448	-.216
225	1071	.757	.259	1.770	-.006
225	1072	-.462	.263	.372	-1.459
225	1073	.101	.261	.856	-.799
225	1074	.459	.245	1.196	-.247
225	1075	.615	.242	1.416	-.168
225	1076	1.110	.230	1.858	.407
225	1077	1.187	.261	2.081	.304
225	1078	1.059	.233	1.839	.223
225	1079	1.018	.230	1.734	.227
225	1080	.824	.243	1.620	.091
225	1081	-1.666	.248	-.844	-2.752
225	1082	-1.774	.258	-.932	-2.754
225	1083	-2.388	.307	-1.424	-3.382
225	1084	-3.337	.363	-2.201	-4.380
225	1085	-1.716	.239	-.914	-2.518
225	1086	-1.552	.232	-.738	-2.402
225	1087	-1.849	.278	-.979	-3.193
225	1088	-1.624	.322	-.666	-2.739
225	1089	-.922	.215	-.211	-1.691
225	1090	-2.729	.685	-.701	-4.733
225	1091	-1.452	.265	-.602	-2.375
225	1092	-1.240	.303	-.135	-2.740
225	1093	-.781	.198	-.088	-1.844
225	1094	-.842	.180	-.146	-1.432
225	1095	-2.634	.377	-1.265	-3.727
225	1096	-1.299	.240	-.497	-2.221
225	1097	-1.043	.210	-.333	-1.682
225	1098	-.959	.190	-.304	-1.748
225	1099	-.884	.213	-.021	-1.680
225	1100	-1.650	.291	-.564	-2.676
225	2001	1.081	.267	1.987	.111
225	2002	1.194	.270	2.124	.294
225	2003	1.134	.259	1.989	.240
225	2004	1.037	.242	1.939	.276
225	2005	.846	.265	1.930	-.006
225	2006	.500	.289	1.355	-.652
225	2008	-1.001	.483	.419	-2.616
225	2010	1.232	.311	2.388	.246
225	2012	-.889	.423	.429	-2.242
225	2014	1.177	.270	2.069	.199
225	2016	-.790	.422	.305	-2.609
225	2018	1.143	.243	1.998	.453
225	2020	-.815	.450	.437	-2.997
225	2022	.922	.286	1.968	-.019

APPENDIX B -- PRESSURE DATA: MOBILE SERVICE TOWER (M.S.T.)

WD	TAP	CPMEAN	CPRMS	CPMAX	CPMIN
225	2024	.144	.512	1.676	-1.955
225	2026	1.208	.283	2.099	.401
225	2027	.875	.263	1.752	-.021
225	2029	.761	.234	1.672	.049
225	2031	.928	.246	1.827	-.021
225	2032	1.204	.280	2.463	.038
225	2035	.539	.240	1.253	-.392
225	2036	.778	.227	1.570	.023
225	2037	.928	.231	1.695	.225
225	2038	1.239	.269	2.236	.340
225	2039	.862	.247	1.660	-.032
225	2041	.644	.222	1.352	-.106
225	2043	.942	.229	1.767	.101
225	2044	1.115	.249	1.840	.230
225	2047	.673	.228	1.378	-.135
225	2048	.742	.226	1.618	-.019
225	2049	.243	.217	1.063	-.434
225	2050	.857	.243	1.887	-.086
225	2051	.620	.239	1.649	-.259
225	2053	.621	.219	1.473	-.296
225	2055	.738	.232	1.537	-.034
225	2057	.796	.245	1.686	-.159
225	2059	.730	.257	1.499	-.260
225	2061	.844	.236	1.623	.097
225	2063	.882	.241	1.711	.102
225	2065	.808	.226	1.679	-.018
225	2067	.926	.251	1.780	.047
225	2069	.771	.235	1.624	.072
225	2071	.877	.258	1.732	.049
225	2073	.746	.216	1.446	-.006
225	2075	.861	.236	1.551	.064
225	2076	1.014	.226	1.769	.216
225	2077	.983	.236	1.653	.275
225	2078	.951	.215	1.654	.221
225	2079	.935	.207	1.702	.188
225	2080	.907	.223	1.657	.192
225	2081	.755	.246	1.562	-.168
225	2082	.770	.222	1.494	.023
225	2084	.814	.253	1.510	.008
225	2085	.830	.242	1.614	.035
225	2086	.761	.252	1.506	-.075
225	2090	.835	.249	1.605	.021
225	2091	.835	.212	1.594	.036
225	2095	.858	.223	1.578	.075
225	2096	.842	.219	1.603	.053
225	2097	.765	.229	1.510	.071
225	2099	.770	.214	1.499	.021
225	2100	.863	.232	1.537	.078
270	1001	1.126	.294	2.110	.211
270	1002	1.107	.293	2.128	.342
270	1003	.858	.312	1.824	-.131
270	1004	.523	.360	1.612	-.931
270	1005	-.246	.578	1.210	-2.113
270	1006	-1.622	.397	-.482	-3.217
270	1007	-1.765	.427	-.513	-3.751
270	1008	-1.819	.425	-.601	-3.398
270	1009	-1.386	.328	-.260	-2.468
270	1010	-1.495	.335	-.629	-2.962
270	1011	-1.649	.354	-.768	-3.286
270	1012	-1.707	.432	-.500	-3.884
270	1013	-1.673	.448	-.410	-3.304
270	1014	-1.433	.323	-.492	-2.608
270	1015	-1.605	.365	-.623	-3.048
270	1016	-1.806	.446	-.560	-3.638
270	1017	-1.622	.463	-.278	-3.866
270	1018	-1.496	.308	-.684	-2.947
270	1019	-1.650	.343	-.794	-3.313
270	1020	-1.821	.394	-.859	-3.704
270	1021	-1.626	.382	-.259	-3.300
270	1022	-1.652	.515	-.353	-4.106
270	1023	-1.559	.399	-.222	-3.279
270	1024	-1.685	.380	-.555	-3.181
270	1025	-1.289	.305	-.317	-2.863
270	1026	-1.190	.286	-.074	-2.265
270	1027	-1.304	.276	-.288	-2.287
270	1028	-1.455	.276	-.470	-2.456
270	1029	-1.269	.264	-.461	-2.267
270	1030	-1.235	.294	-.169	-2.251
270	1031	-1.312	.298	-.358	-2.329
270	1032	-1.237	.328	-.303	-2.241
270	1033	-1.232	.305	-.402	-2.481
270	1034	-1.189	.275	-.398	-2.141
270	1035	-1.131	.247	-.410	-2.024
270	1036	-1.137	.237	-.233	-2.043
270	1037	-1.298	.259	-.416	-2.437
270	1038	-1.212	.350	-.229	-2.950
270	1039	-1.198	.300	-.390	-2.705
270	1040	-1.193	.263	-.256	-2.348
270	1041	-1.029	.240	-.239	-2.013
270	1042	-.979	.276	-.006	-2.174
270	1043	-1.185	.314	-.116	-2.459
270	1044	-1.304	.320	-.196	-2.527
270	1045	-1.316	.314	-.259	-2.596
270	1046	-1.391	.291	-.367	-2.448
270	1047	-1.212	.268	-.379	-2.100
270	1048	-1.307	.303	.008	-2.459
270	1049	-1.482	.306	-.288	-2.539
270	1050	-1.232	.277	-.423	-2.466
270	1051	-1.332	.279	-.466	-2.418
270	1052	-1.512	.279	-.555	-2.587
270	1053	-1.282	.261	-.385	-2.172
270	1054	-1.278	.267	-.242	-2.188
270	1055	-1.332	.267	-.365	-2.274
270	1056	-1.634	.261	-.789	-2.500
270	1057	-1.552	.403	-.367	-3.217
270	1058	-1.462	.341	-.537	-2.972
270	1059	-1.493	.315	-.696	-2.794
270	1060	-1.753	.439	-.137	-3.680
270	1061	-1.534	.352	-.396	-2.928
270	1062	-1.509	.309	-.459	-2.581
270	1063	-1.545	.304	-.446	-2.612
270	1064	-1.831	.479	-.186	-4.802
270	1065	-1.506	.372	-.459	-3.257
270	1066	-1.377	.330	-.439	-3.173
270	1067	-1.429	.323	-.513	-3.226
270	1068	-1.856	.401	-.153	-3.358
270	1069	-1.645	.360	-.673	-3.420
270	1070	-1.614	.423	-.602	-3.882
270	1071	-1.664	.403	-.625	-3.651
270	1072	-1.569	.315	-.244	-3.166
270	1073	-1.455	.322	-.385	-3.147
270	1074	-1.488	.386	-.298	-2.897
270	1075	-1.732	.516	-.566	-3.997
270	1076	1.006	.284	1.988	-.180
270	1077	.896	.293	1.817	-.410
270	1078	.752	.305	1.808	-.666
270	1079	.574	.333	1.448	-1.219
270	1080	-.106	.512	1.159	-1.861
270	1081	-1.739	.329	-.557	-2.804
270	1082	-1.666	.318	-.703	-2.751
270	1083	-1.555	.271	-.713	-2.612
270	1084	-1.733	.306	-.989	-3.054
270	1085	-1.698	.294	-.778	-2.943
270	1086	-1.627	.355	-.528	-3.030
270	1087	-1.647	.349	-.577	-3.318
270	1088	-1.444	.300	-.614	-2.855
270	1089	-1.591	.359	-.673	-3.807
270	1090	-1.515	.346	-.602	-3.675
270	1091	-1.621	.399	-.577	-3.897
270	1092	-1.613	.352	-.643	-3.217
270	1093	-1.450	.360	-.453	-2.832
270	1094	-1.528	.334	-.534	-3.299
270	1095	-1.544	.377	-.659	-3.206
270	1096	-1.474	.358	-.485	-3.005
270	1097	-1.637	.364	-.621	-3.242
270	1098	-1.537	.380	-.212	-3.061
270	1099	-1.603	.355	-.386	-3.736
270	1100	-1.445	.362	-.135	-2.949
270	2001	1.231	.258	2.206	.414
270	2002	1.196	.247	1.957	.290

APPENDIX B -- PRESSURE DATA: MOBILE SERVICE TOWER (M.S.T.)

WD	TAP	CPMEAN	CPRMS	CPMAX	CPMIN
270	2003	1.186	.250	1.958	.349
270	2004	1.173	.250	1.939	.305
270	2005	1.114	.243	2.008	.440
270	2006	.780	.212	1.460	.130
270	2008	.029	.833	2.024	-2.415
270	2010	1.235	.245	2.025	.526
270	2012	.117	.823	1.886	-2.859
270	2014	1.241	.252	2.074	.471
270	2016	-.040	.806	1.806	-2.779
270	2018	1.208	.241	2.018	.147
270	2020	-.042	.857	1.965	-2.689
270	2022	1.141	.229	1.900	.415
270	2024	.981	.422	2.315	-2.170
270	2026	1.379	.271	2.234	.361
270	2027	1.388	.278	2.293	.322
270	2029	1.400	.276	2.418	.314
270	2031	1.349	.256	2.165	.494
270	2032	1.359	.237	2.179	.540
270	2035	1.325	.238	2.115	.482
270	2036	1.365	.276	2.403	.344
270	2037	1.343	.276	2.290	.357
270	2038	1.352	.253	2.187	.496
270	2039	1.329	.267	2.163	.504
270	2041	1.348	.254	2.321	.536
270	2043	1.295	.257	2.189	.373
270	2044	1.199	.256	2.056	.287
270	2047	1.173	.258	2.059	.182
270	2048	1.268	.259	2.222	.478
270	2049	.429	.252	1.251	-.314
270	2050	1.077	.264	1.913	.034
270	2051	1.005	.270	1.884	-.033
270	2053	1.164	.277	2.066	.059
270	2055	1.095	.260	2.048	.199
270	2057	1.380	.268	2.205	.460
270	2059	1.288	.258	2.179	.308
270	2061	1.328	.284	2.338	.412
270	2063	1.242	.248	2.261	.343
270	2065	1.280	.251	2.111	.413
270	2067	1.207	.278	2.032	.373
270	2069	1.244	.266	2.197	.407
270	2071	1.183	.255	2.066	.379
270	2073	1.113	.259	2.040	.331
270	2075	1.122	.242	1.898	.227
270	2076	1.233	.260	2.059	.301
270	2077	1.173	.254	1.975	.161
270	2078	1.197	.252	1.964	.376
270	2079	1.179	.245	1.971	.270
270	2080	1.100	.235	2.105	.422
270	2081	1.303	.242	2.150	.456
270	2082	1.305	.243	2.056	.417
270	2084	1.397	.251	2.250	.552
270	2085	1.345	.241	2.143	.494
270	2086	1.405	.253	2.339	.500
270	2090	1.483	.260	2.274	.590
270	2091	1.348	.233	2.179	.606
270	2095	1.468	.248	2.347	.717
270	2096	1.333	.243	2.193	.665
270	2097	1.304	.261	2.014	.372
270	2099	1.452	.254	2.159	.592
270	2100	1.459	.259	2.377	.692